An Experimental Investigation of the Influence of Mechanical Damage, Rust and Dust on the Ability of Flame Gaps to Prevent Gas Explosion Transmission

Fredrik Solheim

A thesis submitted in partial fulfillment of the requirements
for the degree of Master of Science in the subject of Physics;
Process Safety Technology

Department of Physics and Technology
University of Bergen
Bergen Norway
November 2010

Preface

This thesis is based on the experimental work performed in the Gas Explosion Laboratory at the Department of Physics and Technology, University of Bergen (UoB). The present thesis is a part of a Master Science degree in process safety technology.

I want to express my gratitude to several helpful persons who have supervised and motivated me through the work with this thesis. First of all I want to thank my two supervisors, Professor Rolf K. Eckhoff and Associate Professor Bjørn J. Arntzen. They have contributed in many interesting discussions concerning the physical mechanism related to different aspects of the explosion proof concept. Especially thanks to the former Master students Arild Grov and Harald E. Z. Opsvik who introduced me to the subject of flameproof enclosures and additional contributed in many interesting discussions through the work.

The experimental work required a great deal of special designed joints/slits. I want to thank Leif Egil Sandnes, Roald Langøen and Kåre Slettebakken at the Mechanical workshop for making these experimental parts. I also want to thank Werner Olsen, Chief engineer at the Section of Microelectronic at UoB, who helped me with the experimental setup. He also contributed in reparations when the electrical system failed. I am grateful to Egil S. Erichsen at the Laboratory for Electron Microscopy at UoB for taking magnified photos of the dust particles used in the present work.

I want to thank my friends and family for support and encouragement through the whole study period, both at the spare time and in periods where the time spent at school has been longer than the time spent in their company.

Finally I must thank my parents Bård E. Solheim and Elfrid H. Solheim who always has motivated me to take a good education, and who have supported me financially through tough times.

Bergen 18. November 2010

Fredrik Solheim

Department of Physics and Technology
University of Bergen
Norway

Abstract

Potential ignition sources, such as motors, light switchers and relays that are located in an industrial area where an explosive atmosphere is a threat, must be designed in such a way that the ignition source does not ignite the hazardous atmosphere. Flameproof enclosures designed for electrical apparatus are constructed in such a way that the enclosure can withstand an internal explosion, without causing an external ignition of the explosive atmosphere. All holes and gaps on the enclosure are designed in accuracy to given requirements from international standards. Current international standard (IEC 2007a) require that the maximal average roughness (Ra) of a flame gap surface is $\leq$ 6.3 μm. The standard also requires that any damaged flame gap must be brought back to its original state.

No technical argument is given by the current standard (IEC) to justify the requirements of an average roughness $\leq$ 6.3 μm. In the present work it is applied severe damages on different flame gap surfaces. This involves highly rusted flame gap surfaces and flame gap surfaces with different perforating grooves over the entire length. The purpose of the experimental work has been to investigate how different damages on the flame gap surface affect their ability to prevent ignition of an external explosive gas mixture.

The international standard (IEC 2007a) also requires a maximum allowed gap opening/distance between the two joints that form the flame gap. This distance varies with the inner volume of the flameproof enclosure and the width of the two joints. For the experimental set up in the present work the maximum allowed gap opening is 0.40 mm. This gap opening contains a safety factor, which implies that the actual distance between the joints can be noticeably larger without causing a re-ignition of an external gas mixture. The largest width between the joints in a standardized test apparatus, which prevents transmission of a gas explosion on the inside of the gap to the outside of the gap, is denoted as the MESG value (Maximum Experimental Safe Gap). This value is used in the present work as a parameter for judging if different damage on the gap surface reduce or improve the gap's ability to prevent a re-ignition.

Flameproof enclosures are located in areas where an explosive gas/air mixture can be formed. Dust is represented in almost any atmosphere and many types of dust are combustible. In the present work it has been investigated how the presence of dust inside a flameproof enclosure impacts the flame gaps ability to prevent a transmission of a gas explosion. The dust was not placed in the internal chamber, but sprinkled into the flame gap. This was to assure that the dust possibly found its way into the internal chamber by itself. The purpose of this work has been to investigate if dust can ignite inside the flame gap or the inner chamber, during an internal gas explosion and subsequently penetrate at a burning state into the external chamber and cause a re-ignition. To assure that the gas did not cause the possible re-ignition, the gap opening was set to a width smaller than the respective MESG value for an undamaged slit. It is performed experiments where the gap opening is set to the allowed width of 0.40 mm for flameproof enclosures, given by the standard (IEC 2007a).

The apparatus used in the experimental work was mainly the Plane Rectangular Slit Apparatus (PRSA), but in the experimental work due to dust, two apparatuses were used, the Plane Circular Flange Apparatus (PCFA) and the PRSA. Premixed 4.2 vol. % propane in air was used as a test gas in all experiments.

The overall conclusion from the present investigation of rusted gap surfaces and gap surfaces with perforating crosswise grooves is that the required value for surface roughness (6.3µm) is arbitrary chosen. The gap efficiency was not reduced in any of the performed experiments with different damages on the gap surfaces. This includes rusted surfaces and flame gap surfaces with perforating multiple crosswise grooves of different depths and widths. It is stated that the hot combustion gases that flow through a slit with multiple crosswise grooves have a noticeably lower temperature when they enter the external chamber, than the hot combustion gases that flows through an undamaged slit.

The overall conclusion from the experiments performed with different dust types is that combustible dust must not be underestimated as a potential hazard in areas where flameproof enclosures are located. It is shown through several experiments that dust possibly can cause re-ignition of an external explosive atmosphere, at gap openings where it is impossible to get an ignition of the surrounding explosive atmosphere with only gas present. It is stated that the probability for an ignition of the surrounding explosive atmosphere is greatest if the dust find its way through the flame gap and into the main volume of the flameproof enclosure, prior to the gas explosion. Through several experiments it is shown that this scenario can occur at the allowed gap opening of 0.40 mm, according to the standard (IEC 2007a).

1 Introduction

1.1 Background

Today the consumption of energy per person is greater than ever. The demand for energy increases rapidly. This leads to a great development of new methods that extract more energy from existing and well known sources, such as wind, oil and gas. The potential hazards are enormous in many cases, but man has decided that this is a risk worth taking. There is a constant battle to reduce the probability for potential fatalities. April 20, 2010 we failed again. On this date the oil platform Deepwater Horizon exploded and caused one of the most fatal man-made disasters in history. The platform sank and 11 persons were killed, the oil spill continued to July 15 before it was temporarily closed by a well cap, but then the environmental disaster was already a matter of fact. The initial course of events is unclear, but it is known that a blow out from the well leaded methane into the ventilation plant, which subsequent ignited in series of gas explosions.

An explosive atmosphere can be formed in many industries, as a result of mixing between combustible substances and air. It is therefore of great importance that each industry have detailed knowledge of all potential sources that can lead to an explosion on their plant. Understanding of the explosion phenomena is important to keep the production going, but most of all important to prevent fatal accidents.

1.2 Motivation

The aim at safety in own projects is an inherent quality that most people have, but how much time and resources are appropriate to spend on the development of safety? In the year 1815, Sir Humphrey Davy started the work with an explosion proof oil lamp for use in coal mines. Since 1815 new challenges have constantly occurred. The work with explosion safe electrical equipment started about 100 years ago. Since then the improvements have been great, but nevertheless there has been a growth of potential hazards in the industry world-wide.

From Figure 1-1 it can be seen that a great deal of hydrocarbon leakages above 0.1 Kg/s occurred on Norwegian installations from the year 2000 to 2009. In 2009 alone there were 15 leakages. This implies that the safety routines due to potential ignitions sources must have high priority, and that the equipment that isolates potential sources of ignition from the explosive substance must be reliable. The process industry therefore uses a considerable amount on maintenance of electrical equipment in process plants, especially Ex"d" equipment.

Electrical apparatuses constitute a great deal of the potential ignition sources in the industry. In process areas where an explosive atmosphere can occur it is therefore important to “isolate” all electrical parts that can cause ignition. Today all electrical installations that are situated in process areas with potential explosive atmosphere are conducted to extensive international standardisations. In Europe both the IEC and the Cenelec standards apply. The present work is related to flameproof enclosures (Ex"d") and the international IEC standards that are valid for these. Different series of standardized basic design concepts for electrical

apparatuses are available. One of these concepts is flameproof enclosures (Ex"d"). These enclosures prevent transmission of the explosion from inside of the apparatus to the external atmosphere by a flange/flame gap.

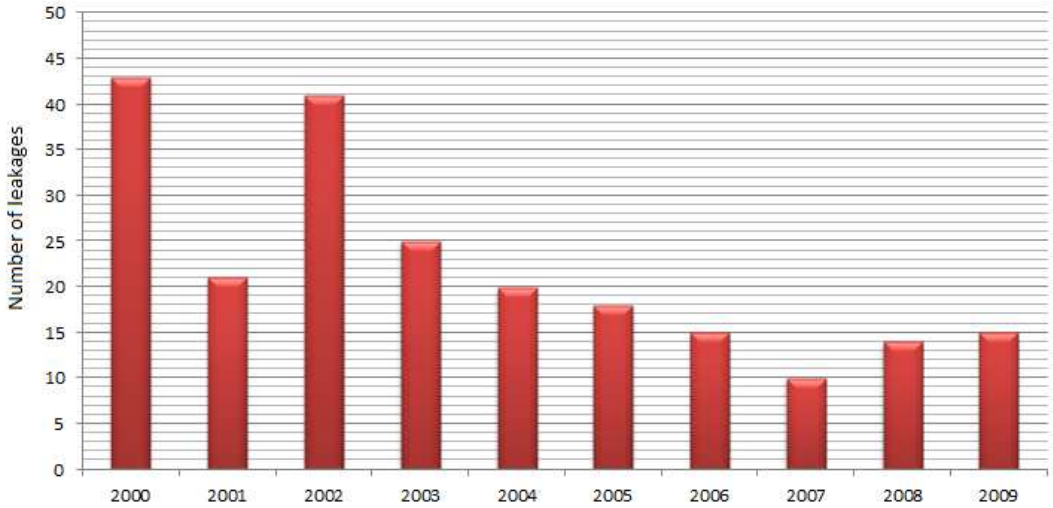

Figure 1-1: *Hydrocarbon leaks on Norwegian installations in the period 2000 to 2009. All leaks are above 0.1 Kg/s. Based on values from (Petroleum Safety Authority Norway 2009).*

The aim of the experimental research in the present work has been to investigate to what extend different damages on flame gap surfaces affects the flame gaps ability to prevent transmission of an explosion. This involves highly rusted surfaces and severe mechanical damage on the gap surface. This work is a continuation of the work performed by (Opsvik 2010) and (Grov 2010), who both studied how different damages on flame gap surfaces affect the flameproof enclosures ability to prevent an transmission of an explosion. They did systematic experiments with flame gap surfaces of different roughness above the permitted value of 6.3 µm from (IEC 2007a).

Additional an investigation of the presence of combustible dust inside the flame gap and flameproof enclosure has been carried out. The motivation for performing these experiments was to investigate if dust inside the flame gap or the inner chamber reduce the flame gap's ability to prevent a transmission of a gas explosion from the inner chamber to the external explosive atmosphere. Dust occurs in nearly any environment, and a great deal of dust substances is combustible. It is therefore of interest to examine if dust possibly can ignite inside the flameproof enclosure during an internal gas explosion and subsequently penetrate back to the external chamber and ignite the surrounding explosive gas mixture.

2 Review of Relevant Literature

2.1 Gas explosion

Leaks of combustible gases and vapors may give rise to an explosion if the main physical conditions for combustion are obtained. The conditions to be obtained are fuel, ignition source and oxygen. If one of these sources is removed you cannot get an explosion. Industries that deal with combustible gases and vapor must always take into account that there can be a leakage of the combustible composition. Consequently they must prevent neither oxygen nor an ignition source to be a part of the environment where leakage is a potential hazard. For obvious reasons it will be most emphasize to obstruct the ignition sources.

An explosion is an exothermal process. This implies that heat release occur because of rapid chemical reactions. (Eckhoff 2005) proposed a definition of the phenomenon explosion: *"An explosion is an exothermal chemical process that, when occurring at constant volume, gives rise to a sudden and significant pressure rise".*

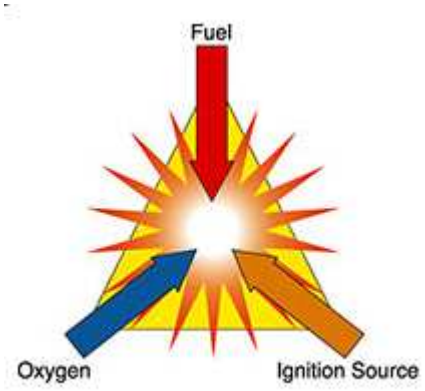

Figure 2-1: The explosion triangle. From (RKI-instruments 2010)

For all ratios of fuel and air there exist an upper and lower flammable limit. The mixture of the combustible gas/vapour and air can't be ignited if the fuel concentration is below the lower flammable limit or higher than the upper flammable limit (see Table 2-1). Different vapours and gases require different energies and consequently temperatures to ignite.

Table 2-1: *Combustibility and ignitability parameters of some combustible gases in air at atmospheric pressure. Based on (Eckhoff 2005)*

Fuel	Flammable limits [vol. % in air]		Min. ign. temp.
	Lower	Upper	[^{0}C]
Acetone	2,6	13	735
Ammonia	15	28	305
Bensene	1,3	7,9	560
Butane	1,8	8,4	370
Etane	3	12,4	515
Ethanol	3,3	19	363
Hydrogen	4	75	560
Propane	2,1	9,5	493

2.2 Flameproof enclosures (Ex"d")

2.2.1 Historical review

Flameproof enclosure is one of the oldest types of protection of potential ignition sources. In the 17th and 18th century it was a rapid increase in the coal mine industries in Europe. Coal produce methane, which is an explosive gas mixed with air. The minors light source was an open flame candle. This open flame frequently ignited the gas mixture inside the mine, which leaded to gas explosions. The pressure wave of the initial explosion further leaded to dispersion of dust layers inside the mine, occasionally the dispersed dust also ignited and a violent secondary explosion occurred.

The conditions in the mines was unbearable, consequently the UK's Sunderland Society for preventing Accidents in Coal Mines asked Sir Humphrey Davy in 1815 to perform a systematic investigation of flame propagation in firedamp/ air mixtures. In January 1816 Sir Davy had invented a revolutionary protection of potential ignition source, the Davy lamp. It was a paraffin lamp where the flame was surrounded by a fine wire mesh of gauze. The mesh prevented the flame to propagate through it, at the same time as it emitted light.

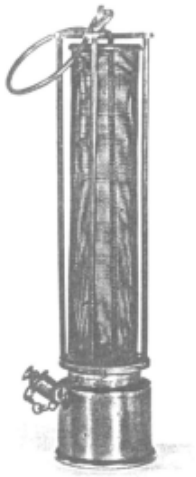

Figure 2-2: Early version of the coal mine lamp developed by Sir Humphrey Davy about 1816. From (Eckhoff 2005).

In the 19th century it was a rapid progress in electrical science and electrical engineering. The electricity went from being a scientific curiosity to be a great implement in the Second Industrial Revolution, and consequently in modern life. As a result of this, delegates to the International Electrical Congress adopted a report in 1904 that included following words: "*steps should be taken to secure the co-operation of the technical societies of the world, by the appointment of a representative Commission to consider the question of the standardization of the nomenclature and ratings of electrical apparatus machinery*". This led to the official foundation of the IEC in June 1906 in London. Since 1906 there has been a great development of the standards that regulate the design and manufacturing of the electrical equipment used in hazardous areas.

In 1935 the first German standard for installation of electrical equipment in hazardous areas came, "Protection of Electrical Installations in Hazardous Areas". This led to a fundamental change in the work with standards; they divided the installation requirements and product

design requirements. Subsequent the basic types of explosion protection such as flameproof enclosures were included in the product design standard. With the new classification the development of increased safety enclosures with flameproof components inside escalated, and all equipment design according to this standard were marked with the symbol (Ex).

CENELEC, The European Committee for Electrotechnical Standardization was established in 1973, as a result of the merger of two previous European committees, CENELCOM and CENEL, both working with coordination of electro technical standards in Europe. The main purpose was to establish a free trade zone in Europe, with technical standards that harmonized. In 1975 the first EU directive for apparatus used in hazardous areas was published, the "Explosion Protection Directive". CENELEC published the first edition of the European standards which included the installation techniques in 1978. Today 31 European countries are members of CENELEC.

But is not only in Europe the work with electro technical standards took place in the 19th and 20th century, both in USA and Canada developed their own standards. In Canada they got the Canadian Electrical Code, CE code that is a standard for maintenance of electrical equipment. National Electrical Code (NEC) is the standard in United States for the safe installation of electrical wiring and equipment.

2.2.2 A description of the concept of flameproof enclosures (Ex "d")

As briefly described in section 2.2.1 the development of electrical equipment was in rapid progress during the 1930s and 1940s. The quantity of electrical instruments used in different industries increased, and the demand for preventive safety precautions consequently increased. This leaded to the development of flameproof enclosures. The concept of these enclosures is to block the ignition sources (engines, switches etc.) from potentially explosive gas clouds to prevent hazardous and violent explosions. But the flameproof enclosures are not necessarily vapor-proof, this implies that the gas can find its way into the enclosure and cause an internal explosion. The internal explosion must not be transmitted to the external atmosphere. The flameproof enclosures must therefore have joints that reduce the internal explosion pressure so the enclosures can withstand the great forces during an explosion. Additional the joints have to be narrow enough so the hot penetrating gas from the internal chamber is sufficiently cooled down when it reaches the surrounding gas mixture (see Figure 2-3). All joints or gap openings has to be in accordance to IEC requirements (IEC 2007a) to secure that the hot gas that penetrates trough the openings does not lead to an external ignition.

Example of requirements related to flameproof enclosures, stated by IEC:

- Joints shall have an average roughness < 6.3 μm (see Figure 2-6)
- The surface temperature of the enclosure should not exceed the minimum ignition temperature for the gas that may be present
- Minimum width of the joint, which varies with varying types of joint (see Figure 2-4).
- Maximum gap opening of joint, which varies with varying type of joint and the volume of the primary chamber (see Figure 2-4)

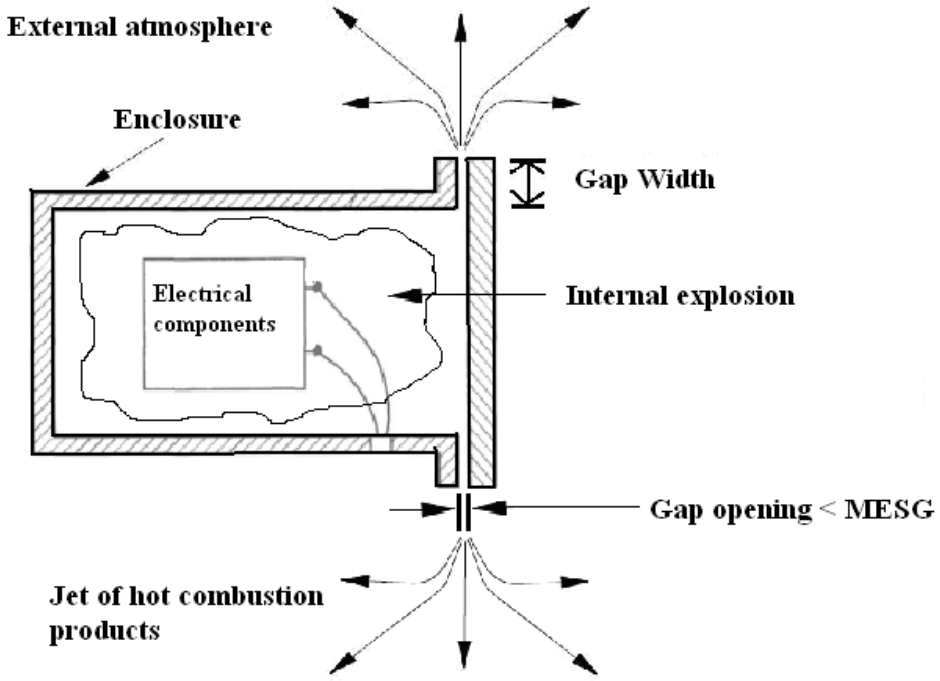

Figure 2-3: *Illustration of flameproof enclosures Ex"d" with an internal explosion.*

Different hazardous areas are subdivided into zones based on the probability of occurrence and duration of a flammable atmosphere. This is traditionally used as a basis for where different types of electrical equipment are allowed to handle. The design concept of Ex"d" proof enclosures can be used for apparatuses to be used in zone 1 and 2, typically transformers, motors, plugs, communication apparatus, heating equipment and light fittings. The zones are defined by the institute of petroleum (Petroleum 2002).

- Zone 0: That part of a hazardous area in which a flammable atmosphere is continuously present or present for long periods.

- Zone 1: That part of a hazardous area in which a flammable atmosphere is likely to occur in normal operation.

- Zone 2: That part of a hazardous area in which a flammable atmosphere is not likely to occur in normal operation and, if it occurs, will exist only for a short period.

The area classified as Zone 1 is a harsh area where a flammable atmosphere is likely to occur, the design concept of Ex"d" enclosures is allowed to use in this area. This implies that the mechanism of the flameproof enclosures that shall prevent an ignition of the surrounding explosive atmosphere must be reliable. There has been a great amount of investigation of which mechanisms that are most important considering the prevention of transmission of an explosion from the internal chamber to the external atmosphere. In chapter 2.3, literature that summarize the basic physically mechanism of flameproof enclosures will be presented.

Type of joint		Minimum width of joint *L* mm	Maximum gap mm											
			For a volume cm³ $V \leq 100$			For a volume cm³ $100 < V \leq 500$			For a volume cm³ $500 < V \leq 2\,000$			For a volume cm³ $V > 2\,000$		
			I	IIA	IIB	I	IIA	IIB	I	IIA	IIB	I	IIA	IIB
Flanged, cylindrical or spigot joints		6	0,30	0,30	0,20	–	–	–	–	–	–	–	–	–
		9,5	0,35	0,30	0,20	0,35	0,30	0,20	0,08	0,08	0,08	–	–	–
		12,5	0,40	0,30	0,20	0,40	0,30	0,20	0,40	0,30	0,20	0,40	0,20	0,15
		25	0,50	0,40	0,20	0,50	0,40	0,20	0,50	0,40	0,20	0,50	0,40	0,20
Cylindrical joints for shaft glands of rotating electrical machines with:	Sleeve bearings	6	0,30	0,30	0,20	–	–	–	–	–	–	–	–	–
		9,5	0,35	0,30	0,20	0,35	0,30	0,20	–	–	–	–	–	–
		12,5	0,40	0,35	0,25	0,40	0,30	0,20	0,40	0,30	0,20	0,40	0,20	–
		25	0,50	0,40	0,30	0,50	0,40	0,25	0,50	0,40	0,25	0,50	0,40	0,20
		40	0,60	0,50	0,40	0,60	0,50	0,30	0,60	0,50	0,30	0,60	0,50	0,25
	Rolling-element bearings	6	0,45	0,45	0,30	–	–	–	–	–	–	–	–	–
		9,5	0,50	0,45	0,35	0,50	0,40	0,25	–	–	–	–	–	–
		12,5	0,60	0,50	0,40	0,60	0,45	0,30	0,60	0,45	0,30	0,60	0,30	0,20
		25	0,75	0,60	0,45	0,75	0,60	0,40	0,75	0,60	0,40	0,75	0,60	0,30
		40	0,80	0,75	0,60	0,80	0,75	0,45	0,80	0,75	0,45	0,80	0,75	0,40
NOTE Constructional values rounded according to ISO 31-0 should be taken when determining the maximum gap.														

Figure 2-4: *Minimum width of joint and maximum gap opening for enclosures of groups I, IIA and IIB. From (IEC 2007a)*

2.2.3 Typical damages on Ex"d" equipment

During operation at an industrial area damages can easily occur on the Ex"d" enclosures. To avoid severe fatalities in hazardous areas it is of great importance to inspect the installed Ex"d" enclosures for damages at a regular basis. Ex"d" enclosures are usually made of steel, stainless steel and bronze alloy, in some cases they are made of plastic. These materials are possibly exposed for different types of damages.

Corrosion is one of the most usual damages on flameproof enclosure. The enclosures are often placed outside in harsh environment. From Figure 2-34 in section 2.6 it can be seen that the environment where the corrosion rate is of greatest extend is in the “droplet zone”. Offshore industries are located between this zone and the “marine atmosphere zone”. This implies that a great deal of Ex"d" enclosures is placed in a highly corrosive atmosphere. On an offshore rig, where there is oil production there will also be drilling sludge. The drilling sludge contains of different hygroscopic chemicals, a hygroscopic substance absorb water molecules. Equipment coated with drilling sludge will therefore be highly corrosive. Cleaning of process areas with water jets can also lead to moisture inside the flameproof enclosure, which can cause both rust formation on the flame gap and failure in the electrical components inside the enclosure.

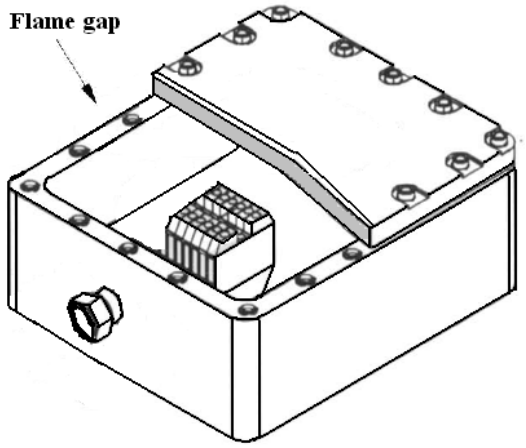

Figure 2-5: *Example of an Ex"d" flameproof enclosure with an electrical component inside.*

Other damages can directly be caused by human errors. Typically examples of this are damages on the enclosure due to welding, sandblasting, cutting and poor handling during inspections. All of these cases can lead to grooves or scratches on the gap surfaces which subsequent can result in an average roughness greater than the (IEC 2007a) requirement of 6.3 µm for flame gaps. Flameproof enclosures made of plastic is obvious more vulnerable for high temperatures than a steel enclosure.

2.2.4 Maintenance and inspection of flameproof equipment as regulated by the IEC standard

As flameproof enclosures is used in areas where a flammable atmosphere is likely to occur the inspection, maintenance and repair of the enclosures is of great importance to secure safe operations during the total lifetime of the equipment. Regular inspection routines of the enclosures are essential to determine if the apparatus requires service. The operations related to inspection of Ex"d" enclosures are described in (IEC 2007c) and the operation related to repair of the enclosures are described in (IEC 2007b).

As a process plant ages the physically conditions of the equipment on the plant tends to deteriorate. This implies that the maintenance and inspection of the equipment has to sustain of high priority. Area drawings and zone maps have to be continuously updated during modifications of a plant, so the essential equipment is installed at the right spot at the plant and easy to find during inspection.

The (IEC 2007c) defines different grades of inspections in three categories; visual inspection, close inspection and detailed inspection. The detailed inspection includes identification of defects which only will be apparent by opening the enclosures. Most companies require a “hot permit” from the person which performs the dismounting of an Ex"d" enclosure. The enclosures must be de-energized prior to the inspection, and the work has to be carried out with caution and in clean condition so the enclosures/flame gap do not get damaged, or get blocked by any objects.

2.2.5 Reparation of Ex"d" enclosure

If an Ex"d" enclosure is sufficient damaged it needs to be repaired to ensure a safe operation. But which damages are sufficient to demand reparation? It exist a great deal uncertainty due to this question. This is because the current standard (IEC 2007b) does not provide any guidance as to what extent of damage is sufficient enough to reduce the gap efficiency of such a level that the Ex"d" enclosure is useless. The only decisive parameter of the physical conditions of an Ex"d" enclosure is that the average roughness of the flame gap shall be lower than 6.3 μm (see Figure 2-6).

As reported in the standard for reparation (IEC 2007b) of Ex"d" equipment: "*Damaged or corroded flameproof joint faces should be machined, after consultation with the manufacturer wherever possible, only if the resultant joint gap and flange dimensions are not affected in such way that they contravene the certification documents."* This implies that all equipment with mechanical damage that can be detected should be machined and brought back to its originally state. The present work has investigated how different damages on the flame gap affect the gap efficiency.

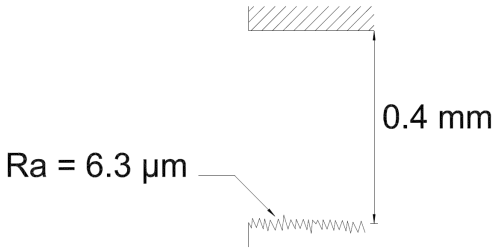

Figure 2-6: *The maximum allowable roughness of the joint/flame gap surface (average depth of 6.3 μm) compared with the maximum allowable flange gap (0.4 mm). From (Opsvik 2010)*

2.3 Basic Theory

2.3.1 Quenching distance, Q_D

The study of flame-wall interaction is of great importance for the understanding of near wall combustion. If a flame should successfully propagate through a narrow hole, the rate of heat production has to exceed the rate of heat loss to the wall. The quenching distance is defined as "the smallest tube diameter (or gap) which a laminar flame can propagate through". The quenching distance depends on many parameters concerning both surface state (material, surface topography, temperature) and burning medium (temperature, pressure, composition).

2.3.2 Maximum Experimental Safe Gap, MESG

The quenching distance is related to the propagation of a laminar flame through a narrow gap, but it does not consider the propagation of an explosion through a narrow gap. During an explosion in a vessel vented through a narrow gap, a jet of hot combustion products will be forced through the gap, due to the pressure rise in the vessel. This jet may achieve conditions favourable for igniting an external explosive mixture surrounding the vessel. The maximum experimental safe gap (MESG) is the widest gap that prevents a re-ignition of a surrounding explosive gas mixture.

The International Electrical Congress (IEC) developed a standardized method for determining the MESG value. Different gases of different ignition sensitivity were tested and classified in a test apparatus. The standard test apparatus consist of a primary chamber of 20 ml connected to a secondary chamber with a 25 mm flange gap (see Figure 2-7). The ignition source is located at the centre of the primary chamber.

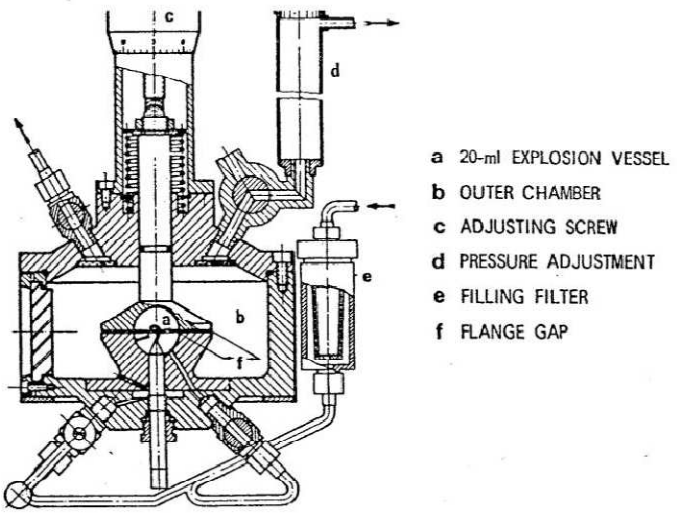

Figure 2-7: *Standard test apparatuses for determining MESG. From (IEC 2002).*

The largest gap opening giving no ignition in 10 subsequently experiments for a given gas is determined as the MESG value for the specific gas. Several studies are performed to determine the MESG values for varying gas mixtures and several definitions of the MESG are

presented. From (IEC 2007a) the MESG is defined as "*maximum gap of joint of 25 mm in width which prevents any transmission of an explosion during 10 tests made under conditions specified in IEC (2002)*". In 1979 Strehlow performed an investigation of the MESG for different components. Some of his results are presented in Table 2-2.

Table 2-2: *MESG values for different gases, determined with a European test apparatus. The experiments are carried out both in a 20 ml chamber and an 8 litre chamber. From (Strehlow, Nicholls et al. 1979)*

MESG (mm)	
Component	European
Propane	0.96
Ammonia	3.18
Ethylenediamine	1.47
Methane	1.15
Diethyl Ether	0.87
Ethylene	0.68
Methyl acetylene	0.74
Dimethyl ether	0.95
Hydrogen	0.28
Propylene oxide	0.7

From Table 2-2 it can be seen that the MESG value for propane is 0.96. In the apparatus used in the present work (see Figure 3-2 in section 3.4) the MESG value for propane is found to be 0.98 mm for an undamaged slit surface. This MESG value is used as an indicator of what impact different damages on the gap surface have on the gap efficiency. The gap efficiency is the ability the gap has to prevent a re-ignition in the secondary chamber (section 2.3.3). To be able to switch between different slits with varying gap surface, the apparatus presented in section 3.4 is used, and not a standard test apparatus, similar to the one in Figure 2-7.

2.3.3 Gap efficiency

If a specific damage on the gap surface leads to a significant reduction of the MESG (see section 2.3.2) compared with that obtained with a standard undamaged gap surface (roughness < 6.3 μm) then the gap efficiency is reduced significantly. If the MESG value increases due to a specific damage on the gap surface, then the gap efficiency also increases.

2.3.4 Elementary Reactions

In all chemical reactions there are reactive intermediate radicals involved, these are essential to maintain the reaction progress. A radical is an atom, molecule or an ion with unpaired electrons on an open shell configuration. The radicals are highly chemically reactive because of the unpaired electrons who always seek stability.

Combustion processes are based on radical chain reactions. One can explain these mechanisms by using the hydrogen-oxygen system. Some vital reactions of this system are shown in Table 2-3.

Table 2-3: *Radical chain reactions. Based on (J. Warnatz 2006)*

a	$H_2 + O_2 = 2\,OH^{\cdot}$	chain initiation
b	$0H^{\cdot} + H_2 = H_2O + H^{\cdot}$	chain propagation
c	$H^{\cdot} + O_2 = OH^{\cdot} + O^{\cdot}$	chain branching
d	$H^{\cdot} = \frac{1}{2} H_2$	chain termination

In the reaction mechanism, there are four main steps. The first step (Reaction a) is the chain initiation step, where stable species reacts to reactive species, radicals. The second step (Reaction b) is the chain propagation step where reactive intermediate radicals react with stable species forming another reactive radical. The third step is the chain branching step (Reaction c) where a stable species reacts with a radical and forming two reactive species. The last step is the chain termination step (Reaction d) where reactive species react to stable species, this can occur at a wall or in the gas phase.

When there is continuously more chain branching reactions then chain termination reactions (c > d) in a reaction zone the concentration [n] of radicals will increase exponentially with increasing time, this leads to an explosion (see Figure 2-8). If there are more chain termination reaction than chain branching reaction (c < d), the solution will get in to a time independent stationary solution and an explosion will not take place.

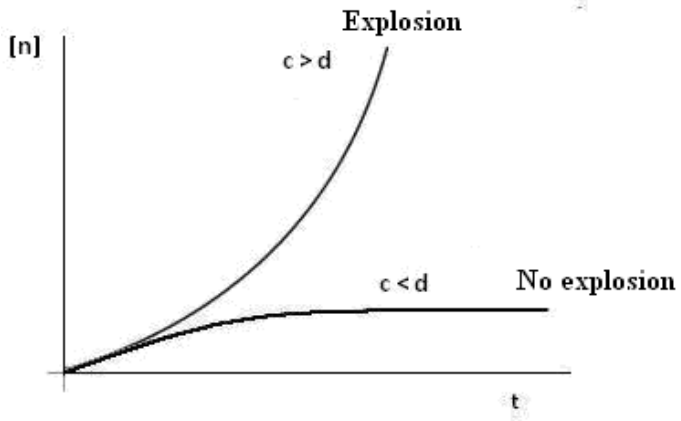

Figure 2-8: *Development of intermediate radicals. Based on (J. Warnatz 2006)*

2.3.5 Ignition of a combustible gas cloud by a jet of hot combustion products

The basic principle of Ex"d" equipment is to prevent ignition of an explosive atmosphere that surrounds the flameproof enclosure. The flame inside the enclosure has to be quenched and the jet of hot combustion gases that penetrates through the narrow gap have to lose its energy and temperature so it is does not ignite an external explosive atmosphere. A thermal explosion

theory formulated by (Frank-Kamenetskii 1955) stated that the heat generation by the combustion reaction must exceed the heat loss to the surrounding to cause an ignition.

The function of the flame gap is to assure that the heat loss to the environments is greater than the heat generated from the combustion process and consequently prevent a re-ignition. The heat loss from the hot jet is caused by cooling inside the flame gap and mixing with cold unburned gas in the external atmosphere, this is described in more detail in section 2.3.8 and 2.4.1.

The thermal explosion theory by Frank-Kamenetskiican is used to explain the basic mechanisms of the heat exchange that arise when a hot jet of combustion gases penetrates into a "cold" explosive atmosphere (see Figure 2-9). Thus determine if the hot jet will cause an ignition in the explosive atmosphere or not. The theory is based on the ratio between heat production ($\dot{Q}_G$) in a fixed volume (V_c), due to chemical reactions and the heat loss ($\dot{Q}_L$) to the surrounding environment by conduction. This ratio is described by the temperature-time development from (Beyer 1996) by the equation :

$$\frac{dT}{dt} = \dot{Q}_G - \dot{Q}_L \qquad \textbf{(2.1)}$$

The behaviour of the heat loss ($\dot{Q}_L$) and heat production ($\dot{Q}_G$) with the temperature (T) is described below and illustrated in Figure 2-10.

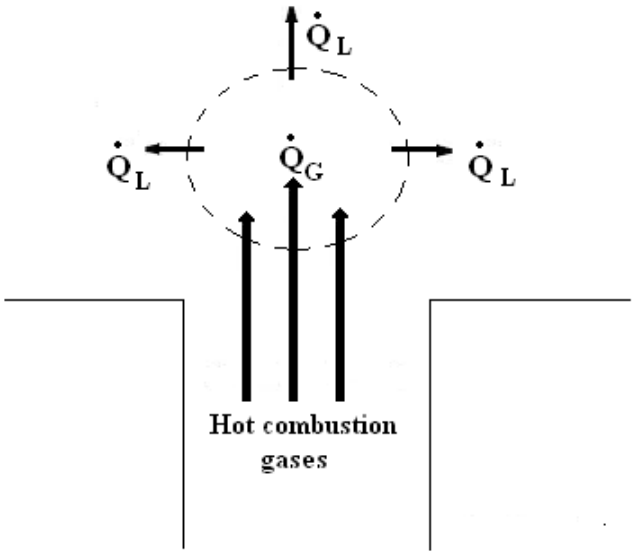

Figure 2-9 : *A fixed volume (V_c) in the external chamber, where it occurs heat generation ($\dot{Q}_G$) due to chemical reactions and heat loss ($\dot{Q}_L$) due to conduction.*

Consider a small "fixed volume" in an external chamber that is occupied by explosive gas. When the hot combustion gases penetrate through the flame gap and into the external

chamber the small volume will be heated. Assume that the volume does not expand during the heating, and that the temperature is uniform inside the small volume. Then the curved line in Figure 2-10 represents heat generation $\dot{Q}_G$. The hot combustion gases are the heating source that leads to an exponential raise in the heat generation inside the small volume due to chemical reactions. The straight line in Figure 2-10 represents the heat loss $\dot{Q}_L$ from the volume. The rate of heat loss increases linearly with the increase in temperature difference between the fixed volume and the surrounding explosive gas. At point 1 in the figure the rate of heat loss will exceed the rate of heat generation and there will be no ignition of the explosive mixture in the fixed volume. To get an ignition inside the volume the temperature must exceed T_2. At this point the rate of heat generation will exceed the rate of heat loss from the fixed volume. As soon as the ignition takes place, one got a self-sustained combustion process in the external volume. But if the external heating of the fixed volume is brought to an end before the rate of heat generation exceeds the rate of heat loss, the temperature in the volume will drop back to the surrounding temperature and there will be no ignition.

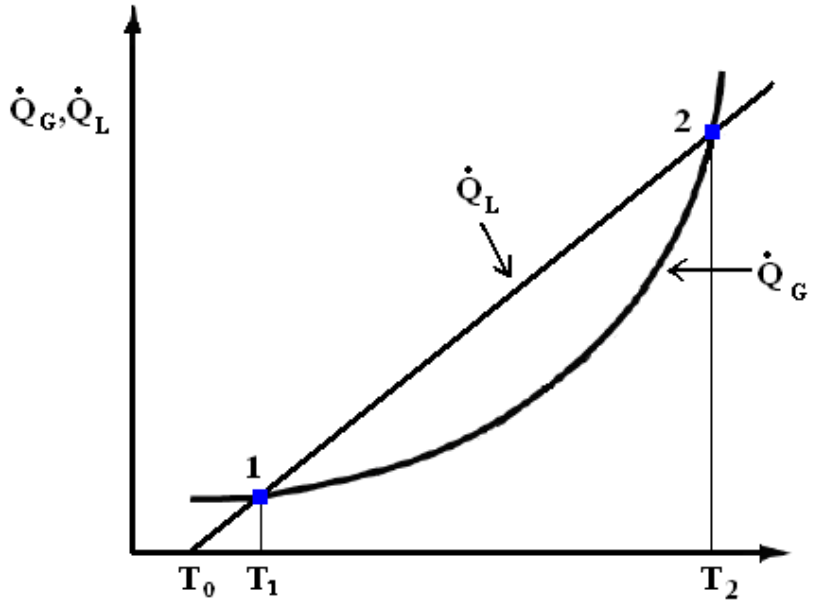

Figure 2-10: *Ignition curve, heat loss by conduction ($\dot{Q}_L$) and heat production ($\dot{Q}_G$) as a function of temperature (T) in the reaction zone. Based on (Beyer 1996)*

The theory presented above is a simplification of the physical phenomenon ignition. There are several assumptions that distinguish this model from the actual phenomenon of ignition. One assumes that the temperature throughout the ignition volume is uniform at any time, which is false because the heating source supply the fixed volume with energy only from one side of the volume. One also assumes that circular volume does not expand during the heating process; this is incorrect, because an increase in the temperature leads to more rapid and greater movement of the atoms, which consequently leads to a larger volume.

2.3.6 Chemical induction time

When an explosive gas mixture is spontaneous exposed for high pressure or high temperatures there is an ignition delay from the moment the explosive gas mixture is exposed to the source

until the mixture possibly ignites, this delay is called induction time. The ignition delay is controlled by the degree of formation of intermediate species (radicals) (see section 2.3.4), that needs a given time to react.

2.3.7 Quenching by a cold wall

Flames extinguish if they enter a sufficiently small passageway, if the passageway is large enough the flame will propagate through it. The smallest tube or gap diameter which a laminar flame can propagate through is defined as the quenching distance. (F.A.Williams 1985) pointed out a rule of thumb due for flame quenching by a cold wall.

- *The rate of liberation of heat by chemical reactions inside the flame must approximately balance the rate of heat loss from the flame by thermal conduction.*

Imagine a flame that has just entered a slit formed by two parallel plates as shown in Figure 2-11.

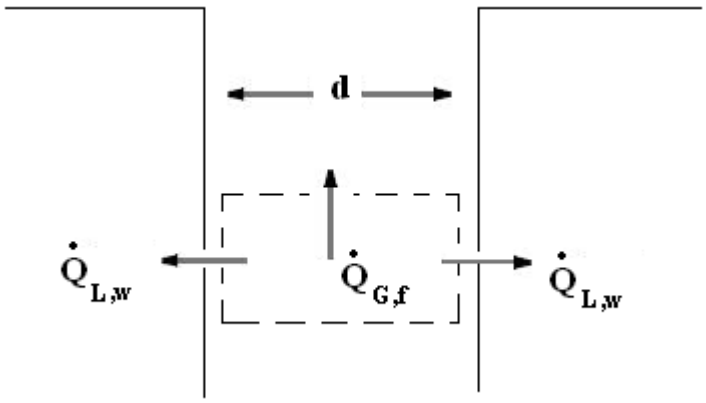

Figure 2-11: *Flame quenching between two parallel walls (based on (Turns 1996))*

We can write an energy balance equation over the system by applying (F.A.Williams 1985) criterion for quenching at a cold wall:

$$\dot{Q}_{G,f} V = \dot{Q}_{L,w} \qquad \textbf{(2.2)}$$

$\dot{Q}_{G,f}$ V = the volumetric heat release rate from the flame

$\dot{Q}_{L,w}$ = the heat loss due to conduction to the walls

From equation (2.2) the heat loss by conduction to the walls is equal to the heat produced by reaction. To successfully propagate a self-sustained flame thorough a tube or gap, the rate of heat production in the flame zone must exceed the rate of heat loss to the wall.

This is a simplified quenching analysis that doesn't take into account the heat loss to the wall due to convection, which is a noticeably parameter in fluid dynamics. In section 2.4.1 a more comprehensive analysis of the heat loss to the wall at turbulent fluid flow is presented. It has

been shown in recent works ((Phillips 1971), (Larsen 1998) and (Grov 2010)) that quenching of a flame in a narrow gap is a complex and versatile phenomenon. Different parameters have to be considered, such as the initial pressure behind the flame, the configuration of the gap and the level of turbulence inside the gap.

2.3.8 Cooling by mixing with cold unburned gas in the secondary chamber

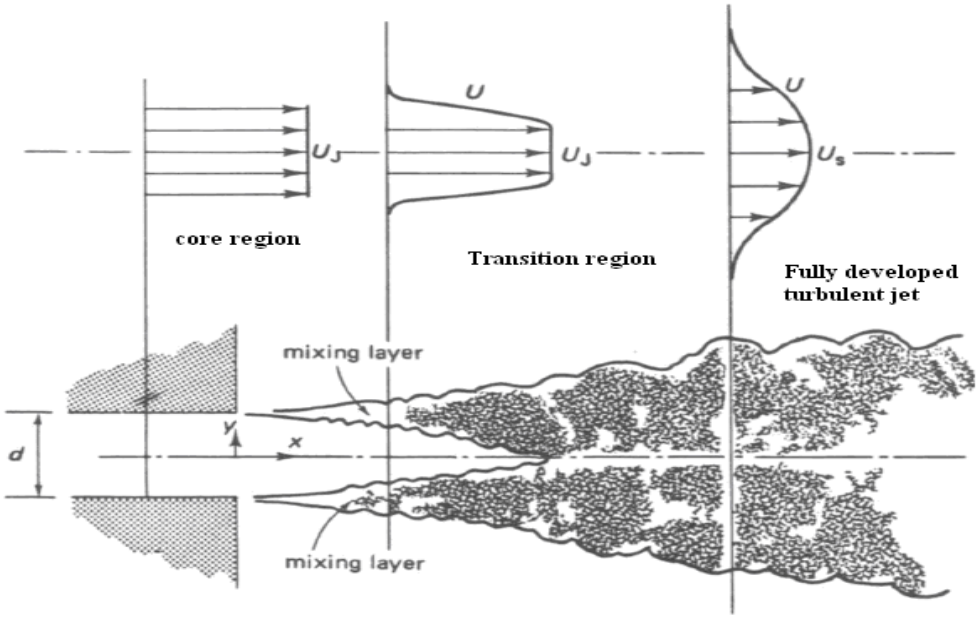

Figure 2-12: *Illustration of a plane turbulent jet. The jet becomes self-preserving some distances after the two mixing layers near the wall exit have merged. From (Tennekes and Lumley 1994)*

Assume an explosion in a flameproof enclosure (see Figure 2-3). Immediately after ignition in the enclosure cold unburned gas will penetrate through the gap opening, subsequent to the cold unburned gas the hot combustion products will reach the gap opening and flow through and form a hot jet in the secondary chamber. The jet becomes turbulent due to the unstable explosion pressure that forces the combustion products through the gap opening at high and fluctuating velocities. The mixing between unburned and burnt gases also contributes to the development of the turbulent jet. The flow field of a turbulent jet can be divided into three different regions. The core region, the transition region and the fully developed turbulent jet region (see Figure 2-12).

The core region is characterized by constant velocity, temperature and concentration in the core of the jet. This region will be "eaten up" by the mixing between unburned and burned gases. The next region is the transition region, in this region the flow will develop to a fully turbulent jet. This means that the efficiency of the cooling increases through the transition region, because the interference between the hot combustion gas and the cold unburned gas increases through the region. The flowing gas is finally turned into a fully developed turbulent jet, where the cooling of the hot combustion gases is at its maximum, because the interaction between cold and warm gases is at a maximum.

In one of the three regions the jet of hot combustion products may achieve conditions favourable for re-ignition. In the core region the velocity on the jet is extremely high, and it expands so rapidly that the time of contact between the cold gas and the hot gas is too short and may be insufficient for igniting the explosive gas mixture in the secondary chamber. As the jet moves into the transition region the velocity on the jet decreases but the mixing rate between cold and hot gas increases. The determining factor for ignition in the transition region and the fully developed turbulent region is the balance between heat generation and heat loss. As soon as the heat generation exceeds the heat loss, the velocity of the hot jet is sufficient and the concentration of the mixture is explosive, the mixture will ignite. In the transition region and the fully developed turbulence region the jet may also be so deformed and the energy so dissipated that the jet is no longer capable to ignite the mixture in the secondary chamber.

2.3.9 Effect of wall roughness on fluid flow

When a flow of hot combustion gases penetrates through a channel the velocity at the interface between fluid and solid material is zero. This is caused by friction at the solid wall. The fluid volume close to the wall is called the viscous sub layer (see Figure 2-16), this sub layer has not a definite thickness and may contain eddies, caused by the turbulent fluid moving into this region. The thickness of the viscous sub layer is difficult to define, it has no sharp upper boundary and it occupies only a very small part of the total cross section of the pipe. At the centerline the velocity gradient is zero for both turbulent and laminar flow.

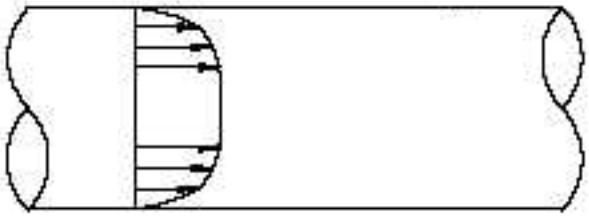

Figure 2-13: *Velocity profile of flow in a pipe. The fluid velocity is nearly zero close to the wall.*

A rough surface leads to higher friction. Friction increases the formation of eddies in the flow. In fluid flow calculations the friction is quantified as a dimensionless number called the friction factor, *f*. If a rough surface is smoothed, the friction factor is reduced. W. Moody (1944) designed a friction factor chart for circular pipes (see Figure 2-14).

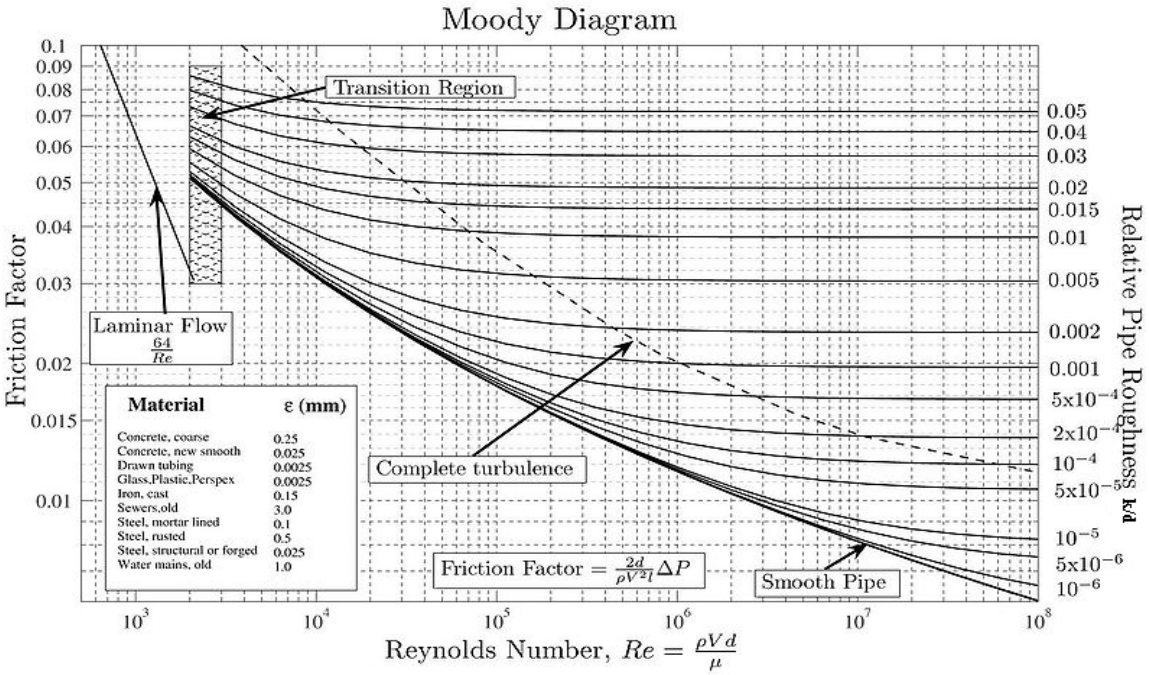

Figure 2-14: *Friction factor chart for circular pipes (L.W. Moody, friction factor for pipe flow, 1944 (McCabe, Harriott et al. 2005)).*

Figure 2-15 shows an idealized picture of roughness. The height of a groove is denoted by *k* and is called the roughness parameter. The diameter of the pipe is denoted as *D* and extends from the bottom of the grooves. The ratio between *k* and *D* is the relative roughness, ξ. In the moody diagram the friction factor is a function of the Reynolds number and the relative roughness, *k/D.*

$$\frac{k}{D} = \xi \qquad \textbf{(2.3)}$$

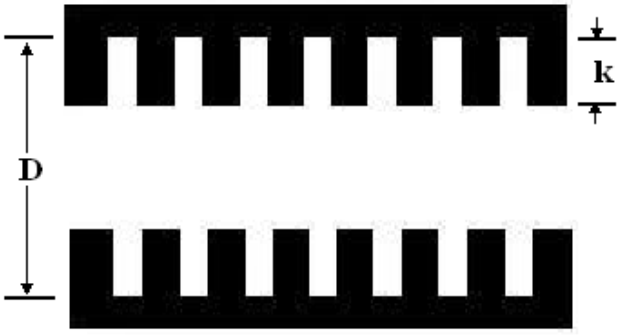

Figure 2-15: *Idealized picture of roughness.*

The Reynolds number is a dimensionless number that gives a measure of the ratio between the viscous forces and the inertial forces. A fully turbulent flow applies when the Reynolds number exceeds 4000. The Reynolds number for a flow in a circular pipe is expressed by:

$$\mathrm{Re} = \frac{\rho v D}{\mu} \qquad \textbf{(2.4)}$$

ρ = density of the fluid

v = velocity of the fluid

D= diameter of the pipe

μ = viscosity of the fluid

The pressure loss over the pipe can be calculated from the Darcys-Weisbach equation:

$$\Delta p = f \frac{L}{D} \frac{\rho V^2}{2} \qquad \textbf{(2.5)}$$

Where the pressure loss due to friction is a function of the ratio of the length to diameter of the pipe, L/D, the density of the fluid, ρ, the mean velocity of the flow, V, and the dimensionless coefficient of laminar or turbulent flow, f.

It can be seen from equation (2.5) that the pressure loss is strongly dependent on the friction factor. This implies that the pressure inside a vessel with venting through a narrow gap is strongly coupled to the friction factor in the narrow gap.

These equations are intended for circular pipes, for fluid flow through non-circular pipe one have to use an equivalent diameter:

$$D_e = 4 \frac{S}{Lp} \qquad \textbf{(2.6)}$$

Where S is the pipes cross sectional area and Lp is that part of the perimeter that is in contact with the fluid.

2.4 Literature review of previous work in relation to turbulent fluid flow through tubes

2.4.1 The roughness effects on friction and heat transfer in turbulent flow.

As it is stated in section 2.3.9 the friction factor in a tube flow is a function of the relative roughness and the Reynolds number. It is also stated by (Kanury 1975) that a viscous sub-layer occurs near the wall in laminar flow and plays an important role in the heat transport process occurring in this area (see Figure 2-16). Destruction of this sub-layer leads to a dramatic change in the conditions of the heat transfer from the fluid to the wall. As the roughness of the wall increases, the convective heat transfer also increases because of both higher turbulence in the flowing fluid and the increase in the fluid-wall contact area. The roughness also leads to greater friction loss through the channel.

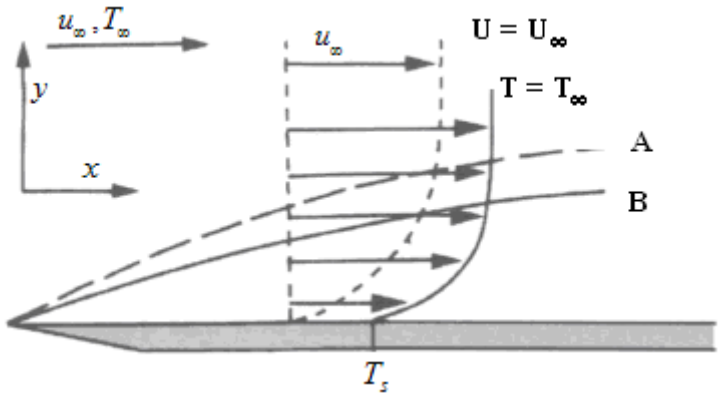

Figure 2-16: *Hydrodynamic (A) and thermal (B) boundary layers on a flat plate under laminar flow. T_s represents the wall surface temperature, T_∞ is the fluid temperature and U is the velocity of the fluid which varies from U = 0 at the wall and U = U_∞ at the outer boundary of the layer. Based on (Kanury 1975).*

The following theory is based on (Ceylan and Kelbaliyev 2003) work: "The roughness effects on friction and heat transfer in the fully developed turbulent flow in pipes". This is an investigation of the effect of roughness on the friction factor and the convective heat transfer in turbulent flow. Ceylan and Kelbaliyev propose a correlation for the friction factor that is applicable in the region of transition to fully developed turbulent flow. They also investigated the effectiveness parameter for the heat transfer as a function of the pipe roughness, the Reynolds number and the Prandtl number.

Friction factor in turbulent flow

As the Reynolds number increase above the transition region (see Figure 2-14), the friction factor at first follow the smooth pipe curve, and it is apparently a function of Re number only. When the Reynolds number further increase, the thickness of the viscous sub-layer decreases, then the roughness of the wall bump through this layer and the friction factor becomes a function of the relative roughness, ξ (ξ =k/D) and the Reynolds number. When the flow turns fully turbulent at high Reynolds numbers the roughness elements perforate through the viscous sub-layer and the friction factor depends only on the relative roughness, ξ.

If the surface roughness is greater than the thickness of the viscous sub-layer, (ψ) then the turbulence in the boundary layer becomes dominant. The thickness of the boundary layer can be estimated as:

$$(\psi/D) = 5Re^{-1/2} \qquad \textbf{(2.7)}$$

It can therefore be stated that the effect of pipe roughness on the friction is of importance when the relative roughness is greater than the thickness of the boundary layer, $\xi > 5Re^{-1/2}$. Then the complete rough zone in Figure 2-14 is valid for the fluid flow.

Ceylan and Kelbaliyev proposed that the flow is fully rough turbulent and the friction factor is independent of the Reynolds number if the relative roughness is, $\xi \geq 2000 / Re$. Otherwise the friction factor depends on both Re and the relative roughness ξ.

As a result of this they proposed a simple equation for the estimation of the friction factor for fully developed turbulent flow in range of $10^4 \leq Re \leq 6\times10^8$ for relative roughness, $\xi \geq 2000/Re$:

$$f = 0.22\xi^{3/8} \qquad \textbf{(2.8)}$$

Heat transfer in turbulent flow

The quenching theory presented in section 2.3.7 only takes into account the heat loss due to conduction to the walls. When a hot gas flows in a tube with lower temperature, a temperature gradient is established, and there will also be heat transfer due to convection. The rate of heat transfer due to convection increases with increased movement in the fluid. The case where you only get heat transfer due to conduction is when the bulk of the fluid is completely at rest. The Nusselt number is the ratio of convective to conductive heat transfer normal to the boundary layer. A large Nusselt number suggests that the heat transfer is mainly due to convection.

Newton`s law of cooling states that the convective flux is usually proportional to the difference between the wall temperature and the temperature of the fluid:

$$\frac{q}{A} = h(T_s - T_f) \qquad \textbf{(2.9)}$$

h = heat transfer coefficient

T_s = Surface temperature

T_f = bulk temperature of the fluid

The heat transfer coefficient, h for the thermal convection is not an intrinsic quality in the fluid, as it is for thermal conduction. It is strongly influenced by the flow pattern in the fluid which is determined by the fluid mechanics, the thermal properties of the fluid and the surface configuration of the gap. There will be heat transfer from the fluid to the wall if $T_s < T_f$.

As the roughness of the wall surface increases, the heat transfer between fluid and wall increases. The heat transfer coefficient may increase up to 350 % if a smooth pipe wall is roughened (Mottahed and Molki 1996). As the roughness increases the resistance in the gap increases, this means that the energy needed to push the fluid through the tube also increases. The heat transfer efficiency, η, may be defined as the ratio between the heat transfer enhancement and the increase in the drag of the fluid, from a smooth to a rough tube. The heat effectiveness is therefore defined in terms of the Nusselt number, Nu, and the friction factor for tube configuration, *f*:

$$\eta = \frac{Nu / Nu_0}{f / f_0} \qquad \textbf{(2.10)}$$

Where f_0 and Nu_0 are friction factor and Nusselt number for tubes with a smooth wall and *Nu* and *f* are friction factor and Nusselt number for the tube with rough wall.

The Nusselt number for rough pipes is defined by Ceylan and Kelbaliyev (2003) as:

$$Nu = 1.15\, Nu_0\, Pr^{1/7}\, (1\text{-}0{,}106\, K_+^{1/4})\, \frac{f}{f_0} \qquad \textbf{(2.11)}$$

Where *Pr* is the Prandtl number, which is a dimensionless number for the ratio of momentum diffusivity. K_+ is a dimensionless roughness parameter that increases with increasing roughness and increasing Reynolds number. K_+ is given by the equation:

$$K_+ = \xi\, \mathrm{Re}(\frac{f}{8})^{1/2} \qquad \textbf{(2.12)}$$

From these equations Ceylan and Kelbaliyev have shown that the convective heat transfer from a hot fluid to a cold wall is strongly influenced by the surface roughness. A very rough surface can cause turbulence that break through the boundary layer at the wall surface, and the contact area between the wall and fluid increases sharply, consequently the heat transfer increases.

2.5 Literature review of previous work in relation to explosions transmission through narrow gaps

As early as 1906 an investigation of the passage of a flame through an narrow hole was carried out by (Beyling 1906). He discovered that if the hole was sufficiently small an explosion of a methane-air mixture inside a enclosure was not transmitted to the surrounding combustible mixture. This laid the foundation for the further investigation of flameproof enclosures by several scientists. In this chapter relevant literature related to flameproof enclosures is introduced.

2.5.1 Investigation of explosion transmission through narrow gaps by H. Phillips

In the following section a small part of the enormous work Harry Phillips performed is presented. He investigated different aspects of the physical mechanisms of flameproof enclosures. He united a great amount of experimental work to a set of equations.

To get a better understanding of the physically mechanisms of the re-ignition process, Phillips recorded the hot jet of combustion products that penetrates through an orifice with a Schlieren system. Phillips stated that the cone angle of the hot jet was constant. When the ignition source was placed further away from the orifice a jet of cold unburned gas established first at the outside of the orifice. When the hot jet was ejected thorough the orifice it establish a jet along the axis of the cold jet, but this hot jet soon spread sideways and formed a jet with the same cone angle as previously. From the Schlieren recordings Phillips also found that the ignition occurred at the head of a spherical vortex that arises a distance from the orifice opening (see Figure 2-17).

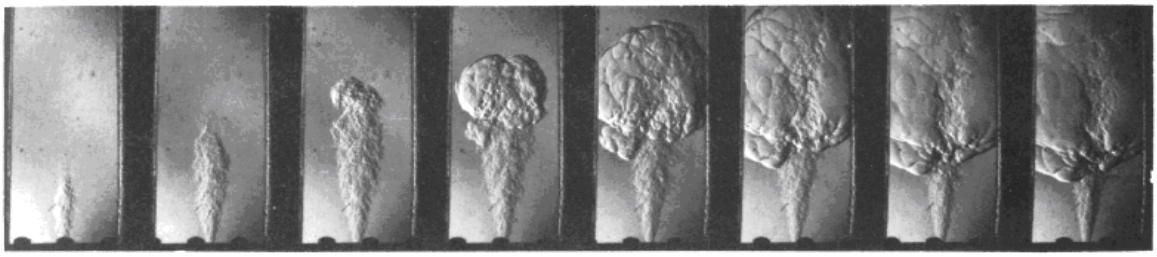

Figure 2-17: *Schlieren photographs of 50 per cent probability for re-ignition. From (Phillips 1971).*

From Figure 2-17 it can be seen that the ignition of the external mixture appears as a flame ball at the head of the penetrating jet. Phillips stated the typically distance from the orifice opening to the point of ignition was 5 to 80 millimeters.

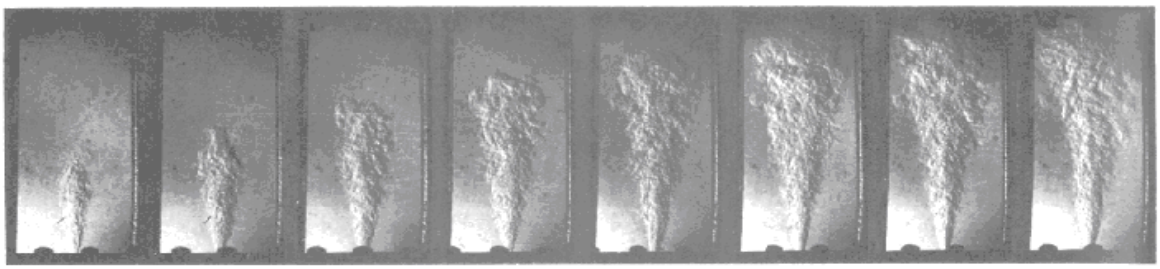

Figure 2-18: *Schlieren photographs of non-ignition. From (Phillips 1971)*

To assess whether or not the hot jet of combustion products lead to an ignition of the external mixture, Phillips developed a numerical analysis of the temperature at the head of the jet as it propagates away from the orifice opening. He stated that a temperature fall at the vortex head due to mixing with "cold" unburned gas and rapid expansion would lead to no ignition, while a temperature increase above the ignition temperature of the surrounding gas mixture will lead to a re-ignition of the external mixture.

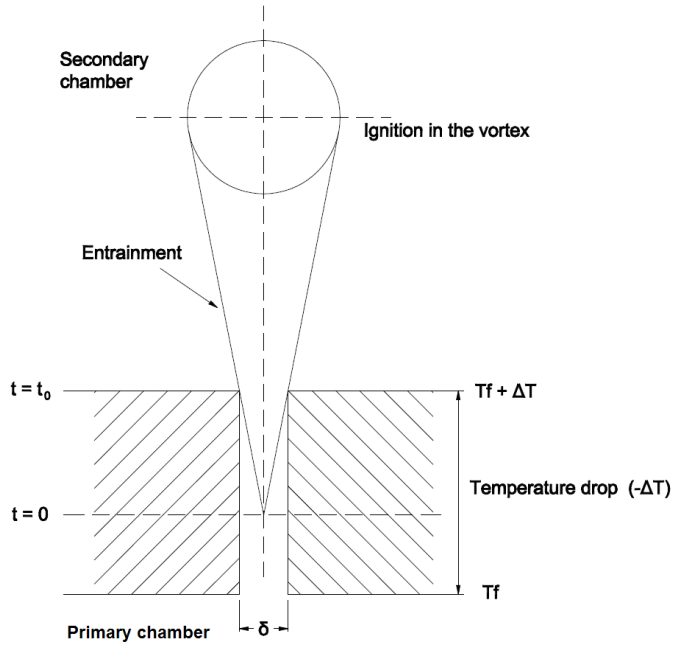

Figure 2-19 : *Two-dimensional model of the hot penetrating jet that causes an ignition a distance away from the gap opening inside a vortex. (Phillips 1971)*

The overall conclusion of Phillips was that the rate of heat generated from the combustion process must exceed the heat loss due to entrainment and mixing with cold gas to obtain a re-ignition above the orifice. The rate of the combustion process depends on the jet temperature and the fuel- oxygen concentration. A short excerpt from the combustion analysis of calculating the dimensions of safe gaps (MESG) by (Phillips 1971) is shown below.

An energy balance over a small volume of the vortex leads to an equation for the rate of combustion, ω:

$$\omega = \frac{1}{\eta_c} \cdot \frac{d\eta}{dt} + \frac{1}{m} \cdot \frac{dm}{dt} \qquad \textbf{(2.13)}$$

Where:

m = the mass of gas in the vortex

η_c = combustion efficiency

The function: $\frac{1}{m} \cdot \frac{dm}{dt} = \frac{z}{t}$ is the rate of entrainment into the jet.

The factor z is an experimental determined entrainment factor for jets. If the velocity of the jet increases with time the jet has a high value of z. Phillips assumed that the jet had constant velocity and used the value, z =1/3.

The combustion efficiency can be calculated from the equation:

$$\eta_c = \frac{T - T_u}{T_m - T_u} \qquad \textbf{(2.14)}$$

T = jet temperature

T_u = ambient temperature

T_m = maximum flame temperature

For low values of T (jet temperature) the heating is never rapid enough to exceed the cooling process. This leads to a temperature drop towards the ambient temperature, and the external mixture will not ignite. This is in accordance to the curve "no combustion" located at the bottom in Figure 2-20. The three lines that are located highest in the graph represents successful ignition of the external mixture. For these curves the initial jet temperature (T) is high. They first fall, but as soon as the heat generating from combustion exceeds the rate of cooling by entrainment, the combustion efficiency increases and the temperature rises, subsequently the gas mixture ignites.

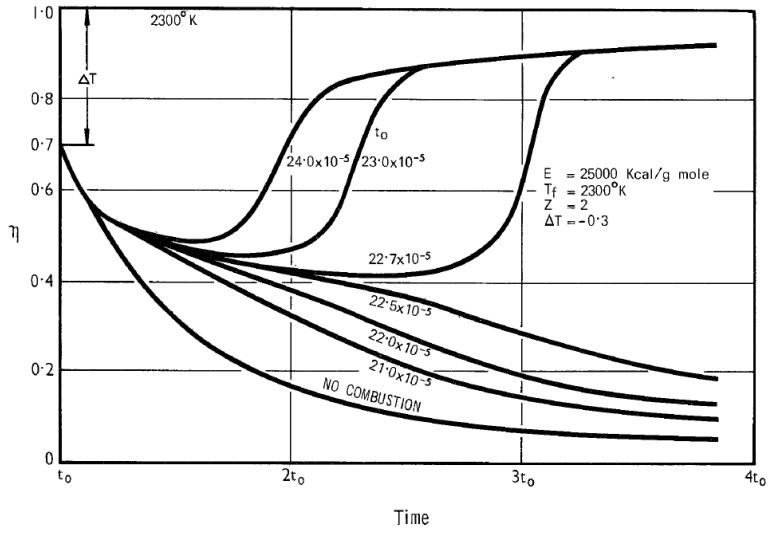

Figure 2-20 : *Analogue computer curves of vortex temperature. η is a non-dimensional temperature (combustion efficiency) and t_0 denotes the starting time in seconds from a point source until the vortex fills the orifice. (Phillips 1971).*

The effect of initial pressure

Phillips showed through his calculations that the pressure in the explosion chamber has a great impact on the maximum explosion safe gap. He compared his calculation of the effect of pressure on the MESG value with (Grobleben 1967) experimental curves. The calculated points by Phillips were in good correlation to the experimental data of Grobleben's, as shown in Figure 2-21. It can be seen that an increase in pressure reduces the safe gap (MESG). In

1987 Phillips found that there was a critical ignition point, where the external ignition is most likely to occur. At this point the pressure was low, and consequently the velocity of the penetrating combustion gases was low. Due to the low velocity he based his equations on heat transfer calculations for laminar flow.

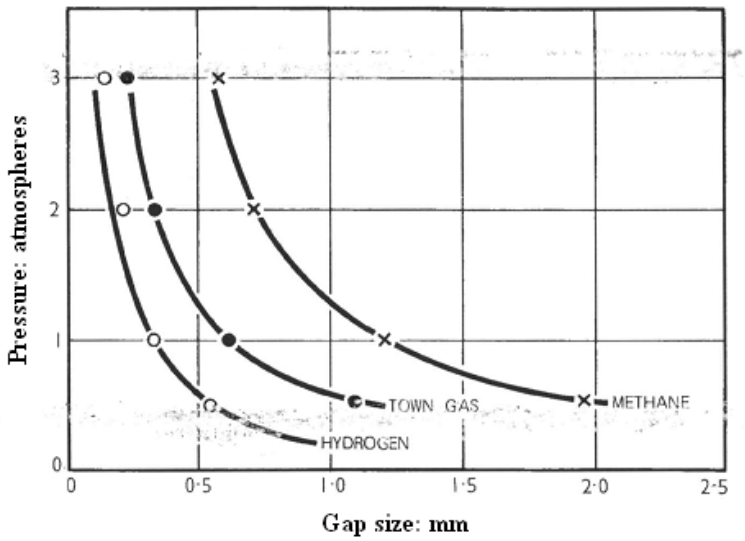

Figure 2-21: *The effect of pressure on the safe gap (MESG). Calculated points compared with (Grobleben 1967) experimental curves. From (Phillips 1971).*

From the curve in Figure 2-22 it can be seen that the safe gap (MESG) varies with the pressure. This is a curve based on calculations by (Phillips 1988). At low pressures, an increase in the pressure leads to a reduction in the safe gap. The pressure falls to a minimum of approximately 1.5 bars. Due to the low pressure in the chamber the velocity of the jet is relatively low and consequently the cooling by entrainment and mixing with the cold unburned gas is low. This leads to the critical point where the safe gap is smallest. When the pressure is further increased the safe gap also increases due to the increase in the rate of cooling which exceeds the heat generating by the combustion process. At a pressure of approximately 2.5 bar the safe gap reaches its maximum. Any further increase in pressure leads to a decrease in the safe gap. At the break point the safe gap is at its minimum, this is because the pressure reached at this point can't be exceeded by the test apparatuses used in the experimental work of Phillips.

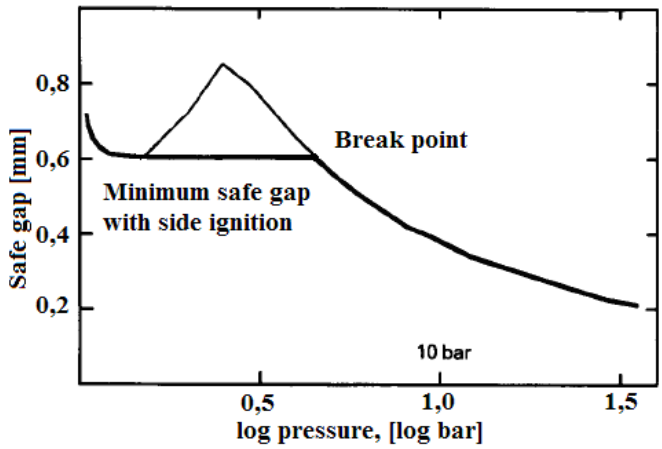

Figure 2-22: *The 's' curve showing a minimum in safe gap at 1.5 bar and a break point at 4.6 bar. From (Phillips 1988).*

2.5.2 The effect of turbulence on minimum ignition energy (MIE) and quenching distance

The theory in this section is based on the work that (Ballal and Lefebvre 1975) presented in the article "*The influence of flow parameters on minimum ignition energy"*. They performed several experiments were they examined the effect of turbulence on the minimum ignition energy and quenching distance.

The overall conclusion from Ballal and Lefebvre`s work was that an increase in turbulence raises the minimum ignition energy and leads to an increase of the quenching distance. They explain that turbulence give raise to a lacerating flame, which leads to an increase of the flame front surface. When the surface of the flame increases the heat loss to the surrounding environment increases. This is due to increased contact area between the hot fluid and the cold wall or cold gas. The heat transport between the hot and cold gas occurs through molecular diffusion. The consequence of the increased heat transfer is that the minimum ignition energy increases and the quenching distance increases, as shown in Figure 2-23.

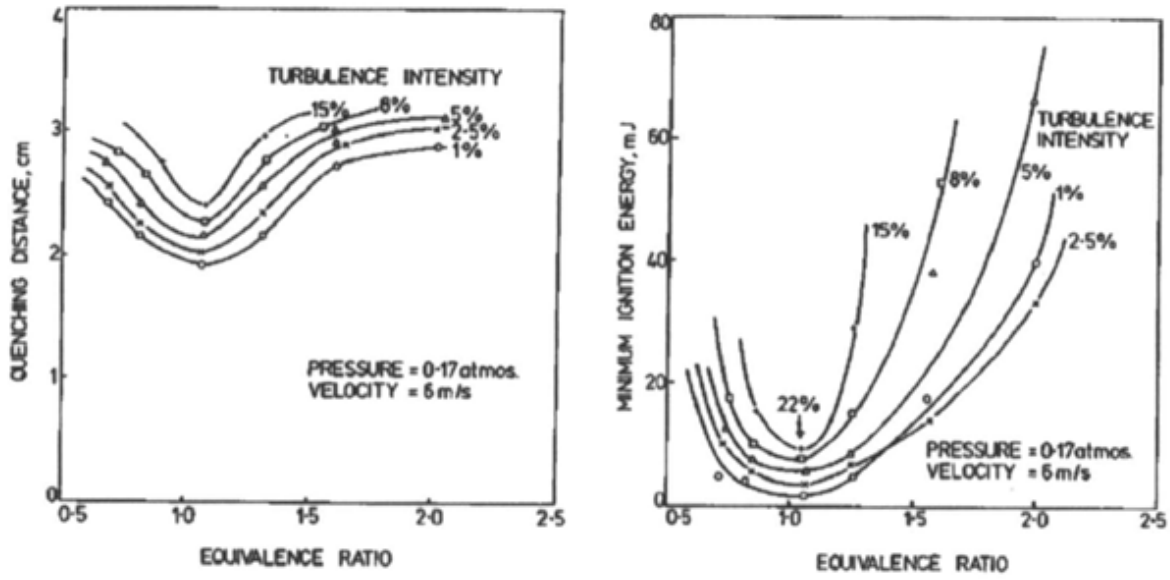

Figure 2-23: *Effect of turbulence intensity on quenching distance and minimum ignition energy at different equivalence ratios (Ballal and Lefebvre 1975).*

From the two graphs in Figure 2-23 it is shown several curves for different turbulence intensities. It can be seen that the curve with the greatest turbulence intensity is represented with the highest value for quenching distance and MIE at all equivalence ratios.

The experiments performed in the present work are carried out with an equivalent ratio of 1.0. It is presumed that the results presented by Ballal and Lefebvre are valid for the experiments carried out in this master thesis. This includes the influence turbulence intensity will have upon different parameters, such as quenching distance and MIE.

2.5.3 A Study of Critical Dimensions of Holes for Transmission of Gas Explosions and Development & Testing of a Schlieren System for Studying Jets of Hot Combustion Products (Larsen 1998)

(Larsen 1998) focused his master thesis on critical dimensions of holes for transmission of a gas explosion from a primary chamber to a secondary chamber. He proved that the probability for ignition of an explosive atmosphere in an external chamber depends on diameter of the perforated hole, the point of ignition inside the enclosure, the gas concentration and the enclosure volume.

Larsen constructed an apparatus (see Figure 3-2) which he used in his study of transmission of a gas explosion from a primary to a secondary chamber. With this apparatus Larsen had the opportunity to vary the channel hole diameter and the ignition distance to the flame path. Larsen showed that the explosion pressure increased by moving the ignition source away from hole inlet (see Figure 2-25). Further he explained that as the pressure increases, the flow through the hole increases and thus the cooling to the channel wall is reduced. This effect leads to the most "dangerous ignition position", where the probability for ignition in the secondary chamber is at its maximum (see Figure 2-24). He determined that the most dangerous ignition position is a function of both the enclosures volume and the ignition distance to the flame path.

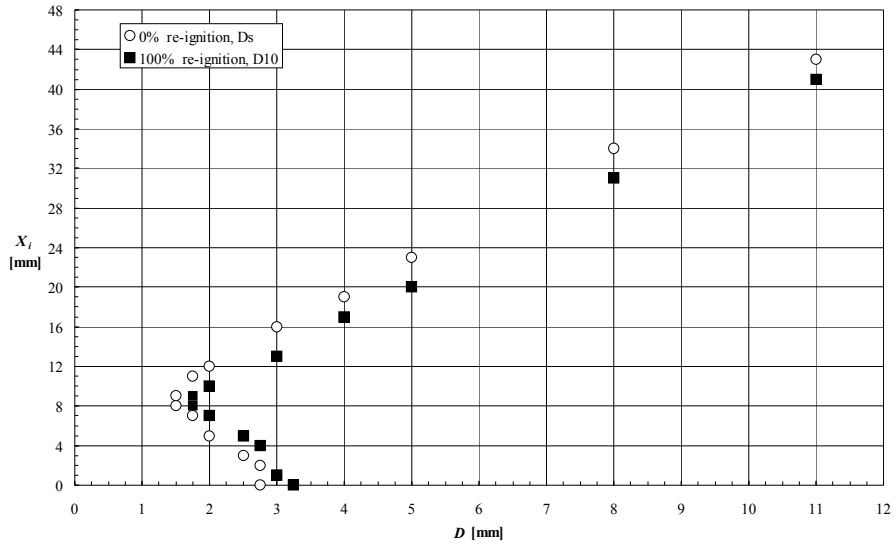

Figure 2-24: *Safe diameter D_s and D_{10} for various ignition-distances X_i. Primary volume V = 1 l and 4.2 vol. % propane-air. From (Larsen 1998).*

Larsen introduced a new denotation, MESD (Maximum Safe Gap Diameter,) for the widest limiting hole-diameter that can prevent a transmission of an explosion at the most dangerous ignition position.

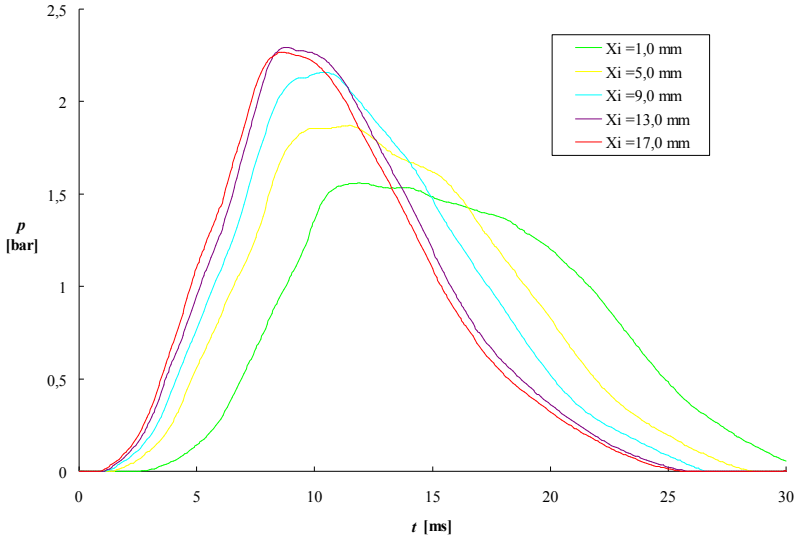

Figure 2-25: *Explosion pressure as a function of time for various ignition distances. Hole diameter D = 2.0 mm, primary volume V = 21 ml and 4.2 vol. % propane-air concentrations. From (Larsen 1998).*

He also found the fuel-air composition that gave the smallest safe gap. He called this the most dangerous concentration. Starting with a lean and a rich concentration he proceeded towards stoichiometric mixture concentration. He found that the region of stoichiometric mixture gave the smallest safe gap. The fuel-air composition used in the present work is therefore of stoichiometric concentration.

Larsen also studied the re-ignition process through Schlieren recordings. He found that the point of external ignition varied between 2 mm and 30 mm from the hole outlet. Larsen confirmed that all of the jets had a given angle (20^{o}- 25^{o} from the jet axis) when they penetrated out from the hole outlet.

2.5.4 Experimental investigation of the influence of mechanical and corrosion damage of gap surfaces on the efficiency of flame gaps in flameproof apparatus (Opsvik 2010)

(Opsvik 2010) performed an experimental investigation of the critical dimensions, and the effect of damages on flame gaps on flameproof Ex"d" equipment. He determined MESG values for three different flange structures, both sand blasted, undamaged and rusted (see Figure 2-26). He found that even with severe damages on the flame path surface the MESG value did not fall to an unacceptable level according to the limiting values in IEC (2007a).
This statement was supported by the observation, which showed that rusted flanges, with roughness greater than the undamaged flange and a noticeable higher roughness than the IEC requirement of 6.3 µm, gave a larger MESG value than the undamaged flange.

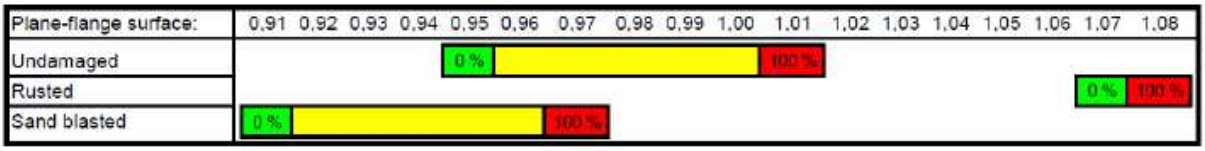

Figure 2-26: *Explosion experiments with variation of circular flange openings. No re-ignition is indicated with green colour, while 100 % re-ignition is red. The transition range is the yellow bar. From (Opsvik 2010).*

Most of Opsvik's experimental work was performed in a self-constructed apparatus (PCFA) with the cylindrical flange arrangement made as realistic as possible (see Figure 2-27 and described in section 3.6). The main reason for building this apparatus was to get great flexibility to change between flanges with different surface structures, and to produce experimental results from an apparatus that fulfill adequate requirements from IEC.

The rusted cylindrical flanges that Opsvik conducted several experiments with (see Figure 2-28) were placed in the sea side separately, and screwed together initial to the explosion tests. From Figure 2-26 it can be seen that these rusted flanges increased the MESG from 0.95 mm to 1.07 mm.

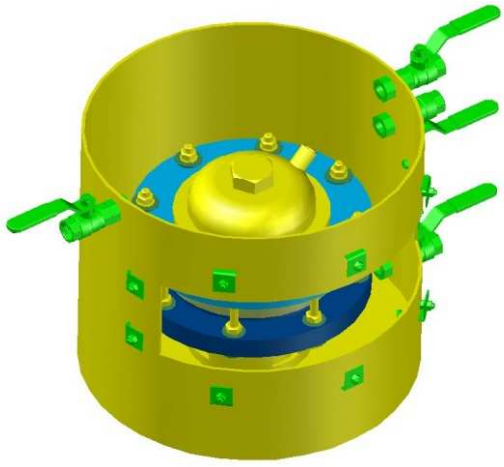

Figure 2-27: *"Opsvik bomb" The primary and secondary chamber assembled. From (Opsvik 2010)*

Figure 2-28: *Picture of the plane rusted flange mounted on the flange adapter. From (Opsvik 2010)*

2.5.5 An Experimental Study of the Influence of Major Damage of Flame Gap Surfaces in Flameproof Apparatus on the Ability of the Gaps to Prevent Gas Explosion Transmission (Grov 2010)

(Grov 2010) continued the experimental study (Opsvik 2010) started a year earlier. Grov focused his master thesis on the influence of major damages on flame gap surfaces. He investigated different types of flame surfaces, such as rusted, sandblasted and fabricated configurations to tell something about how different types of flame gap damages affect the Maximum Experimental Safe Gap (MESG).

Grov did experiments in the apparatus that Opsvik built (PCFA) and the Plane Rectangular Slit Apparatus (PRSA) (see Figure 3-2 in section 3.4). He observed that the experiments performed in the two apparatuses with similar gap surface structures were in good correlation, despite the large differences between the apparatuses themselves. Thus the greater parts of Grov's experimental work were carried out in the PRSA, which demanded less time per experiment than the PCFA due to a simpler flame gap system, consisting of slits (Figure 2-31) instead of flanges (Figure 2-28) and since a smaller volume had to be filled of gas.

Grov stated that the most favorable ignition position for a re-ignition in the secondary chamber for an undamaged slit was at a distance 14 mm from the gap opening (see Figure 2-29). He also found through this investigation that the MESG value for an undamaged slit was 0.98 mm in the PRSA.

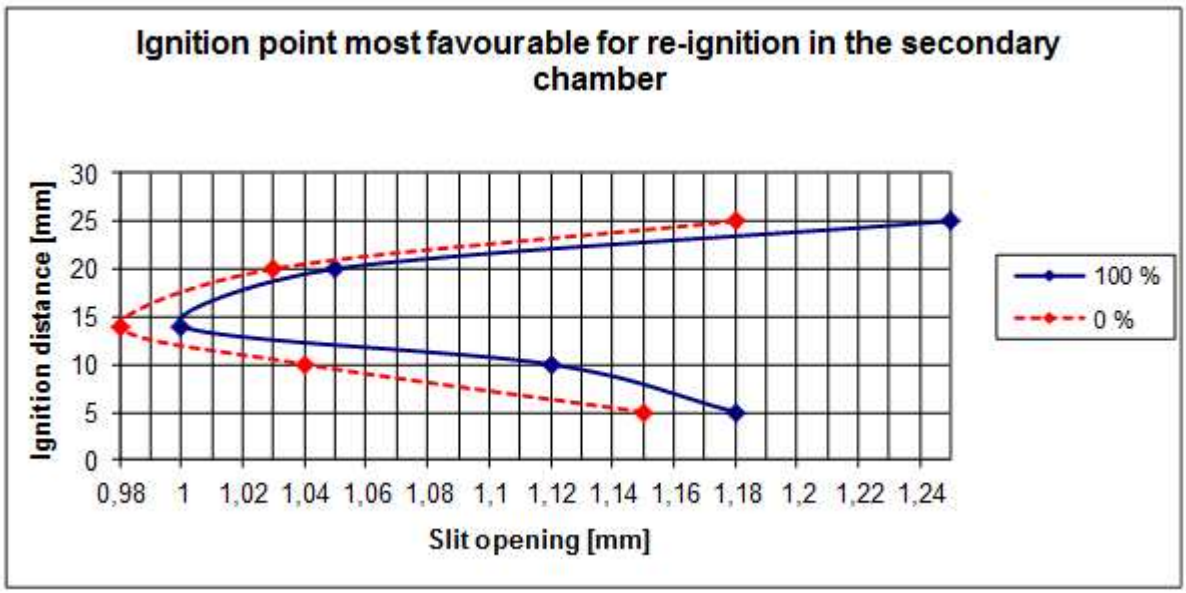

Figure 2-29: *Determination of the most favourable ignition position for re-ignition in the secondary chamber in the Plane Rectangular Slit Apparatus with 4.2vol. % in air. This curve is valid for an undamaged slit. The solid line is the gap opening giving re-ignition for ten experiments for the given ignition position, the dotted line is the gap opening giving no re-ignition for ten experiments for the given ignition position (MESG for an undamaged slit is 0.98 mm). From (Grov 2010).*

Grov's investigation of rusted flame gap surfaces

Grov continued the work with rusted gap surfaces as a result of the surprising observations made by Opsvik, where Opsvik proved noticeable improvements of the gap efficiency. Grov tested two rusted gap surfaces in the PRSA. These slits were placed in the sea for rusting separately, and on a later stage attached to each other with a given torque before the explosion test. Grov got a reduction of the MESG value of approximately 15 %. He observed that the first explosion did not give a re-ignition in the secondary chamber with a gap opening at 0.98 mm. He explains that this is a consequence of the most porous rust formation was blown of the slit surface during the first explosion. Grov assumed that the reduction and the great variance in the MESG values he found compared with those values Opsvik found, are a result of compression of porous iron oxide. He explained that the torque used in Opsvik's work on the Plane Circular Flange Apparatus (PCFA) was higher than the torque used in the Plane Rectangular Slit Apparatus (PRSA), leading to the actually distance between the flanges in the PCFA is smaller than the value reported.

Grovs's investigation of fabricated damages on the flame gap surface

Grov did several experiments with fabricated grooves on the flame gap surface. He distinguished between grooves that go in the same direction as the flow through the flame gap, which he called lengthwise grooves, and grooves that go in the opposite direction of the flow which he called crosswise grooves (see Figure 2-30 and Figure 2-31).

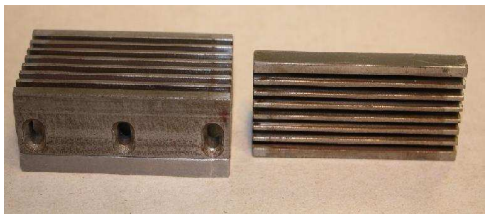

Figure 2-30: *Photograph of a flame gap surface with seven crosswise grooves. From (Grov 2010)*

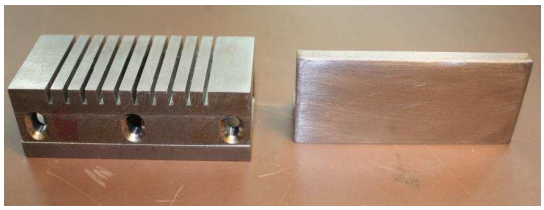

Figure 2-31: *Photograph of a flame gap surface with 10 lengthwise grooves. From (Grov 2010)*

The motivation for making these large fabricated grooves was to see how it would affect the MESG value and the efficiency of the gap. The multiple crosswise slit had seven grooves of 2.0 mm width and 3.0 mm depth. Surprisingly Grov found that the MESG value increased from 0.98 mm for undamaged slits to 1.10 mm for slits with the specific crosswise configuration. This is an improvement of 12.2 %. He also showed that the pressure build up from the surface with crosswise grooves were significantly higher when comparing with same gap opening for the undamaged surfaces. He suggested that the pressure build up interacting with the grooves led to increased turbulence and velocity of the gases that propagates through the gap opening. He explained that the increased turbulence and velocity leads to a more efficient cooling of the hot combustion jet that propagates into the secondary chamber, and therefore creates a flow regime that is less favorable for re-ignition.

The experiments performed with ten lengthwise grooves of width 1 mm and depth 4 mm gave an increase in the MESG value of 14.3 % in the PRSA,but this result did not correlate in the PCFA where he just got a slightly increase in the gap efficiency. Grov stated that the lengthwise grooves had to have a width as large as 3 mm before they started to influence the efficiency of the flame gap in a negative way. The mean pressure measured during the experiments with lengthwise grooves is lower than the mean pressure for an undamaged slit. Grov explained that this was due to the increased venting area obtained by the perforating grooves was added on the slit surface in the lengthwise direction, which is the flow direction (see Figure 2-31).

Grov's investigation of flame gap surface made of Plexiglas

Grov performed experiments with undamaged flame gaps made of Plexiglas. The motivation for this was to see if the MESG values changed if he had a flame surface with different thermal capacity from steel. He discovered that the MESG value for undamaged gap surface of Plexiglas and steel was equal, and assumed therefore that the cooling of the combustion gases to the gap wall is of second order significance.

2.6 Basic corrosion theory

Ex"d" equipment is typical made of a material called carbon steel. The bulk of carbon steel consists of iron [Fe]. Formation of rust on iron is one of the most familiar examples of corrosion. Corrosion is an electrochemical process; this means that chemical reaction take place through the exchange of electrons. This process requires the presence of oxygen, water and an electrolyte. Corrosion does not occur to any significant extend in the absence of any one of these. Therefore industries that operate in an environment where the equipment are exposed to sea water are especially vulnerable for rust.

Solid iron [Fe] will start oxidizing as soon as a droplet of water containing a little dissolved oxygen falls on a steel surface.

$$Fe(s) \rightarrow (aq) + 2e^-$$

The electrons are consumed by the hydrogen ions from water and produce acidic water. Thus the hydrogen ions are consumed by the process. As the iron corrodes, the pH in the droplet rises.

$$2H^+ (aq)\ 2e^- \rightarrow H_2 (g)$$

Hydroxide ions (OH-) arise in the water as the hydrogen ion concentration falls. Hydroxide ions react with iron ions [Fe^{2+}] and produce insoluble iron hydroxides ($Fe(OH)_2$ (s) or rust.

$$Fe^{2+}(aq) + 2OH^- (aq) \rightarrow Fe(OH)_2 (s)$$

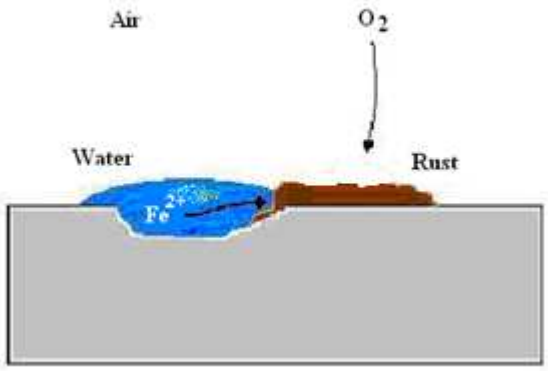

Figure 2-32: *The formation of rust on a surface of steel. Based on (Chang 2006).*

In Figure 2-32 rust formation is illustrated. It can be seen how the corrosion process steals iron ions from the gap surface, and oxygen from the air to form iron oxides (rust). This causes irregular sunken areas on the surface and it causes elevations of rust formation. The solid of the rust is porous, but it does not leave the gap surface immediately. There is an interface between steel and rust, which keep a layer of rust bound to the carbon steel and consequently form undefined elevations on the gap surface. But as the corrosion process steals more iron ions, the interface between rust and steel moves even lower on the carbon steel surface, and the porous rust at a higher altitude peel off. The corrosion process slowly “eats” up the solid carbon steel, as shown in Figure 2-33.

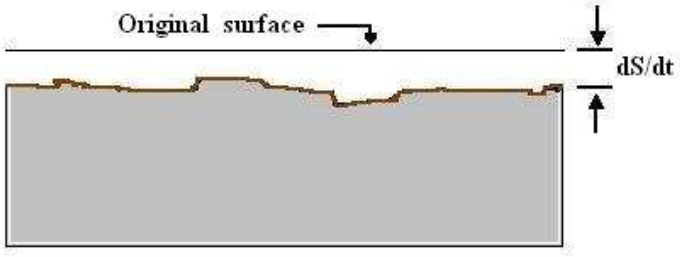

Figure 2-33: *The corrosion process "eats" up the solid carbon steel over time, dS/dt.*

In Figure 2-34 typical corrosion rates for steel are presented at different marine environments. The rate of corrosion depends on the oxygen supply, and will therefore be of the greatest extend in droplet zone, where there will be intermittent thin water layers that supply the corrosion process on the steel surface. The intermittent water may also contribute to wash away the most porous rust, and consequently leads to an increase in corrosion rate. A typically offshore installation is located between the marine atmosphere zone and the droplet zone. Typical corrosion rate in this environment is 0.1 mm -0.15 mm/ year (Bardal 1994).

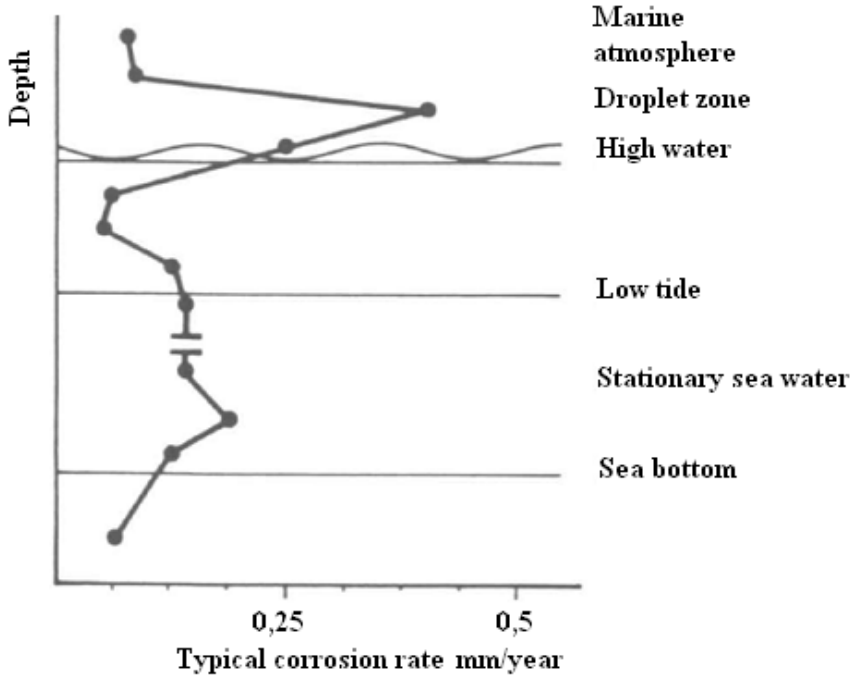

Figure 2-34: *Typically corrosion rates (mm/year) for steel that is placed in different marine environments. Based on (Bardal 1994).*

2.7 Review of relevant dust theory

Ex"d" enclosures are located in “zones” where a gas leakage is a potential hazard. Dust is not considered as a potential source of ignition. But dust is represented in almost any atmosphere. In this thesis there have been performed experiments that can tell if dust can ignite inside the flame gap or inside the main volume of the Ex"d" enclosure and subsequent penetrate into external chamber and cause an ignition. To understand physical mechanisms related to combustion of dust, a review of relevant dust theory is presented in this section.

2.7.1 Combustion of dust (Based on (Eckhoff 2005))

Any solid materials that can burn in air will combust with increased burning rate when the solid material is divided into smaller parts. This is because the total ratio between air and surface of combustible material will increase when you split the solid into smaller parts. When a material is subdivided down to sizes in the order of 0.1 mm the required minimum ignition energy will decrease significantly.

If the particles of a combustible material are small enough they can easily be dispersed and appear as a dust cloud. If the dust cloud is dispersed in a sufficiently large volume of air, so each particle can burn separately, the dust cloud can turn into a dust explosion in the presence of an ignition source. It is therefore important to keep process modules and areas clean from dust. A great number of dust types are combustible, and can generate hazards if they get dispersed and ignited. Various substances generate various levels of heat per mole O_2 consumed (see Table 2-4). This means that one type of dust can be more hazardous and violent than another.

The main materials that can cause dust explosions include:

- Natural organic materials, examples are grain, linen and sugar.
- Metals, examples are aluminium, magnesium, and iron.
- Synthetic organic material, examples are organic pigments and plastic.
- Coal and peat.

Table 2-4: Heats of combustion (oxidation) of different common substances per mole O_2 consumed. (Eckhoff 2005)

Material	Oxidation products	Heat of combustion (kJ/mol O_2)
Calcium	CaO	1270
Magnesium	MgO	1240
Aluminium	Al_2O_2	1100
Silicon	SiO_2	830
Chromium	Cr_2O_2	750
Zinc	ZnO	700
Iron	Fe_2O_3	530
Copper	CuO	300
Sucrose	$CO_2 + H_2O$	470
Starch	$CO_2 + H_2O$	470
Polyethylene	$CO_2 + H_2O$	390
Carbon	CO_2	400
Coal	$CO_2 + H_2O$	400
Sulphur	SO_2	300

2.7.2 Ignition and combustion of single particles

Almost all organic particles contain combustible volatiles which will stream out of the particle during heating. In the presence of an ignition source it is the volatiles and vapour gases that ignites. Because the particle first has to be heated to realise the combustible substances which subsequently ignites, the necessary ignition energy is higher for particles than for gases.

In the ignition process of metal particles an exothermic reaction between the metal atom and the oxygen occurs. In 1962 (Friedman and Macek 1962) stated that the ignition occurred after melting the oxide layer that coats the aluminium particle, this is a controversial and discussed theory. (Ermakov, Razdobreev et al. 1982) measured the temperature of aluminium particles at the moment of ignition, the temperature measured was approximately 2070 K. They also measured the burning temperature of 2170 K subsequently to the ignition. This temperature is lower than the melting point of oxide which is of 2300 K. From this observation (Ermakov, Razdobreev et al. 1982) stated that the ignition of aluminium was not due to the melting of the coating oxide layer, but due to the destruction of the integrity of the layer caused by thermo mechanical stresses arising during the heating process.

2.7.3 Influence of particle size on the minimum ignition energy of a dust cloud. From (Bartknecht 1987).

From Figure 2-35 it can be seen that the minimum ignition energy of a dust cloud is strongly coupled to the size of the particles in the cloud. The vertical scale is logarithmic, so an

increase in particle size of aluminium and optical brightener leads to a great increase in the energy needed to ignite the dust cloud.

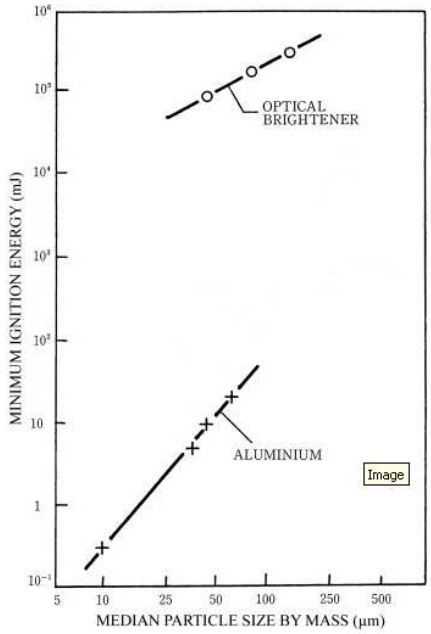

Figure 2-35: *The minimum particle size for aluminium and optical brightener as a function of the median particle size. From (Bartknecht 1987)*

2.7.4 Influence of turbulence on the minimum ignition energy of dust clouds

From the curves in Figure 2-36 (Glarner 1984) it can be seen that the minimum ignition energy for a dust cloud decreases with increasing delay between dust dispersion and ignition. The shorter delay, the higher the turbulence level. This implies that the energy needed to ignite a dust cloud increases with increasing initial turbulence of the dust cloud.

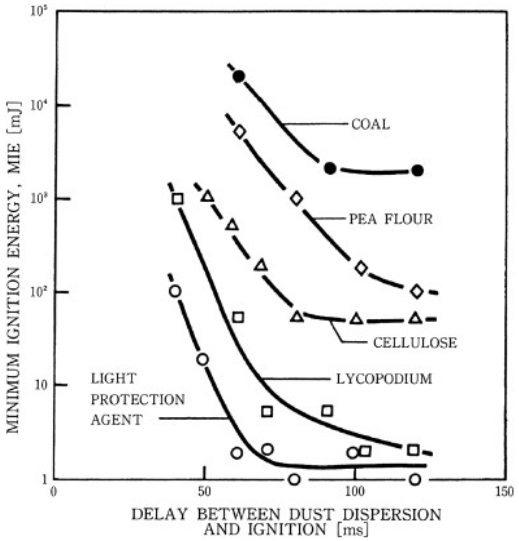

Figure 2-36: *Influence of initial turbulence at the moment of ignition on the minimum electrical spark energies required for igniting different explosive dust clouds (Glarner 1984).*

2.7.5 Combustible dust mixed with an explosive gas (Hybrid mixtures)

As early as 1885 it was performed experiments by (Engler 1885) which stated that the physical properties of the participating substances in a mixture of combustible dust and explosive gas will be affected. Engler filled a box with methane at a concentration of 2.5 vol. % methane in air (the flammability limit is 5 vol.% methane in air) and a cloud of subdivided charcoal dust. Separately it was impossible to ignite the cloud of charcoal dust and the methane concentration in air, but Engler showed that these to substances mixed together in a limited volume could ignite.

It is shown by (Pellmont 1979) that a small amount of combustible gas can influence the ignitability of dust clouds noticeable. He investigated the influence of combustible gas in air on the minimum ignition energy (MIE) of dust clouds. The minimum ignition energy for some of the dust materials decreased almost linearly with the amount of propane in air (see Figure 2-37). These results were quite surprising. They tell that in process areas with potential gas leakages one should be alert in relation to dust accumulation, because a hybrid mixture of gas and dust may increase the probability for an ignition of a combustible substance.

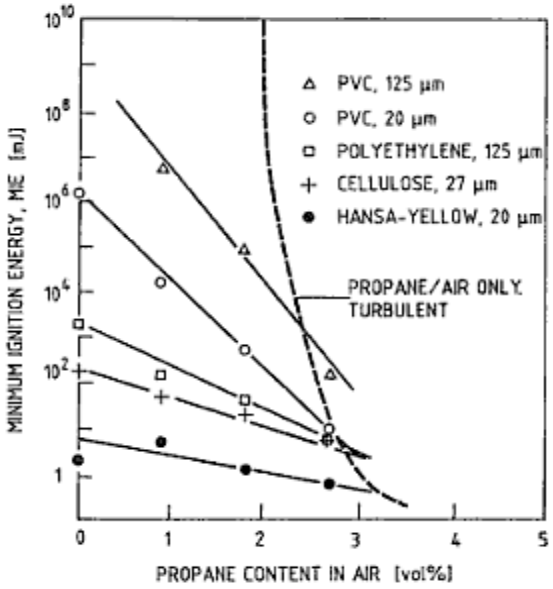

Figure 2-37: *The influence of propane content in air on the minimum ignition energy of different clouds of combustible dust. From (Pellmont 1979).*

2.7.6 Dust/gas mixtures explosion regimes (Garcia-Agreda, Di Benedetto et al.)

(Garcia-Agreda, Di Benedetto et al. 2010) performed an investigation of the explosive violence of a hybrid mixture of methane and nicotinic acid dust in air in a spherical bomb of 20 l, hence how different substances affect each other's lower combustible limits.

The experimental setup is shown in shown in Figure 2-38. The system consists of two feed lines into a 20 l standard apparatus (bomb). The feed line on the right side of the bomb is for the gases, and feed line under the bomb is for dust/air mixtures. A spark generator capable to supply 15 kV, 30 mA is used. A spark electrode of two rounded tungsten rods with tips at

distance 6 mm was used to ignite the mixture. The experiments were carried out by varying the methane concentration (v/v-%) in the range of 1.0 to 10 % and the nicotinic acid dust in the range of 30 to 250 g m^{-3}.

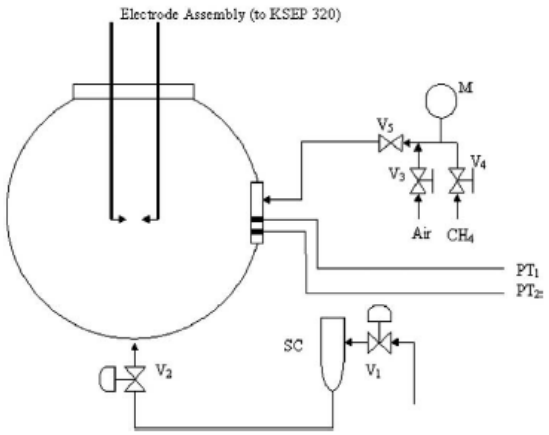

Figure 2-38: *Scheme of the 20 l bomb From (Garcia-Agreda, Di Benedetto et al. 2010).*

The nicotinic acid dust is a combustible organic compound used in the pharmaceutical industries, classified as a B-vitamin. The minimum explosion concentration (MEC) is 125 g nicotinic acid dust/m^3 air. The lower flammability limit (LFL) for methane is 5 vol. % in air.

From the results of the experimental work it has been made a map (Figure 2-39) for the explosion behaviour of the CH_4 /nicotinic acid dust/ air mixtures, where methane content (vol.% / LFL) and dust concentration (C/MEC) are the x- and y- axes. The solid circles are the measured data from the [1]deflagration index, $K_{st.}$ The circles increase proportionally to the value of K_{st}. The white circles represent the experiments where the given mixture of dust and gas does not ignite. From the map it can be seen that it is possible to ignite a mixture of nicotinic acid dust and methane even if one or both of the components is below their respective concentration limits for igniting. The map is divided into five zones. The "no explosion" zone, meaning the mixture can't be ignited. The synergic explosion zone where explosion is possible, despite it is below the lower flammable limit for methane and the MEC for nicotinic acid dust. The dust driven explosion zone is the region where the dust concentration is higher than the minimum explosion concentration and the methane concentration is lower than the LFL. From the map it can be seen that several explosion of different violence occurred in this zone. The gas driven zone is the region where the methane concentration is higher than the LFL and the dust concentration is lower than the MEC, several explosions with varying violence occurred in this zone also. In the dual –fuel explosion zone both methane and nicotinic acid contributes to the explosion. The maximum values of the deflagration index, K_{st} (the solid circles) can be found close to the stoichiometric line.

[1] The deflagration index, K_{st} (bar m/s), is a constant of direct proportionality which defines the maximum rate of pressure rise with time (dp/dt) of a deflagration in a volume V.

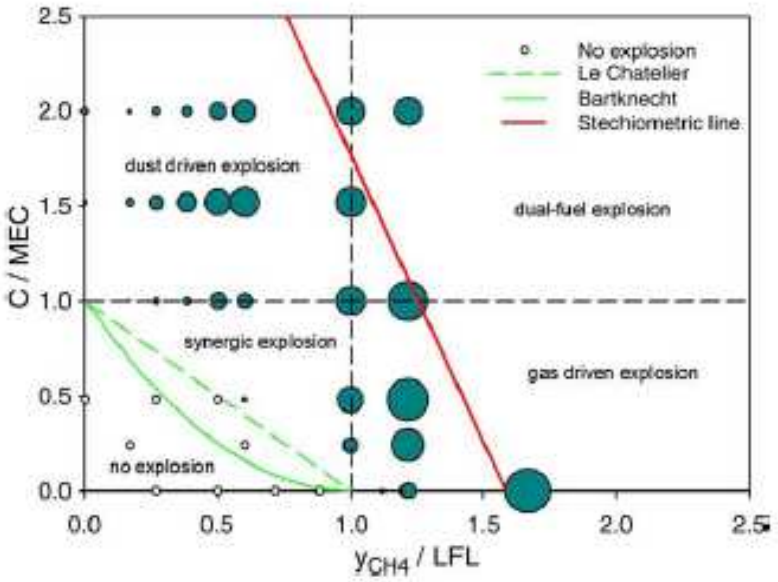

Figure 2-39: *Explosion regimes in the plane methane content/nicotinic acid dust concentration. From (Garcia-Agreda, Di Benedetto et al. 2010)*

The overall conclusion from this work was that the volatile content of dust significantly affects the stoichiometric and the minimum explosion concentrations of the components in a gas/dust/ air mixture. They also concluded that the results are applicable for varying gas/dust/air mixtures.

3 Experimental Procedures and Apparatuses

3.1 Overall experimental approach

To do an accurate and efficient experimental work it depends on a functional and reliable apparatus. The apparatus that (Larsen 1998) and Professor Eckhoff built fulfills these requirements at the same time as it is robust and effective, and therefore it has been used in later experiments by (Einarsen 2001) and (Grov 2010). By making slightly modifications on the rig (see section 3.4.2), it has been a convenient and reliable apparatus in the experimental work of this master's thesis too. The apparatuses are denoted as the "Plane Rectangular Slit Apparatus" (PRSA) throughout this work, detailed description of the PRSA is given in section 3.4.

Some of the experiments carried out with dust in this work are performed with the apparatus (Opsvik 2010) built, referred to as the "Plane Circular Flange Apparatus" (PCFA). This apparatus was designed in accordance to the IEC standard to fulfill requirements for parameters as geometry, widths and hydraulic test pressure. A description of the PCFA is given in section 3.6.

Most of the experiments in this work are performed in the Plane Rectangular Slit Apparatus (PRSA). (Grov 2010) showed that experiments carried out with similar gap configuration in the two different apparatus gave results that correlated surprisingly well, despite the great difference of the two apparatuses. The PRSA is a less time consuming apparatus than the PCFA, due to a 10 liter smaller secondary chamber. The PRSA was therefore primarily used. The experimental procedures for the two apparatuses are described in Appendix A.

In the present work MESG (see description in section 2.3.2) is chosen as a parameter for deciding whether the ability of the flame gap to prevent a re-ignition in the secondary chamber is reduced or improved. The ability to prevent a flame transmission is denoted as the gap efficiency further in this thesis. In the present experiments the test gas is 4.2 vol.% propane in air.

3.2 Crosswise and lenghtwise grooves

(Grov 2010) distinguished between grooves that go in the same direction as the flow through the flame gap (lengthwise grooves, see Figure 2-31) and grooves that go in the opposite direction in relation to the direction of flow (crosswise grooves, see Figure 2-30).

In this thesis an investigation of the physical mechanisms regarding the crosswise grooves is carried out (section 4.2, 0, 4.4, 4.5, 4.6 and 4.7).

3.3 Naming of gap surfaces with grooves

The name system was made by (Grov 2010) to distinguish between the different slit sets with different slit configurations. In Figure 3-1 the naming system is illustrated.

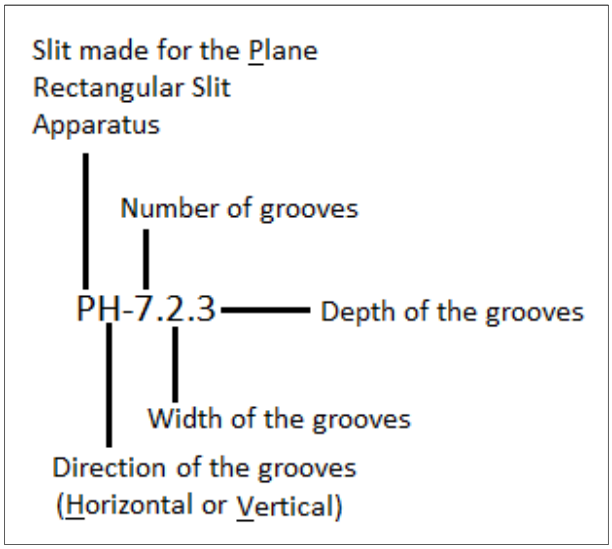

Figure 3-1 *Illustration of the name system for different slit configurations.*

3.4 The Plane Rectangular Slit Appartus

The majority of the experiments in the present work are carried out in the Plane Rectangular Slit Apparatus (PRSA) (see Figure 3-2). As mentioned in section 3.1, it is a reliable and effective apparatus.

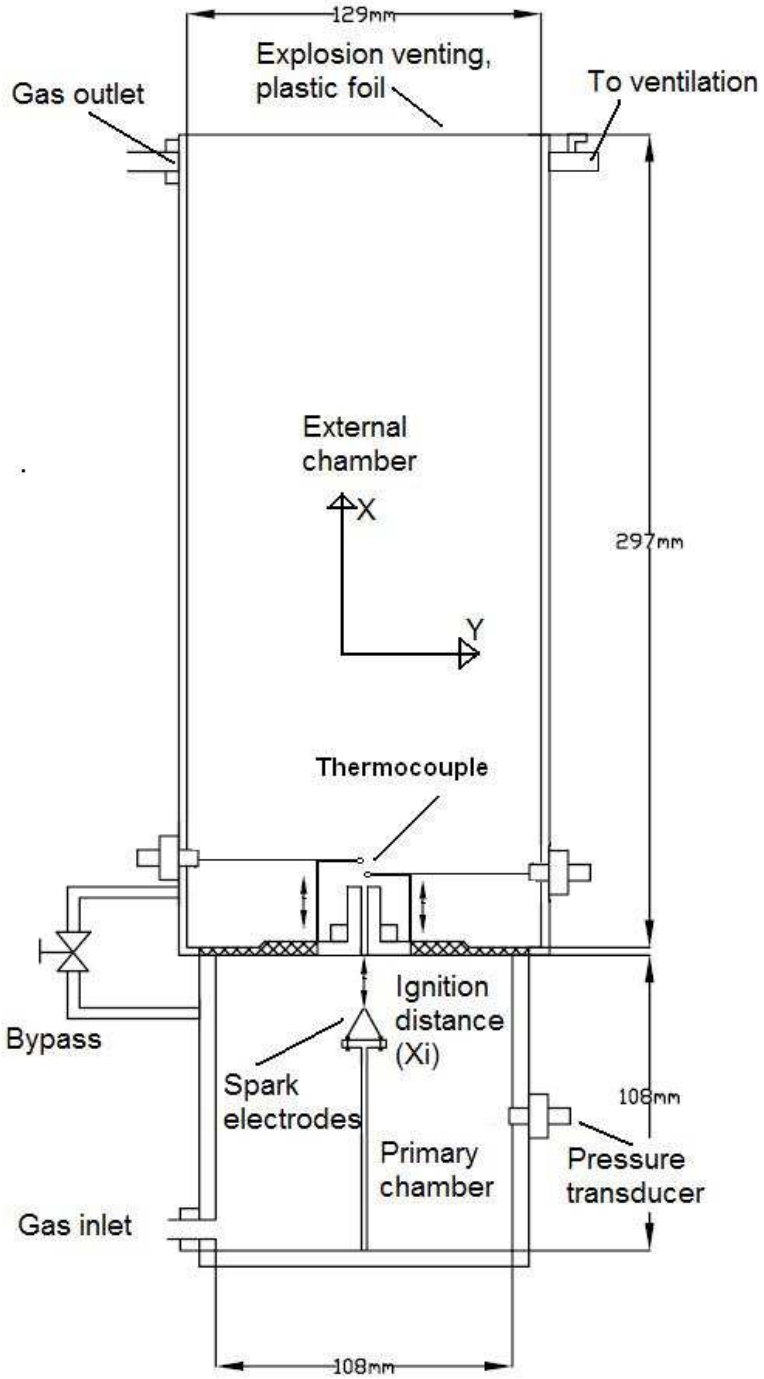

Figure 3-2: *A cross section of the Plane Rectangular Slit Apparatus. Consist of 1 liter primary chamber, a plane flame gap with 25 mm width to a secondary chamber of 3 liters. The plane flame gap is used for determining MESG for different surfaces in propane/air mixture. Based on (Grov 2010).*

The apparatus used in the present work was originally designed by Prof R. K. Eckhoff and (Larsen 1998), it was used in the experimental work of (Larsen 1998), (Einarsen 2001) and (Grov 2010). It has primary chamber of 1 litre with an adjustable ignition source vertically from a flame gap. The secondary chamber has a volume of 3 litres. The two chambers are connected via a rectangular flame gap. The flame gap is replaceable, so different flam gap surfaces can be examined.

The apparatus has been modified several times since it first was constructed. For the present work some adjustable thermocouples are installed above the gap opening in the secondary chamber (see Figure 3-2). This was to be able to measure the temperature of the hot combustion gases that penetrates through the flame gap in different altitudes above the gap opening. As mentioned it is also possible to vary the ignition distance vertically from the gap opening in the PRSA. The temperature measurement system (see section 3.4.2) is somewhat inconvenient and time consuming. It is therefore manly used in the investigation of multiple crosswise grooves.

(Einarsen 2001) was the first one to do an investigation of damages on flame gap surfaces in the apparatus of (Larsen 1998) and professor Eckhoff. The work that Einarsen did proved to be inaccurate due to inaccurate distance pieces. The distance pieces should provide an exact distance between the slits in the flame gap, in Einarsen work the distance varied through the flame gap due to the inaccurate distance pieces and a varying tightening of the flame. The gap was tightened at the upper part of the slits. From this work it was decided by (Opsvik 2010) and (Grov 2010) to use industrial distance "shims", which is used as a tool in motor mechanics. This implies that the gap opening can be varied in steps of 0.01 mm. It was also decided to fasten the slit with a low torque of 20 cNm at both the upper and the lower part of the slit, to ensure a uniform pressure and consequently a constant gap distance throughout the slit, as shown in Figure 3-3. The same procedure for mounting the flame gap is used in the present work. The specifications of the Plane Rectangular Slit Appartus can be seen in Table 3-1.

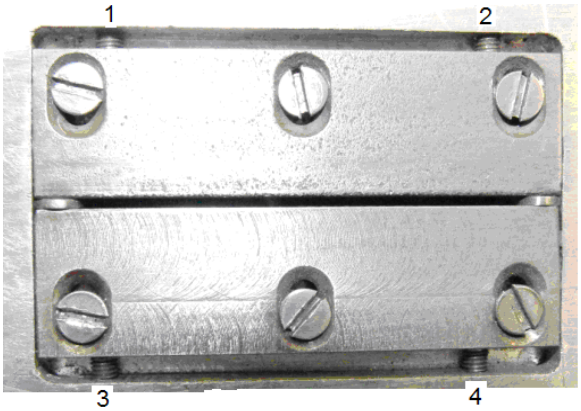

Figure 3-3: *The flame gap entrance, which is located inside the primary chamber, and ends in the secondary chamber. The screws 1- 4 in the picture are screws that are tightened with the same torque as the screws that are located in the upper part of the flame gap, ensuring an uniform gap opening over the whole width of the gap. The distance "shims" can be seen on the side of the slit. From (Grov 2010).*

Table 3-1: *Specification of the Plane Rectangular Slit Apparatus (PRSA).*

Specifications of the PRSA	
Volume, primary chamber	1000 cm^3
Volume, secondary chamber	3000 cm^3
Slit width	25 mm
Slit length	56 mm
Distance "shims"	Varying distances
Ignition source	Spark electrodes, located in the primary chamber
Thermocouples	Adjustable in secondary chamber
Pressure gauge	Located in the primary chamber

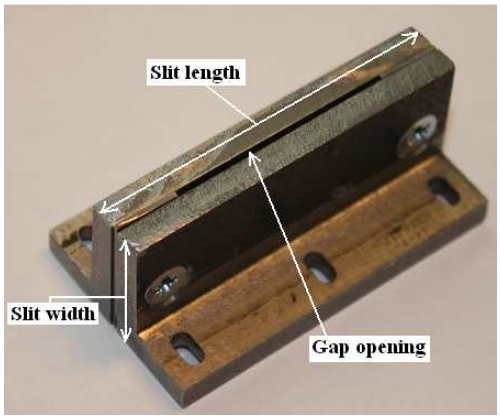

Figure 3-4: *Photography that illustrates the slit width, the slit length and the gap opening.*

3.4.1 Adjustment of the thermocouple position in the Plane Rectangular Slit Apparatus

Modifications on the PRSA were made to be able to measure the temperature of the hot penetrating combustion gas in different altitudes in the secondary chamber. It was mounted two steel "rods" on the plate that separates the primary chamber from the secondary chamber (see Figure 3-5). The thermocouple wires were fastened with small clips on the steel "rods", so each thermocouple was located a given distance vertically above the gap opening. Both of the steel "rods" is replaceable, so it is possible to adjust the distance from the gap opening by mounting a new "rod" with different length.

Figure 3-5: *Photography of the replaceable steel rods on which the thermocouples were "clips" on.*

3.4.2 Adjustment of ignition position in the Plane Rectangular Slit Apparatus

The ignition source located in the primary chamber is adjustable. It can be adjusted vertically from the gap opening and towards the bottom of the primary chamber. From experiments performed by (Grov 2010) and in this thesis a "worst case ignition position" of 14 mm is found (see section 4.2). This implies that the ignition position is placed at distance 14 mm from the gap opening when the MESG value for different flame gap surfaces should be determined. The spark electrodes located in the primary chamber can be seen in Figure 3-6.

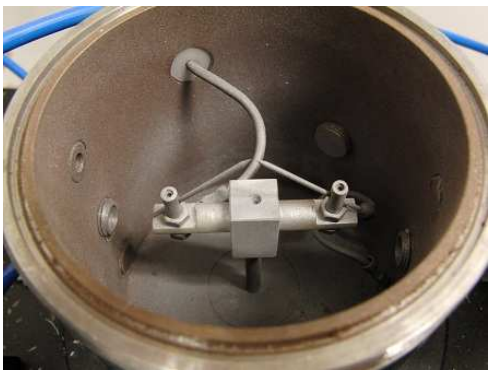

Figure 3-6 : *Photography of the adjustable ignition source located in the primary chamber.*

3.4.3 Direction of the flow in the Plane Rectangular Slit Apparatus

An ignition in the primary chamber will lead to a growing spherical flame front which "pushes" unburned gas through the flame gap. Subsequent the flame will be quenched in the flame gap and hot combustion gases will penetrate through the gap and into the secondary chamber due to the explosion pressure in the primary chamber. The flow direction is illustrated in Figure 3-7.

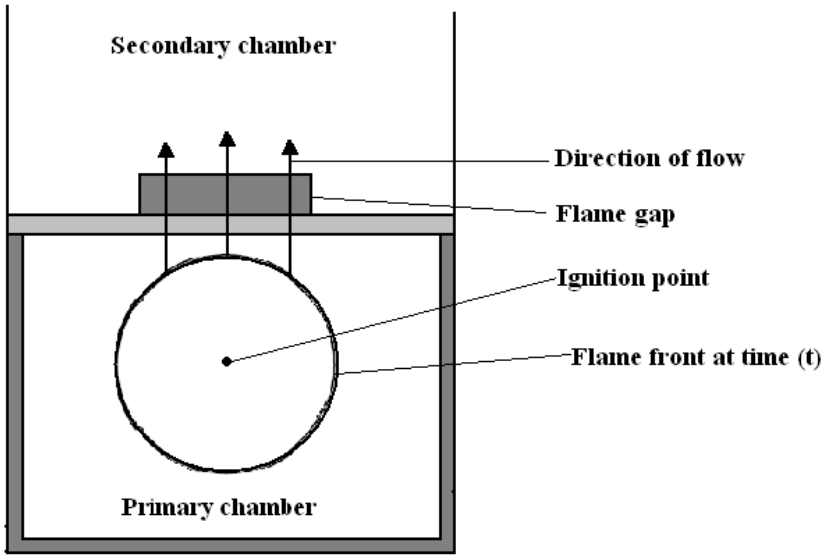

Figure 3-7: *Illustration of which direction the venting of the hot combustion gases will appear in the PRSA. The flame front develops as a sphere from the ignition point.*

3.5 Different experiments carried out and the motivation for implementing these experiments

3.5.1 Experiments with rusted gap surface

Five attached slit sets with undamaged flame gap surface were placed at the sea side for about three months (see Figure 3-8 and Figure 3-9). To generate a great deal of rust the slits were placed at a highly corrosive environment, midway between high and low water. Fifty experiments were conducted on the undamaged slits and fifty new experiments were conducted on the same, but now rusty slit sets after the exposure of saltwater.

The five attached slit sets were fitted with different gap openings, from 0.97 mm to 1.01 mm. The MESG value for undamaged flame gap surface is found by (Grov 2010) to be at a gap opening of 0.98 mm. This means that in the area of the selected gap openings it ideally should be two slit sets giving no re-igniting and three slit sets giving one or more re-ignitions at undamaged state.

Table 3-2: *Specifications of the undamaged slit sets and the rusted slit sets with gap openings, 0.97 mm, 0.98 mm, 0.99 mm, 1.00 mm and 1,01 mm.*

Specifications	Undamaged gap surface	Rusted gap surfaces
Material	Carbon steel	Carbon steel coated with rust
Rz [µm]	2.0	60*
Ra [µm]	0.2	11.5*
Length of slit [mm]	25	25
Width of slit [mm]	56.3	56.3
Thickness of slit [mm]	5	5*
Heat capacity [J/g-C°]	0.452	0.452*
Thermal conductivity [W/mK]	45	45*

*The thermal conductivity and the heat capacity will change when the steel corrodes, but it is uncertain how great the change of the parameters will be. This depends on the molecular structure and the degree of porosity of the coating rust on the gap surface. The values of roughness are estimated values based on the measurements that (Grov 2010) did. The reason for estimating the values is because the measurement equipment for roughness is not made for such great values for roughness as the corrosion forms.

Motivation

In various types of industry rust formation is one of the most common damages on different equipment. Especially vulnerable are equipment that is placed outdoor and exposed for sea water. Ex"d" proof enclosures are often placed in such critical environment. It is therefore of great interest to investigate how rust formation on the flame gap surface affect the gap efficiency and the MESG value.

Experiments with rusted slit surface have been carried out earlier by (Opsvik 2010) and (Grov 2010). In these experiments the slits have been placed in the sea for rusting separately, and on a later stage been attached to each other before the explosion test. However, an explosion proof enclosure used in the industry is one single unit and will be exposed for rust as one

single unit. Therefore, to make a more realistic experiment the slits has now been attached to each other before rusting. This increases the probability of finding new and more realistic side effects of rust. The previous experiments performed by Grov on rusted gap surfaces gave a reduction in the MESG value of 15.3 % in the Plane Rectangular Slit Apparatus. Opsvik presented surprising results where he got an increase in the MESG value of 12.6 % in the Plane Circular Flange Apparatus. With these conflicting results it was decided to do further investigation on rusted flame gap surface.

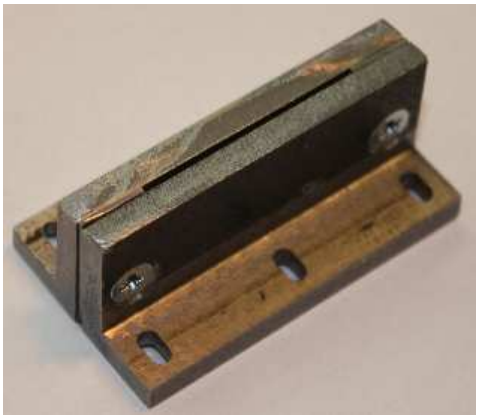

Figure 3-8: *Two plane slits attached to each other with screws prior to the exposure of rust.*

Figure 3-9: *The same slit set after 3 months at sea side. Significant rust formation over the entire surface, including the flame gap surface.*

3.5.2 Experiments to find the most favorable ignition point for re-ignition in the secondary chamber for the slit with seven perforated crosswise grooves

Experiments with the slit with configuration PH-7.2.3 has been carried out to find the ignition point most favorable for re-ignition in the secondary chamber. The grooves on the slit surface are 2 mm wide and 3 mm deep, they perforate over the whole crosswise length of the slit (illustrated in Figure 3-10). The specification for the slit set with configuration PH-7.2.3 is presented in Table 3-3.

Table 3-3: *Specification of the slit with configuration PH-7.2.3*

Specifications	PH-7.2.3
Material	Carbon steel
Rz [µm]	2.0
Ra [µm]	0.2
Length of slit [mm]	25
Width of slit [mm]	56.3
Thickness of slit [mm]	5
Number of grooves	7
Width of grooves [mm]	2.0
Depth of grooves [mm]	3.0
Heat capacity [J/g-C°]	0.452
Thermal conductivity [W/mK]	45

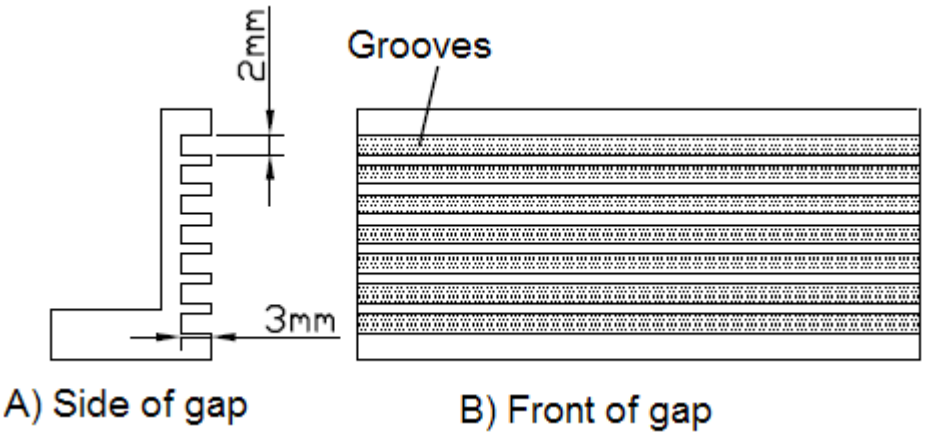

Figure 3-10: *Illustration of the slit with configuration PH-7.2.3. From (Grov 2010).*

Motivation

It was stated by (Grov 2010) that flanges and slits with multiple crosswise grooves on the gap surface improved the gap efficiency noticeably. It was therefore decided to do further investigation of this specific gap configuration, and hopefully get a better understanding of the physical mechanism related to flow through a slit with multiple crosswise grooves.

As described in section 2.5.3, Larsen stated that there exists a limiting hole-diameter (MESD) for transmission of an explosion. This limiting hole-diameter varied with varying ignition position in the primary chamber. When dealing with flameproof enclosures it is necessary to find to what extend the ignition positions affects the probability for re-ignition outside the enclosure, and finally find the most "dangerous" ignition position.

(Grov 2010) did experiments to find the most "dangerous" ignition position for undamaged flame gap surfaces in the PRSA. He found that the ignition position that gave the lowest gap opening in respect to re-ignition in the secondary chamber was 14 mm from the gap opening as described in section 2.5.5. The ignition position at 14 mm was then used in all of the different experiments with various damaged flame gap surfaces. Further it was found that the flame gap surface with multiple crosswise grooves gave a significant increase in the MESG value, with the assumption that the most "dangerous" ignition position for this specific configuration was 14 mm.

To be able to determine definitely that the multiple crosswise groves increase the MESG value, and that the ignition position of 14 mm from the gap entrance is the most favorable for re-ignition for this slit configuration, several experiments at different ignition positions were conducted in this thesis (see section 4.2).

3.5.3 Temperature measurements over the safe gap

It was made a modification on the PRSA to implement temperature measurements in different altitudes straight above the safe gap opening in the external chamber, as shown in Figure 3-5. Several temperature measurements were performed on the combustion gases that penetrate through the slit with multiple crosswise grooves. The results of these experiments were compared with temperature measurements carried out on the combustion gases that penetrate

out of an undamaged slit. Several experiments were carried out with different gap openings on both of the slit configurations.

As seen in Figure 3-5 there are two thermocouples mounted inside the secondary chamber. These two thermocouples are attached to two replaceable metal "rods". This means that it can easily be performed temperature measurements in different altitudes by replacing the rods with new, longer or shorter rods. It is conducted temperature measurements in three different heights (1 mm, 2cm and 4cm) above the gap opening in this work. The sampling rate of the temperature was thousand measures per second, 1000/sec.

The motivation for temperature measurements over the safe gap

The motivation for the temperature measurements was to see how the temperature in the exhaust gases varied above the gap opening with different types of flame gap surfaces. An additional motivation was to see how the temperature varied in different altitudes over a given flame gap surface during an explosion in the primary chamber. Thus be able to say something about the altitude re-ignition occurs.

(Grov 2010) found that the MESG value increased from 0.98 mm to 1.10 mm by replacing the undamaged gap surface with a gap with surface multiple crosswise grooves with specification PH-7.2.3. This implies that the configuration of the multiple crosswise grooves have an effect on the probability for re-ignition in the secondary chamber. The temperature measurements are performed to approach a solution to why this specific configuration has such great importance when it comes to prevent re-ignition in the secondary chamber.

The reason for mounting a thermocouple 1 mm above the gap opening was to examine the hot combustion product that penetrates through the slit before they start mixing with the gas mixture in the secondary chamber. This may give valuable information about the cooling process of the hot combustion products. It can tell if the hot gases mainly cool down above the gap opening in the secondary chamber or if the main cooling process is inside the flame gap.

3.5.4 High speed camera

A casio EX-F1 (see Figure- XI in Appendix C-1) was used to record several experiments. This was placed on a tripod in front of the apparatus prior to the experiments. For detailed information see Appendix C-1.

Motivation

Several experiments on different types of slits and holes in the PRSA have been carried out earlier, and various illustrations and theories have been presented when the re-ignition process shall be explained. One of the most common illustrations used for explaining this is the re-ignition process shown in Figure 2-19, where it is illustrated by (Phillips 1971) that the re-ignition occurs inside a vortex at a distance from the gap opening. To support this explanation and to do further research on the theme, several re-ignitions in the secondary chamber have been recorded with a high speed camera that can shoot 1200 frames per second. This means that the re-ignition process can be observed from a new and hopefully informative approach.

3.5.5 Flame gap surfaces with different depths on the multiple crosswise grooves

Experiments are carried out in the Plane Rectangular Slit Apparatus with different configurations on the flame gap surface. The specifications of four slits sets with seven crosswise grooves of varying depth are presented in Table 3-4. In addition the motivation for performing these experiments are stated. The results from the experiments carried out are shown in section 4.6.

Table 3-4: *Specifications of the four different slit sets with different depth.*

Specifications	PH-7.2.3	PH-7.2.2	PH-7.2.1	PH-7.2.0,5
Material	Carbon steel	Carbon steel	Carbon steel	Carbon steel
Rz [µm]	2.0	2.0	2.0	2.0
Ra [µm]	0.2	0.2	0.2	0.2
Length of slit [mm]	25	25	25	25
Width of slit [mm]	56.3	56.3	56.3	56.3
Thickness of slit [mm]	5.0	5.0	5.0	5.0
Number of grooves	7	7	7	7
Width of grooves [mm]	2.0	2.0	2.0	2.0
Depth of grooves [mm]	**3.0**	**2.0**	**1.0**	**0.5**
Heat capacity [J/g-C°]	0.452	0.452	0.452	0.452
Thermal conductivity [W/mK]	45	45	45	45

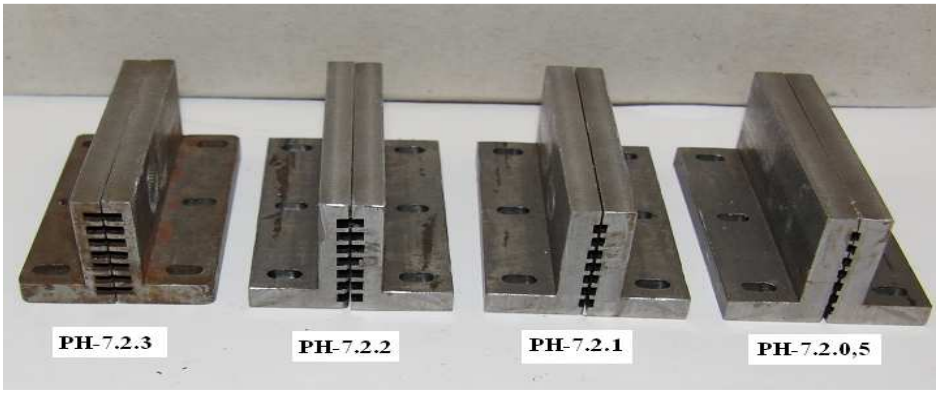

Figure 3-11: *The four different slits sets with multiple crosswise grooves with different depth.*

Motivation

Previously it has been carried out experiments with slits with seven crosswise grooves on the gap surface (Grov 2010). The grooves had a depth of 3 cm and a width of 2 cm. The examination of the slits showed that gap efficiency and consequently the MESG value increased after milling these seven grooves into an undamaged gap surface. The MESG value increased from 0.98 mm to 1.10 mm, which is a radically improvement of the gap. To investigate if there are other dimensions of the seven crosswise grooves that may improve the gap efficiency even more, or lead to new side effects, there have been made four new slit sets with different gap configuration. Three of the slit sets have the same width as the original, but different depth on the seven crosswise grooves (see Table 3-4). It should be mentioned that experiments are performed on the original slit set with depth 3.0 mm as well, in order to

verify the result obtained by (Grov 2010). The results from the experiments performed with different gap configuration are presented and compared in section 4.6.

3.5.6 Flame gap surface with different width on the multiple crosswise grooves

In this section two slit sets with different width on the seven perforating crosswise grooves are examined and compared. The configuration tested are the original and earlier tested configuration PH-7.2.3 which has crosswise grooves of 2 mm width, and a new slit set PH-7.1.3, which has crosswise grooves of 1 mm width. The results from these experiments are presented in section 4.7.

Table 3-5: *Specifications of flame gap surfaces with different width on the multiple crosswise grooves.*

Specifications	PH-7.1.3	PH-7.2.3
Material	Carbon steel	Carbon steel
Rz [µm]	2.0	2.0
Ra [µm]	0.2	0.2
Length of slit [mm]	25	25
Width of slit [mm]	56.3	56.3
Thickness of slit [mm]	5	5
Number of grooves	7	7
Width of grooves [mm]	**1.0**	**2.0**
Depth of grooves [mm]	3.0	3.0
Heat capacity [J/g-C°]	0.452	0.452
Thermal conductivity [W/mK]	45	45

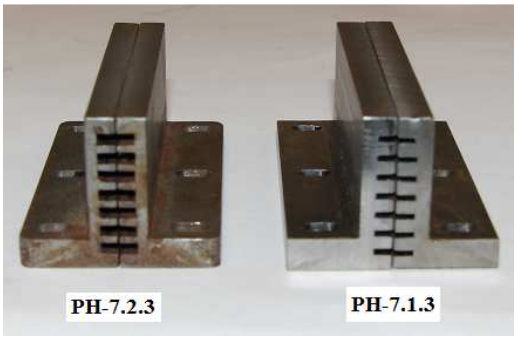

Figure 3-12: *The two different slit sets with multiple crosswise grooves with different width.*

Motivation

The motivation for performing experiments on these slit sets was to examine if there are any significant diverse effects on the gap efficiency of different widths of perforating multiple crosswise grooves. (Grov 2010) stated that multiple lengthwise grooves of 1 mm width, did not affect the gap efficiency. It is therefore interesting to investigate if the MESG value remains unaffected in experiments with crosswise grooves of 1 mm width.

3.5.7 Flame gap surface of Plexiglas with seven perforating crosswise grooves

A slit with the same configuration as PH-7.2.3 was made of Plexiglas (Poly-methyl methacrylate). The specification of the flame gap made of Plexiglas is presented in Table 3-6.

Table 3-6 : *Specification of the flame gap surface made of Plexiglas with multiple crosswise grooves.*

Specifications	PH-7.2.3(Plexiglas)
Material	Poly (methyl methacrylate)
Rz [µm]	14,6
Ra [µm]	2,9
Length of slit [mm]	25
Width of slit [mm]	56.3
Thickness of slit [mm]	5
Number of grooves	7
Width of grooves [mm]	2.0
Depth of grooves [mm]	3.0
Heat capacity [J/g-C°]	1,47
Thermal conductivity [W/mK]	0,2

Figure 3-13: *Photography of one of the slits made of Plexiglas with seven multiple crosswise grooves.*

Motivation

(Grov 2010) carried out experiments with undamaged flame gap surface made of Plexiglas, and found that the MESG value did not change due to change in flame gap material. He found a radically increase in the gap efficiency when adding seven perforating crosswise grooves to an undamaged steel surface. It is conceivable that the crosswise grooves increase the turbulence inside the gap and consequently the fluid- wall contact area. All literature reviewed agrees upon the fact (see section 2.4.1) that an increase of fluid- wall contact area leads to a more efficient heat exchange process. From literature (Mottahed and Molki 1996) it is proposed that the heat transfer coefficient may increase up to 350 % if a smooth surface is roughened. (Grov 2010) did not perform any experiments with a slit made of a material with low thermal conductivity (Plexiglas) combined with a rough gap surface. It is therefore of great interest to see if the gap efficiency decreases when the material of the flame gap surface with crosswise grooves are changed from steel to Plexiglas, which implies a great reduction in the thermal conductivity. The experiments may therefore demonstrate whether heat transfer to the slit material with high roughness is important or of secondary order.

3.5.8 Experiments with dust inside the flame gap

A slit with undamaged gap surface was placed in the flange gap. The slit were fastened at a gap opening lower than its own MESG value at 0.98 mm, found by (Grov 2010). This was to ensure that the hot penetrating combustion gases did not cause an ignition of the explosive atmosphere in the external chamber. The only possible source of ignition was the dust (atomized aluminium and pollen). A quantity of 0.01 g dust were weighted and placed in the flame gap with a spatula. Subsequently the primary and secondary chambers were filled with a uniform gas mixture of 4.2 vol. % propane in air. All of the experiments were recorded with a high speed camera, Casio Exilim EX-F1 (see Appendix C-1). The results from the experiments are presented in section 4.9.

Table 3-7: *Specifications of atomized aluminium flakes and pollen particles. From (Eckhoff 2003) and from observation from magnified photos of the particles (see Appendix F).*

	Atomized aluminium flakes	Pollen particles
Particle size [µm]	Diameter 1-25, Thickness 0.1	10-30 (spherical)
Average bulk density [g/ cm3]	0.30 – 0.60	1.18
Boiling point (°C)	2000	
Melting point (°C)	650	
Heat of combustion (kJ/mol 02)	1100	470

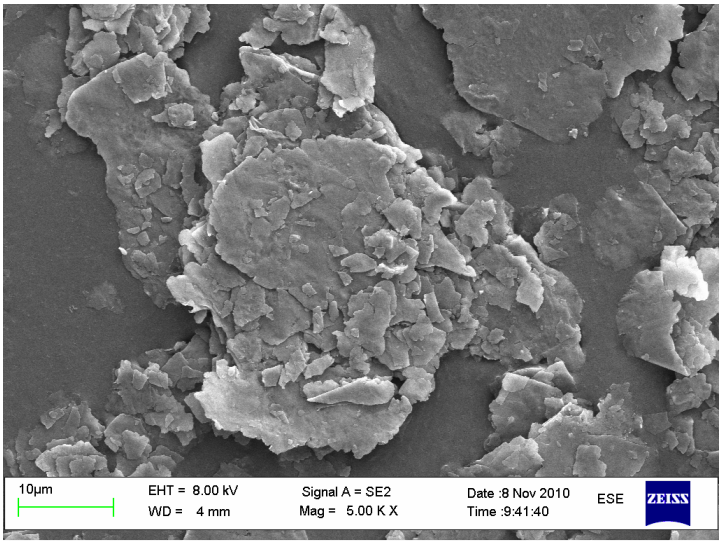

Figure 3-14: *Aluminium flakes used in the present experimental work. Magnified 5000 times with Zeiss supra 55 VP (electron microscope) at UoB. It can be seen that the diameter of the aluminium flakes varies from approximately 1- 25µm. Several photos in Appendix F.*

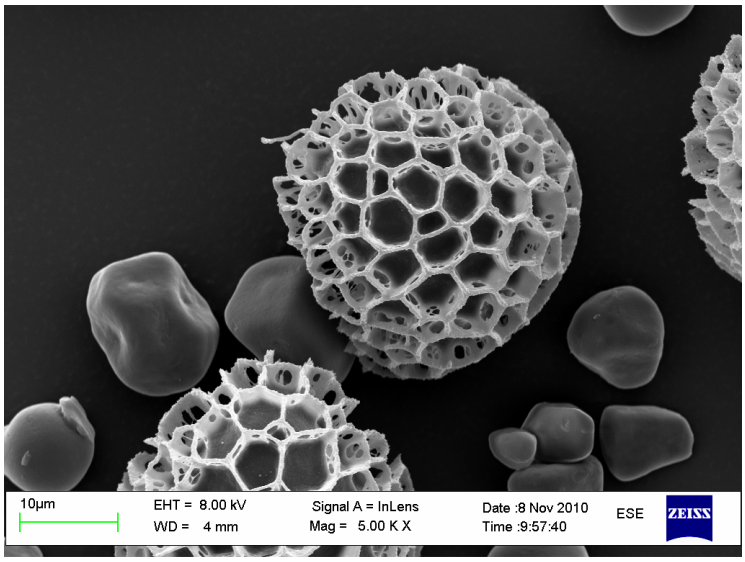

Figure 3-15: *Pollen particles used in the present experimental work. Magnified 5000 times with Zeiss supra 55 VP (electron microscope) at UoB. It can be seen that two different types of pollen is present in the sample, the substances with the mesh structure is lycopodium particles. The diameter of these particles is approximately 25 µm. The other pollen substance present in the sample has a diameter of approximately 10 µm.*

Motivation

Almost any environment is exposed to dust. The Ex"d" enclosures are located in "zones" where a gas leakage is a potential hazard. Dust is not considered as a potential source of ignition. From a survey carried out by (Opsvik 2010) and (Grov 2010) to a company that repair Ex"d" equipment the interviewee explicitly tells that the focus of combustible dust as a potential hazard is totally ignored in several industries. This even applies in some of the most obvious industries, as the wood-processing industry and the food industry. The motivation for this work is to carry out experiments that can tell if dust of any sort can ignite inside the flame gap or inside the main volume of the Ex"d" enclosure and subsequent penetrate into external chamber and cause an ignition.

To get the most complete perspective of this issue, the two dust types that are tested is atomized aluminium powder, which is one of most reactive substances and pollen which is a much less reactive substance. The particle size has great impact on the minimum ignition energy as shown in section 2.7.3. The atomized aluminium flakes has a thickness of approximately 0.1 µm, which makes it more reactive than the spherical pollen particles of diameter 10-25 µm.

3.5.9 Experiments with dust, carried out in the Plane Circular Flange Apparatus

Experiments were performed with atomized aluminium and pollen dust placed on an undamaged circular flame gap in the PCFA (see specifications in section 3.6). The slit were fastened at a gap opening lower than its own MESG value at 0.95 mm, found by (Grov 2010). This was to ensure that the hot penetrating combustion gases did not cause an ignition of the explosive atmosphere in the external chamber. The only possible source of ignition was the dust. A given quantity of dust were weighted and placed on the flame gap with a spatula.

Subsequently the primary and secondary chambers were filled with a uniform gas mixture of 4.2 vol % propan in air. The results from the experiments are presented in section 4.9.3.

Similar specifications of the dust as in Table 3-7.

Motivation

During the experiments with dust in the Plane Rectangular Slit Apparatus the dust fell into the primary chamber due to the gravitational force. To investigate if the combustible dust can ignite when it is only present inside the flame gap the Plane Circular Flange Apparatus was used (see detailed description in section 3.6). This apparatus has a flame gap which is placed horizontal to the ground, so the dust will not fall into the primary volume due to the gravitational force.

A brief introduction of the Plane Circular Flange Apparatus is given below.

3.6 A brief introduction of the Plane Circular Flange Apparatus (PCFA)

The Plane Circular Flange Apparatus

The Plane Circular Flange Apparatus (PCFA) was designed by (Opsvik 2010). He constructed this apparatus to get an apparatus with a flange arrangement as realistic as possible compared to flanges in the industry, while at the same time being in accordance with current IEC standards for MESG determination. A cross section of the apparatus is given in Figure 3-16. The apparatus was built with a flange system that is replaceable. This was with the intent to investigate what influence various damages on the flame gap surface have on the MESG value.

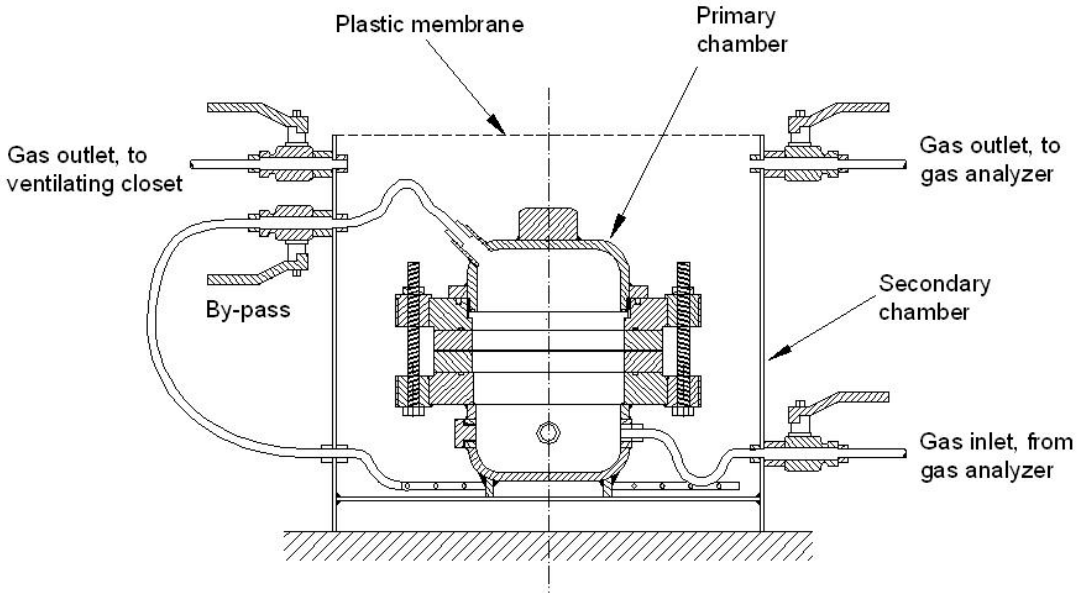

Figure 3-16: *Cross section of the PCFA constructed by Opsvik, used to examine different flame/flange gap surfaces and determine their respective MESG values. From (Opsvik 2010)*

(Opsvik 2010) and (Grov 2010) performed several experiments in the PCFA to determine MESG values for different flange gap surfaces. (Grov 2010) stated that experiments carried out with similar flame gap configurations in the PCFA and the PRSA gave results that were in very good correlation. The volume of the secondary chamber in the PCFA is 13 litres, compared to the PRSA's secondary chamber of 3 litres. This means that the PCFA is a more time consuming apparatus. The greater part of the experimental work in this thesis and the work performed by (Grov 2010) was therefore performed in the PRSA.

The ignition source in the primary chamber is adjustable. It can be moved from the gap entrance towards the centre of the primary chamber. The experiments performed in this work were carried out at the "worst case ignition distance" of 14 mm from the gap opening.

Table 3-8: *Specifications of the PCFA.*

Specifications of the PRSA	
Volume primary chamber	1150 cm^3
Volume secondary chamber	13000 cm^3
Slit width	25 mm
Slit length	Cylindrical
Distance "shims"	varying distance
Ignition source	spark electrodes located in the primary chamber

3.6.1 Flow from Primary Chamber in the Plane Circular Flange Apparatus (PCFA)

The flow direction of the hot combustion gases in the PCFA is horizontal to the ground. This implies that the dust will not fall into the primary chamber, but stay in the flame gap until an ignition is trigged in the primary chamber. If the ignition source is placed at the centre of the primary chamber the flame front will develop as a spherical ball, and unburned gas will first penetrate through the circular flange gap. Subsequently the flame will be quenched in the flame gap and hot combustion gases will penetrate through the gap opening.

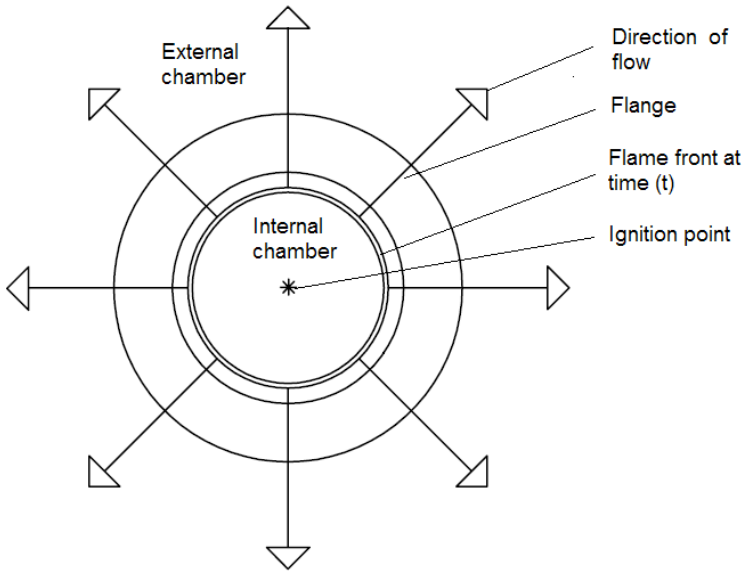

Figure 3-17: *Illustration of the flow directions of hot combustion gases that penetrate out from the primary chamber in the PCFA, the ignition source is located in the centre. From (Grov 2010).*

3.7 Gas mixture preparation, analysis and filling

The method for gas mixture preparation, analysis and filling is the same as used in (Opsvik 2010), this chapter is similar to chapter 3.4 in (Opsvik 2010).

The same system for gas mixture preparation, analysis and filling was used for both the Plane Rectangular Slit Apparatus (PRSA) and the plane cylindrical flange apparatus (PCFA). The system is shown Figure 3-18. The gas filling system consists of various vents, valves, tubes flow meters and a gas analyser. All these components assure that the mixture of propane and air is uniform uniformly distributed in the entire volume of the apparatus.

The gas mixture used in the present work was 4.2 vol. % propane in air. The propane was mixed with air from the pressurized air system of the laboratory. The propane concentration was measured by an infrared gas analyser (Servomex 1991). The premixed gas was introduced into the primary chamber close to the bottom. The subsequent flow to the secondary chamber occurred through the flame gap and a bypass mounted directly from the primary chamber to the secondary chamber. This bypass reduces the gas filling time.

In the present experimental work both the calibration and test gas were of purity of 99.95 % (propane), despite the lower requirement from (IEC 2002) of purity of 95 % of the test gas. It was chosen to have a gas of high quality to minimize the uncertainty due to the chemical composition of the gas. Detailed procedures for us of the gas analyser are given in Appendix A and the gas quality certificate is enclosed in Appendix E.

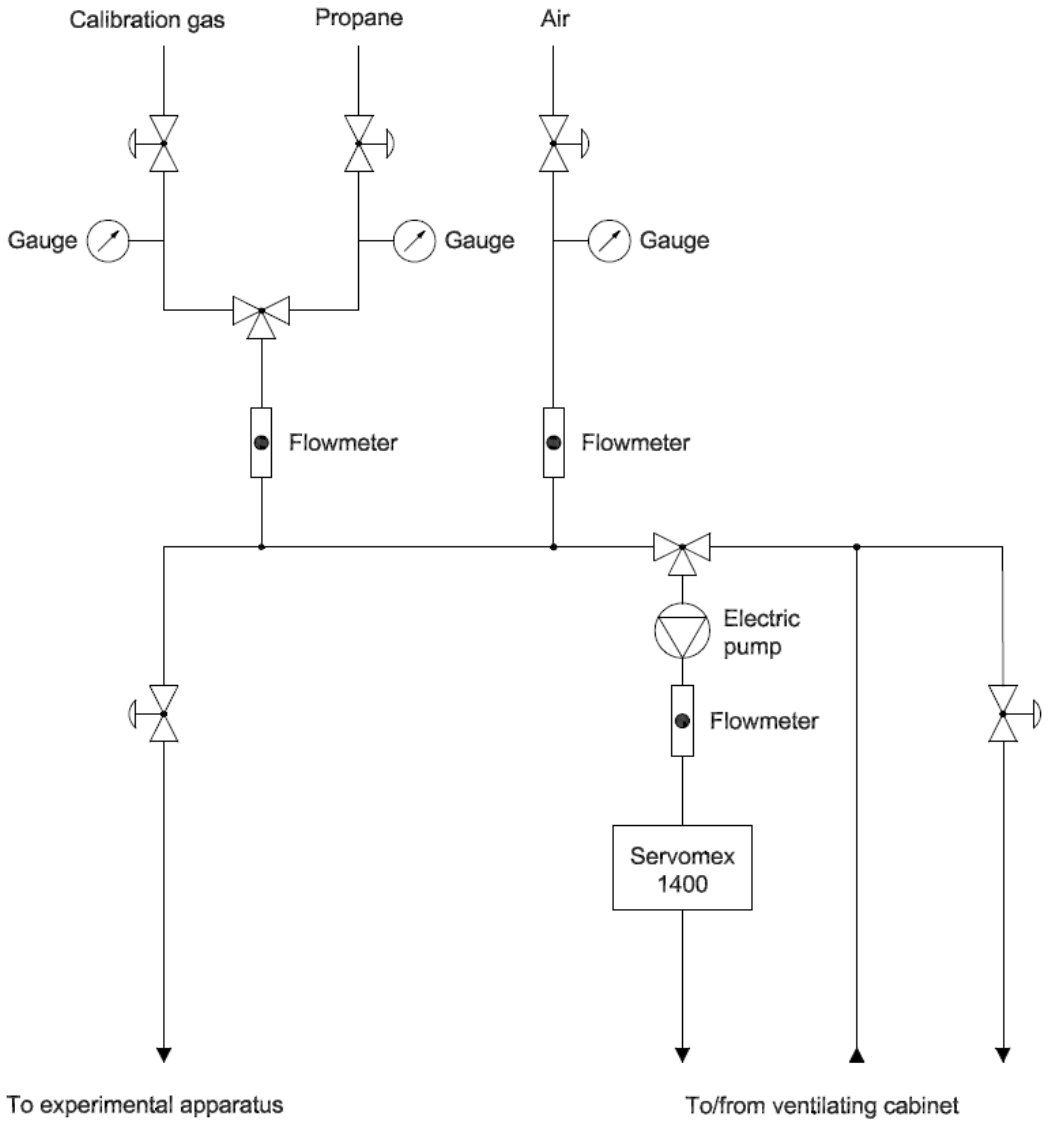

Figure 3-18: *The gas filling system with the servomex 1400 B4 SPX infrared gas analyser. The different pressure gauges, valves, supply pump and flow meters can be seen. From* (Opsvik 2010)**.**

3.8 Measurement and data logging system

This chapter is similar to chapter 3.4 in (Opsvik 2010). The method for gas mixture preparation, analysis and filling is the same as used in (Opsvik 2010), apart from a new charge amplifier.

3.8.1 Data acquisition system

When the homogenous propane-air mixture was contained within the explosion apparatus a spark was generated in the primary chamber and the explosion pressure build up in the primary chamber was measured. Measurement data were stored after each experiment on a computer in such way that it could easily be analysed at a later stage.

A NI USB 6009 card, connected to a computer, performed both controlling and logging of the experiment. This NI-CAD card is programmed by Lab view software, which is documented in

Appendix A-2.5. The software enables the user to change all setup parameters, within the limitations of the card and the hardware.

3.8.2 Control system

A tailor made data acquisition and control system was made to control the experiments. Digital ports are used for remote triggering of the experiment and to reset and activate the pressure measurement system. Figure 3-19 shows the control and measurement system.

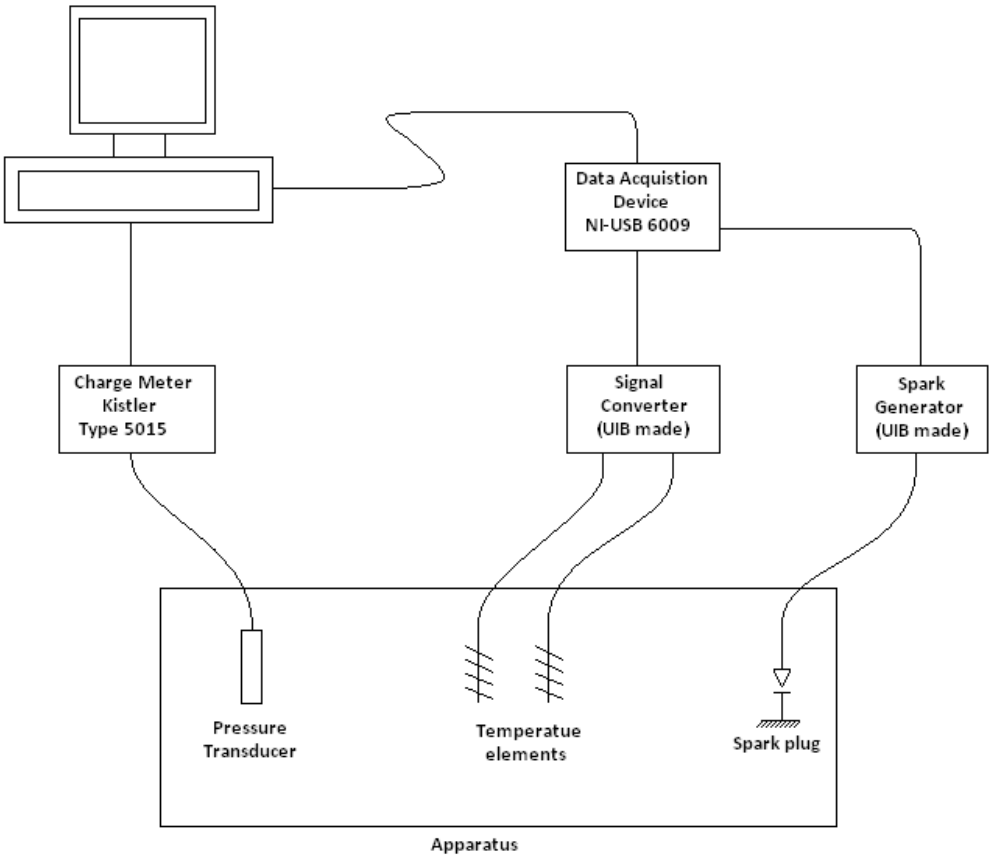

Figure 3-19: *Data acquisition and control system.*

3.8.3 Pressure measurements

In order to measure the explosion pressure in the primary chamber as a function of time pi(t), a piezo electric transducer with a charge amplifier was mounted in the cylinder wall in both apparatuses. In connection with each experiment a zero-calibration of the pressure transducers where conducted just prior the release of the igniting spark in the primary chamber. Additional information and calibration certificates are enclosed in Appendix E.

3.8.4 Temperature measurements

It was performed temperature measurements for the experiments carried out with slits with multiple crosswise grooves. In order to measure the temperature of the hot combustion gases penetrating from the gap opening two thermocouples classified as type k is used. Type k thermocouples consist of a junction of two different metals. The junction creates a small voltage which increases with temperature. The signal was amplified through an operational amplifier (AD597) and logged on the computer.

3.9 Sources of Error

This chapter is similar to chapter 3.8 in (Opsvik 2010). Except the section (3.9.6) which discuss the temperature system.

3.9.1 Data Acquisition system

The experience from the work performed in this thesis shows that amplification of measured signal is important. One A/D converter reads all the channels and have switches inside the card which chooses which channel to read. If one channel is not satisfactorily amplified, then the signal from one channel would influence the signal from the next reading.

3.9.2 Gas concentration measurements

Calibration of the gas analyser was done with a certified span gas containing 5.00 % propane in nitrogen. The measurements close to these values would have the highest accuracy and as the gas mixture departs from these values then the accuracy would be somewhat lower. For mixtures far from the reference point, the accuracy depends on the linearity between the two points or the extrapolation towards a richer mixture. The alternative is how well the analyser calibrates for nonlinearity.

During experiments the gas concentration has to be 4.2 vol.% +/- 0.1 % as stated in (IEC 2007a). Insufficient calibration could result in uncertainties with respect to concentration measurements. To ensure that there is performed an adequate amount of calibration a calibration log has been established. All calibration of the gas analyser has been executed in accordance with the calibration procedure enclosed in Appendix A-2-4.

Changes in flow rate effects accuracy and a change from 0 to 200 ml will introduce an error <0.1 % (Servomex 1991). Adjustment of flow was done with a flow meter that actually measures the momentum of the moving gas particles rather than volume flow, so the flow could also change as a result of variation in specific gravity between air and propane. In general the flow was not changed for every interval and was on some occasions not changed at all so it is assumed that variation of flow is not likely to affect the accuracy of the gas concentration measurement.

Another parameter which can have an influence on the actual gas concentration both in the primary and secondary chamber is that the mixture in the chambers may not always be homogenous.

3.9.3 Atmospheric pressure and temperature

The normal mode of operation of the gas analyser is to discharge the gas sample from the measuring cell at atmospheric pressure. The sensitivity of the cell will be proportional to the atmospheric pressure. The effect is that of a span change, so the error introduced is zero at zero concentration and maximum error at full scale. This leads to a change of 1 % in the atmospheric pressure thus will cause a change of typical 1 % of reading.

The manufacturer has stated that the effect of temperature change is less than (0.2 % of full scale display + 0.4 of reading) per degree Celsius.

3.9.4 Air humidity

The propane used in the experiments is mixed with pressurized air supplied from local distribution network. No measurements of humidity are done, but the air is filtrated and dried in a unit downstream the air compressor. In any case the quality of the air is not documented and pollution in form of oil, dust particles or water may exist in the supplied air. This may have effects on the results.

3.9.5 Pressure

There is uncertainty in the pressure readings due to the resolution of the pressure transducer. Kistler, the manufacturer of the piezoelectric transducer, states that the accuracy of the transducer is $\leq \pm 0.08\%$ of Full Scale Output when the calibration range is in the area of 0 to 25 bar. This gives an accuracy of $\pm$ 0.02 bar at the used measuring range, which is well within acceptable limits.

The pressure transducer is mounted a fixed distance at the vertical chamber wall of the primary chamber. The transducer may not detect local pressure gradients in the chamber.

3.9.6 Temperature

The thermocouples used in this work are not constructed to measure temperatures in explosions (or jets). The extremely rapid increase in temperature due to the explosion causes some uncertainty to the measured temperature, but it is assumed that the temperature difference measured between different experiments is valid.

3.9.7 Condensed water

After a few explosions water will typically condense on the inside of the walls of the primary chamber and may represent a significant source of error. Water may evaporate from the warm

vessel walls during gas filling and the subsequent period of turbulence settling, altering the gas composition. Water in the gas mixture may affect reaction mechanisms and heat capacity, whereas a small portion of the water at the vessel walls may evaporate during the explosion. It is generally assumed that the explosions will be too rapid for significant amounts of water to evaporate.

3.9.8 Experiments

There are uncertainties due to construction tolerances in size of volumes, ignition positions and flange diameters and distances. In addition there is accuracy related to the experimental work, although good experimental procedures would counteract this, with reference to Appendix A.

The dimension of the distance "shims" is observed to have a variation of approximately $^{+}$/- 1 hundredths of a millimetre.

4 Experimental Results and Discussion

In this chapter the results from different experimental work is presented and discussed. The experimental results vary in a plurality of parameters, such as temperature, pressure, flame surface configurations, flame surface damages and position of spark in the primary chamber.

In section 4.9 the results from the experiments performed with a hybrid mixture of dust/gas is presented. The aim of these experiments was to see how dust inside a flameproof enclosure can affect the probability for re-ignition of a surrounding explosive gas cloud. To get most possible information from the experiments performed with a hybrid mixture, both of the apparatuses (PRSA and PCFA) were used.

4.1 Result and discussion from the experiments on rusted flame gap surfaces

Five sets of bolted slits, each with a given gap opening were explosion tested before and after rusting. A total of 100 experiments were conducted with these slits. The results from the experiments are summarized in Table 4-1, Figure 4-1,Figure 4-2 and Figure 4-3.

It was conducted twenty explosion tests on each of the five sets of slits. Ten experiments in undamaged state and ten after rusting. The first explosion test on each of the rusted slit sets is the most critical, because the first ignition source that is exposed to an explosive gas cloud would most likely ignite the entire gas cloud.

4.1.1 Results

Table 4-1: *Experiments carried out with five slit sets at undamaged state and the same slit sets at corroded state.*

Gap opening, Yi (mm)	Ignition distance [mm]	Number of re-ignitions		Mean pressure [barg]		Pressure due to the first explosion [barg]
		Undamaged	Rusted	Undamaged	Rusted	Rusted
1.01	14	10	0	2.30	2.56	2.68
1.00	14	10	0	2.37	1.44	1.55
0.99	14	3	0	2.39	3.30	3.43
0.98	14	0	0	2.40	3.51	3.61
0.97	14	0	0	2.73	3.59	3.88

It was not observed one single re-ignition for any of the five slit sets after the exposure to rust. The two slit set with largest gap opening gave both 100 % re-ignition in undamaged state. The two slits with smallest gap openings (0.97 mm and 0.98 mm) gave no re-ignitions in undamaged state. This is consistent with the MESG value of 0.98 found in the PRSA for undamaged gap surface. The slit with gap opening 0.99 mm gave three re-ignitions in undamaged state.

After exposure to sea water for about three months the slits were significantly corroded. The gap openings were almost completely blocked by rust (see Figure 4-3). On all of the slit sets it was observed that a noticeable quantity of rust was blown of the gap surface by the first explosion. When the rust leaves the gap surface the effective venting area increases, consequently the maximum pressure in the primary chamber decreases. This is showed in Figure 4-1, where the pressure drop due to ten subsequent explosions is presented. But despite the decrease in rust formation on the gap surface, not a single re-ignition was observed for any of the five highly corroded slit sets, as shown in Table 4-1.

From Table 4-1 it can be seen that there is a significant variance in the mean maximum pressure for the different rusted slit sets. Especially the mean pressure for the rusted slit set of gap opening 1.00 mm stands out from the rest. The pressure measured was 1.44 bar(g) after rusting, which is approximately 1 bar less than measured for the same slit set before rusting. For all of the other slit sets there is a significant pressure increase after rusting. This will be discussed in section 4.1.2.

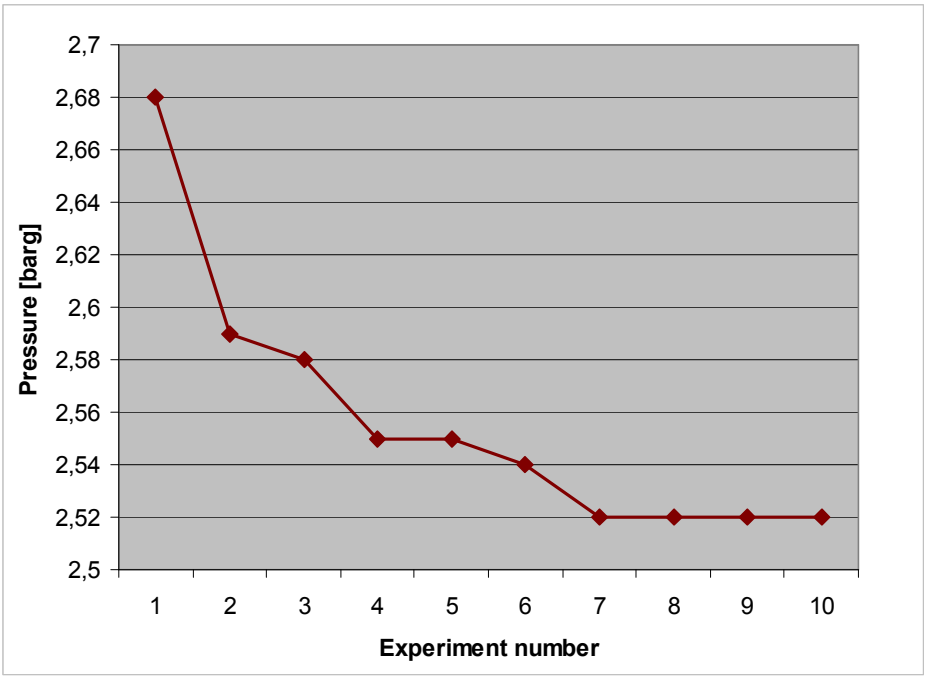

Figure 4-1: *Pressure due to ten subsequent explosions with rusted gap surface, with gap opening 1.01 mm.*

An interesting observation was made from high speed recordings taken during the explosion tests of rusted gap surfaces. Sparks were observed penetrating into the secondary chamber (see Figure 4-2). The sparks were only observed during the first explosion test of the five rusted slit sets. The experiments were recorded with 1200 frames per second. From the recordings it can be seen that the sparks has a fairly random path. The typically duration of one spark is 3 ms to 6 ms. The total time were the explosive gas mixture in the secondary chamber is exposed for sparks is varying from 10 ms to 25 ms.

Figure 4-2: *A spark inside the secondary chamber. The experiment is performed with a rusted gap surface at gap opening 1.00 mm. Photography from high speed recordings, 1200 frames/second.*

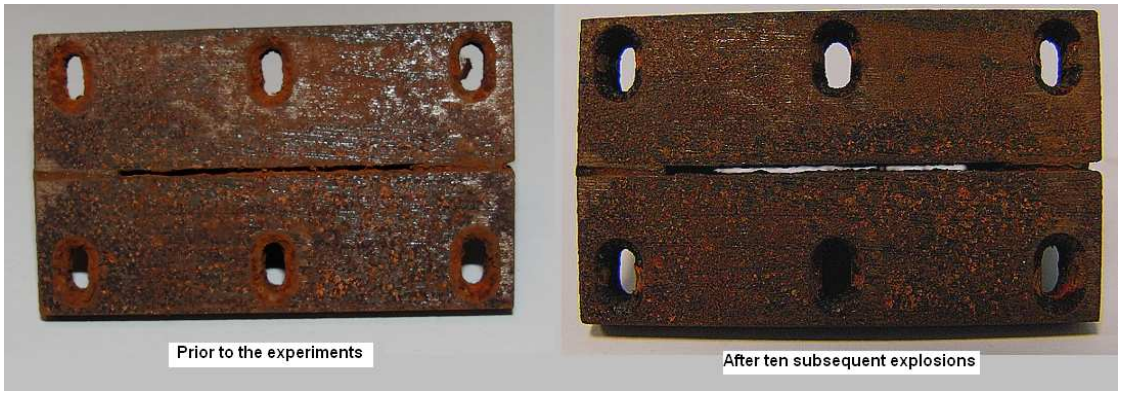

Figure 4-3: *Rusted slit at gap opening 1.01 mm prior to explosion tests on the left side and the same slit after ten subsequent explosion on the right side.*

4.1.2 Discussion

It is shown in Table 4-1 that the mean explosion pressure for gap opening 1.00 mm decreased after rusting. It is observed that some of the solid from the distance "shims" used in this slit is blown away during the ten subsequent explosions (see on the right side in Figure 4-3). By removing some of the solids, the effective venting area increases, this leads to a decrease in the maximum explosion pressure in the primary chamber. This does not affect the efficiency of the gap, because the distance between the slits (gap width) is not changed.

From the theory in section 2.6 different corrosion rates for steel in sea water is presented. The slits used in this work was placed at the sea side middle between high and low tide, this corresponds to the droplet zone in Figure 2-34 in section 2.6. This is the zone where the corrosion rate is highest, approximately 0.4 mm/ year. A typical offshore installation is placed in an environment where the corrosion rate is 0.1 mm to 0.15 mm/ year (Bardal 1994). The slits used in this work were at the sea side for 3 months, from the given corrosion rate this implies that 0.1 mm of the steel will be "eaten" up by rust on both sides of the gap surface. The new gap opening should then be 0.81 mm for the slit that had a gap opening of 1.01 mm at undamaged state. From Figure 4-3 it can be seen that this is not valid. The steel seems to swell when it corrodes, and the bond strength between the steel surface and the rust is so

strong that only the outer layer of the porous rust formation is blown away during the explosion.

From Table 4-1 it is shown that the mean pressure for four out of five slit sets have increased after the exposure for rust. An increase in the maximum pressure indicates a smaller venting area. This implies that the corroded configuration has not been totally blown out of the gap but occupies some of the venting volume. It is stated in this work and by (Grov 2010) that the maximum pressure also may increase when applying multiple crosswise grooves to previous undamaged slits. It is explained that the multiple crosswise grooves lead to greater resistance in the gap, which leads to increased initial pressure (this will be further discussed in section 4.4). This means that it is not necessarily a smaller venting area that leads to the increased maximum pressure, but it may be a result of the undefined rough configuration of the rust. But when the five gap openings are examined after ten subsequent explosions there are no doubt that four out of five gap volumes are smaller than they were at undamaged state. In this case it means that the corrosion of the gap surface both result in a smaller gap opening and a gap surface with increased roughness that most likely leads to increased initial pressure. An increase of the roughness at the gap surface combined with an increase of the initial pressure leads to highly turbulent jet of combustion gases that penetrates through the gap and into the secondary chamber. According to (Smith 1953) a jet at high speed will cause high turbulence in the external chamber. The jet gets so deformed and the energy is so dispersed that it may not reach the temperature necessary for ignition. This can be the reason why no re-ignition occurred in the secondary chamber when explosion tests were conducted with the five rusted slit sets.

From Figure 4-1 it is shown that the pressure decreases gradually from experiment one to seven. This graph is based on the pressure measurements from ten subsequent explosions of the same rusted slit set with gap opening 1.01 mm. The pressure measured for the other rusted slit sets is nearly equally distributed. It can be seen that the largest pressure drop measured is from experiment one to two. This indicates that the greatest part of the porous rust formation was blown away during the first explosion. From experiment two to seven the pressure drop is more random, but still significant. From experiment seven to ten there is no pressure drop, this indicates that all of the porous rust formation that potential could leave the gap surface under these conditions has left the gap surface. This implies that the MESG value probably will decrease from explosion one to seven, but stay constant from explosion seven to ten. Reviewed, explosion number one is the most critical, because the first ignition source that is exposed to an explosive environment normally causes the main explosion.

During the first explosion for each of the different rusted slits sets sparks were observed in the secondary chamber as shown Figure 4-2. The sparks did not ignite the explosive gas mixture in the secondary chamber in any of the experiments. It is assumed that the observed sparks is porous iron atoms that combust. From Table 2-4 it can be seen that the heat of combustion per mole O_2 consumed for [Fe] atoms is 530 kJ/ mole O_2. In section 4.9 it is shown that burning aluminum particles can ignite a gas mixture of 4.2 vol. % propane in air. An explanation for this is that the heat of combustion of the aluminum particles (1100 kJ/ mole O_2) is significantly higher than the heat of combustion of iron atoms.

The experimental work on rusted flame gap surfaces in this work differs from the work performed by (Opsvik 2010) and (Grov 2010). The flame gaps examined in this thesis has been exposed for corrosion as one flameproof unit, not as two surfaces that on a later stage has been screwed together forming a flame gap. This implies that the disputed source of error

(Grov 2010) due to how much torque one can turn the screws with, without affect the gap opening is removed. Consequently the experiments with rusted flame gap surfaces performed in this work are more realistic. They indicate that rust formation on the gap surface reduce the probability for transmission of a gas explosion from an internal chamber to an external chamber. Thus the gap efficiency increases with rust on the flame gap surface.

But more experiments are needed to investigate the effect of rust. The effect of different degree of rust formation on the flame gap surface has not been systematically investigated. Additional it could be interesting to investigate for how long period of time the slits can be exposed for a highly corrosive environment without causing a reduction of the MESG value.

4.2 Experiments performed to find the most favorable ignition point for re-ignition in the secondary chamber with multiple crosswise grooves on the gap surface

Several experiments were carried out with the gap surface of configuration PH-7.2.3 (see section 3.5.2) in order to determine the most favorable ignition position for re-ignition in the secondary chamber. To limit the number of experiments the ignition positions examined were: 5mm, 10mm, 14mm, 20mm and 25mm. These are the vertical distances between the ignition source and the gap entrance inside the primary chamber. The mean maximum pressure were measured and at the different ignition positions. The results from the measurements are presented in section 4.2.2.

4.2.1 Results

The smallest gap opening that gave 100 % re-ignition and the largest gap opening that gave 0 % re-ignition in ten subsequent experiments at a given ignition position were determined and are plotted in Figure 4-4.

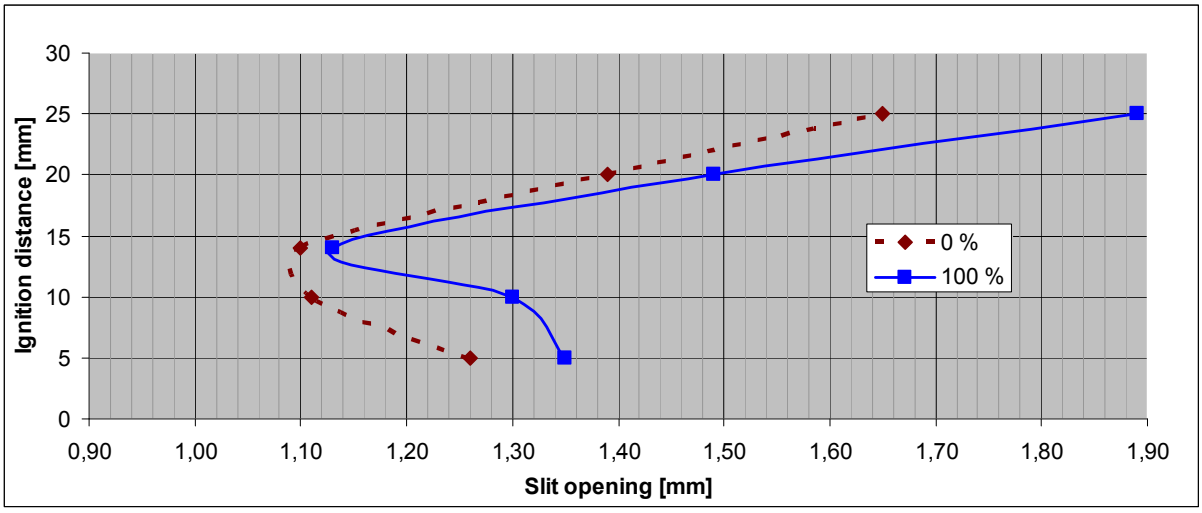

Figure 4-4: *The most favorable ignition point for re-ignition in the secondary chamber in experiments with multiple crosswise grooves (PH-7.2.3) in the gap surface. The red dotted line represents the largest gap opening that gave no re-ignition in the secondary chamber after ten subsequent*

experiments, whereas the blue line represents the smallest gap opening that gave 100 % re-ignition in ten subsequent experiments. All experiments were performed with 4.2 vol. % propane in air.

Figure 4-4 show that an ignition position at 14 mm from the gap entrance is the most favorable ignition distance for re-ignition in the secondary chamber, and consequently gives re-ignition at the smallest gap opening. This ignition position was therefore used throughout the experiments carried out in this work with slits with crosswise grooves. As shown in Figure 4-5 the optimal point for ignition at 14 mm from the gap entrance is in good agreement with the results presented by (Grov 2010) for undamaged gap surfaces.

Figure 4-4 show that an increase in the ignition distance from 14 mm towards 25 mm leads to a radical increase in the minimum gap opening that can cause a re-ignition in the secondary chamber. This will be discussed in section 4.2.3. A decrease in the ignition position from 14 mm towards 5 mm leads to an increase of the minimum gap opening that will cause re-ignition in the secondary chamber, but not to the same extend as one get if the ignition distance is greater than 14 mm.

In Figure 4-5, the results from experiments finding the ignition position giving 100 % re-ignition for the slit with multiple crosswise grooves (PH-7.2.3) are compared with formerly found values (Grov 2010) for the ignition position giving 100 % re-ignition for an undamaged slit.

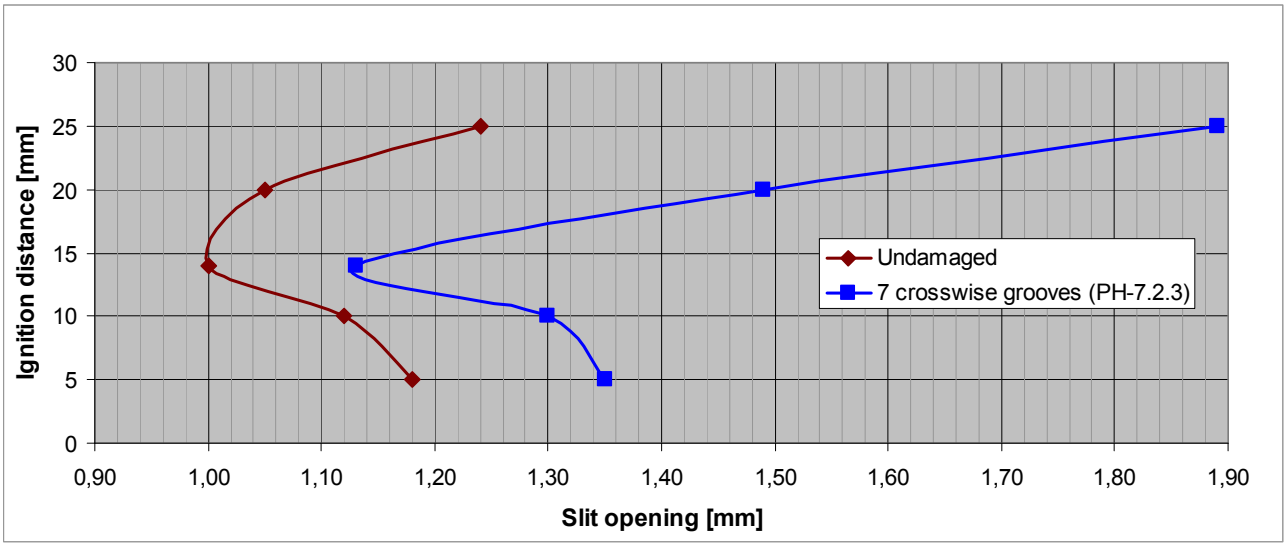

Figure 4-5: *Comparison of the most favourable ignition position for re-ignition (100 % re-ignition) in the secondary chamber for undamaged slits and slits with multiple crosswise grooves (PH-7.2.3). The mixture used was 4.2 vol. % propane in air.*

From Figure 4-5 it is shown that the ignition curve for the slit with multiple crosswise grooves correlate to some extend with the ignition curve for undamaged slit. This indicates that similar physical phenomena are applicable for various combinations of ignition distances and slit openings for the two gap configurations. But in spite of the correlation the curve for the slit with multiple crosswise grooves is placed remarkably to the right in the graph in relation to the curve for the undamaged slit. This will be discussed in section 4.2.3.

At an ignition distance of 25 mm the slit opening giving 100 % re-ignition for a gap with configuration PH-7.2.3 is 1.89 mm, this width is 52 % greater than the width (1.24 mm) that

gives 100 % re-ignition for an undamaged slit. This is a radical and surprising difference in the gap efficiency for the two diverse slit sets at ignition distances 25 mm from the gap entrance. This will be discussed in section 4.2.3.

4.2.2 Explosion pressure for various ignition distances

Table 4-2: *Mean maximum pressure for experiments performed with ignition distances of 5 mm, 10 mm, 14 mm, 20 mm and 25 mm. A total of ten subsequent experiments on each specific setup were conducted. Gap width Yi = 1.20 mm. Slit set with seven crosswise grooves used, PH-7.2.3.*

Date:	30.06.2010
Surface configuration:	PH-7.2.3
Apparatus:	PRSA
Gap width, Yi [mm]	1.20
Ignition distance, Zi [mm]	**Mean maximum pressure [barg]**
5	2.61
10	2.70
14	2.73
20	2.87
25	2.90

From Table 4-2 it is shown that the maximum pressure in the primary explosion chamber increases when the ignition source is moved vertically away from the gap entrance. This is in accordance to the results obtained by (Larsen 1998) (see theory in section 2.5.3). An interesting observation is that the pressure increases to the greatest extend when you move the ignition source from 14 mm to 20 mm, and that the ignition curve for 0 % re-ignition in Figure 4-4 shows the same tendency. It can be observed from the curve that the gap opening for no re-ignition increases in the largest extend when you move the ignition source from 14 mm to 20 mm away from the gap entrance. This indicates that there is a strong coupling between ignition distance, pressure and the probability for re-ignition.

In Figure 4-6 is the pressure development from the five experiments with a gap opening at 1.20 mm and variable ignition distance from 5 mm to 25 mm presented. An interesting observation from the graph is that the farther the ignition source is placed from the gap entrance the shorter is the time to reach a gauge pressure of zero in the primary chamber. This will be discussed in section 4.2.3

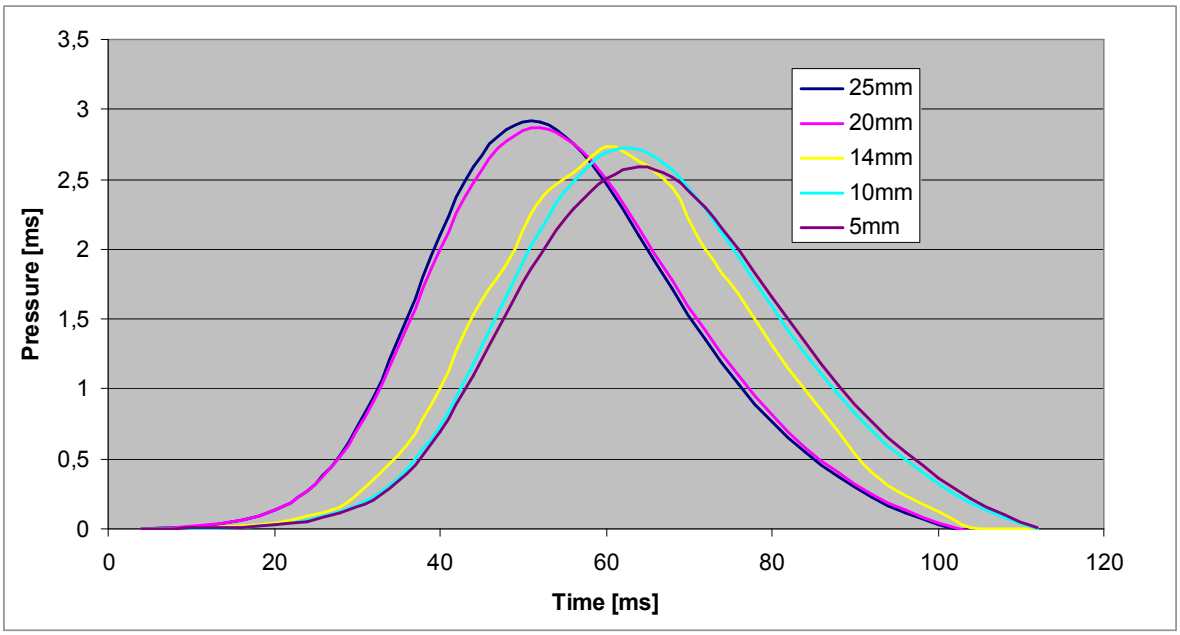

Figure 4-6: *Pressure development in the primary chamber for explosion with ignition distances 5 mm, 10 mm, 14 mm, 20 mm and 25 mm. Gap width Yi =1, 20 mm and 4,20 vol % propane- air concentration. Slit set with seven crosswise grooves used, PH-7.2.3.*

4.2.3 Discussion

The experiments performed for finding the ignition point most favorable for re-ignition in the secondary chamber for slits with multiple crosswise grooves is based on existing literature, (Larsen 1998) and (Grov 2010). Larsen stated that there exist a "most dangerous ignition position", and that the maximum pressure increased when the ignition source was moved from the gap entrance towards the center of the primary chamber (see section 2.5.3). The experimental findings in this work correspond to Larsen's results.

In Figure 4-5 the ignition curves for the slit with multiple crosswise grooves and the curve for the undamaged slit are compared. The curve for multiple crosswise grooves is located at remarkably higher slit opening values in the graph than the curve for undamaged slits at the same ignition distances. This means that the two different surface configurations influence the flow patterns of the hot combustion gases that penetrate through the slit on diverse ways. It is shown in this work (see section 4.4) and by (Grov 2010) that the mean maximum explosion pressure is significantly higher for an explosion performed with venting through a slit with multiple crosswise grooves than venting through an undamaged slit. An increasing pressure indicates increasing resistance in the gap. The increase in resistance is probably caused by the highly rough surface of the slit, due to crosswise grooves (see section 2.3.9). Rough surfaces give rise to turbulent flow. When the hot combustion gases are forced into the external chamber at a higher turbulent state, they will be dispersed over a larger area and the probability for re-ignition decreases, as discussed in section 4.4. The great difference in location of the curve for undamaged slit surface and the slit surface with multiple crosswise grooves can therefore be explained by the difference in turbulence level caused by the rough surface, the pressure difference for the two gap configurations.

From pressure measurements presented in Figure 4-6 it is shown that the pressure increases when the ignition source is moved away from the gap entrance, this is in good correlation

with Larsen's results presented in section 2.5.3. This implies that the same physical mechanism is applicable in relation to pressure build up for an explosion in a vessel with venting through a slit surface with crosswise grooves, as a slit with undamaged surface. When the ignition source is moved away from the gap inlet and towards center of the primary chamber, the flame front will reach the gap opening and the wall at a later stage than it would do if the ignition source was close to the gap inlet. As soon as the flame front reaches the wall there will be chain terminated reactions (see section 2.3.4, elementary reactions) and the combustion process will end by the wall. The consequence of the limited combustion process is that it takes longer time to combust the total volume of explosive mixture in the primary chamber, and the rate of hot combustion gases that leaves the primary chamber per millisecond decreases. Accordingly the pressure build up is not as great as it would have been if the ignition source was in the center of the chamber. The flame front had then reacted as a spherical flame ball throughout the entire volume and the chain termination (see section 2.3.4) reaction had started at a later stage.

Another possible explanation for the increase in explosion pressure when the ignition source is moved towards the center of the chamber is that a greater amount of unburned gas is forced through flame gap when the ignition source is placed further from the gap opening. The cold unburned gas mixture requires a greater force to be pushed through the slit than the warm combustion gases, due to the difference in density of the gases.

From Figure 4-6 it is shown that the pressure increases with increasing ignition distance, but one can also observe from this figure that the time it takes to reach a gauge pressure of zero increases with decreasing ignition distance. This indicates that the flux of combustion gases through the slit increase with increasing ignition distance from the gap entrance in the primary chamber. This is in agreement with the theory Larsen presented (see section 2.5.3), where he stated that an increase in ignition distance leads to increase of the pressure, which further leads to an increase of the flow through the gap. The faster the primary chamber is emptied, the shorter is the time for cooling of the hot combustion gases inside the chamber and the slit. This means that a larger quantity of hot combustion gases reaches the explosive gas mixture in the external chamber within a limited time when the ignition distance and consequently the pressure is increased. But as the velocity of the penetrating jet increases through the gap the turbulence-build up above the gap opening also increases. If the velocity of the hot combustion gases causes a great deal of turbulence, the energy that possibly ignites the external mixture will be dispersed over a larger area above the gap outlet and the probability for a re-ignition decreases, this is supported by (Smith 1953). Thus the ignition position of 14 mm vertically from the gap entrance is a critical ignition position. At this point the interaction between the pressure, the velocity, and the turbulence level of the hot combustion gases that penetrates through the slit favors an ignition of the explosive mixture in the external chamber.

4.3 Results and discussion from temperature measurements above the flame gap

Some modifications were made on the PRSA to be able to measure the temperature in the secondary chamber in different altitudes above the flame gap. It was performed temperature measurement in three different heights, 1 mm, 2 cm and 4 cm above the flame gap opening. Several experiments were performed with a slit with undamaged surface and the slit with multiple crosswise grooves (PH-7.2.3). It was carried out a minimum of five identical experiments on every specific set up to verify that the measured temperature was repetitive. All of the temperatures presented in this section descend from explosions in the primary chamber that didn't cause a re-ignition in the secondary chamber.

4.3.1 Results

Table 4-3: *The mean temperature measured at three different altitudes (1mm, 2cm and 4 cm) vertically above the gap opening. The surface examined is the undamaged gap surface and the gap surfaces with seven multiple crosswise grooves. The mean temperature is based on a minimum of five subsequent explosions in the primary chamber.*

Date:	**19.05-27.05.2010**		
Apparatus	**PRSA**		
Gap opening [mm]	**0.98 mm**		
	Mean temperature °C		
Surface configuration	**1mm**	**2cm**	**4cm**
Undamaged	634	317.4	220.6
PH-7.2.3	328.3	131.2	86.4

In Table 4-3 the temperatures measured in the experiments carried out with the undamaged slit and the slit with multiple crosswise grooves are presented. It is the hot combustion products that penetrate from the primary chamber and into to the secondary chamber that leads to the temperature rise and possible re-ignition in the secondary chamber. It can be seen from the table that the temperature above the two different gap surfaces differs significantly. The temperature is 40 to 60 percent higher for the hot combustion gases that penetrate through the undamaged slit compared to the hot combustion gas that penetrates through the slit with multiple crosswise grooves. This is a remarkable temperature difference above the flame gap, which will be discussed in section 4.3.2.

In Figure 4-7 the temperature development at different altitudes vertically above the gap opening for the undamaged slit and the slit with crosswise grooves are shown. Note that the temperature measurements originate from several experiments that subsequently are united and compared in these graphs. From the figure it can be seen that the temperature increases rapidly at all altitudes during an explosion in the primary chamber. The maximum temperatures reached are significant higher in all altitudes for the undamaged slit than the slit with multiple crosswise grooves, as shown in Table 4-3. This will be further discussed in section 4.3.2.

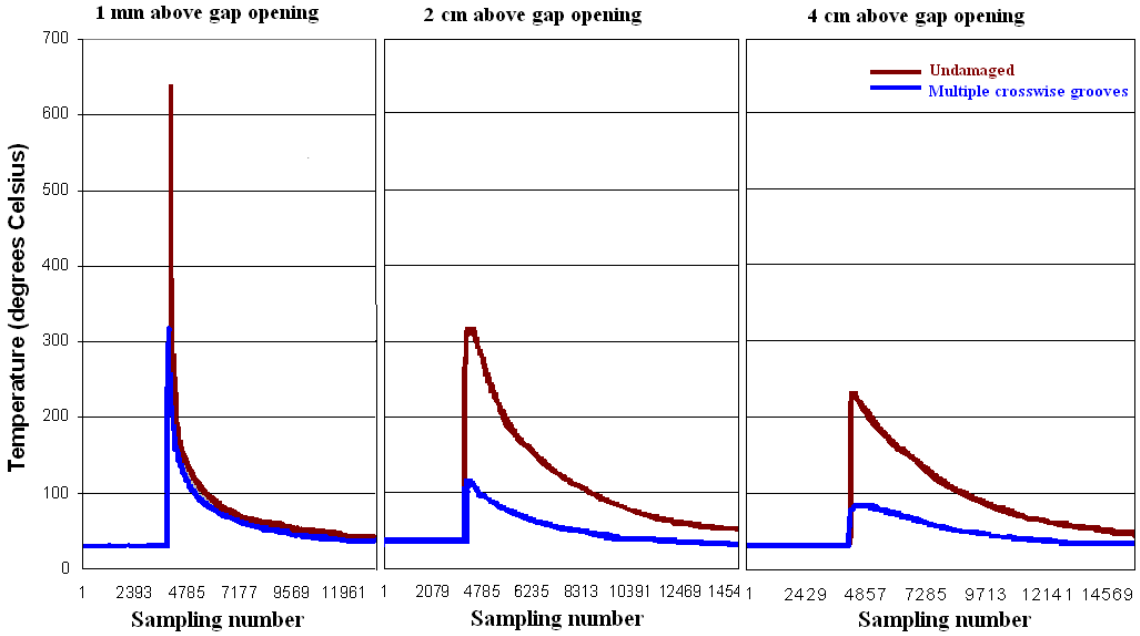

Figure 4-7: *Difference in mean temperatures for undamaged slit and slit with configuration PH-7.2.3 at gap opening 1.00 mm.*

4.3.2 Discussion

The thermocouples used in the experiments are thermocouple type K, and can measure temperatures in a range of -200 °C to 1350 °C. In an explosion there is a rapid temperature rise as shown in Figure 4-7. These thermocouples are not designed to measure temperatures in an explosion. The given temperatures may therefore deviate from the actual temperatures, but it is assumed that the temperature difference between the different experiments is correct. The temperature measurements are therefore considered as valid.

The reason for measure the temperature 1 millimeter above the gap opening was to get as close to the gap as possible, and consequently measure the temperature of the hot combustion gas before they get influenced by the cold gas in the secondary chamber. This can possibly show if the rate of cooling inside the gap is of any importance, or if the cooling process mainly appears a distance above the gap opening. From the measurements performed in this work it can be seen that the mean temperature differs with approximately 300 degree Celsius one millimeter above the gap opening for the two different gap configurations. This is a very surprising finding, which must have its origin in totally different physical mechanisms of the hot fluid flow through the gaps. It is a clear indication that the cooling process inside the flame gap of the slit with seven perforated crosswise grooves is of great importance, and that the cooling process inside the undamaged gap is remarkably less important. This information will be used in the further investigation of the gap surfaces with multiple crosswise grooves.

Figure 4-7 show that the cooling process is of the greatest extent between the altitudes of 1 mm and 2 cm above the gap opening for the undamaged slit and the slit with multiple crosswise grooves. But the temperature recorded 1 mm above the gap opening for the slit with multiple crosswise grooves is noticeably lower than for the undamaged slit. This observation also suggests that the main cooling process for the slit with multiple crosswise grooves occurs inside the flame gap. To investigate this phenomenon the temperature should optimally have been measured in different positions inside the flame gap, but this is practically difficult.

4.4 Comparison of pressure measurements from slit with multiple crosswise grooves (PH-7.2.3) and an undamaged slit

In this section pressure measurement from experiments with crosswise grooves on the gap surfaces will be compared with pressure measurement from slits with undamaged gap surface. All of the experiments are performed at the most favorable ignition position for re-ignition (14 mm from gap entrance). It was carried out a minimum of ten subsequent experiments on each specific setup to verify the pressure measurement. The results from the experiments are summarized in Table 4-4.

4.4.1 Results

Table 4-4: *Mean pressure from experiments performed with undamaged slit and the slit with configuration PH-7.2.3 at gap openings 0.98mm and 1.10mm.*

Date:	27.04-27.05.2010		
Apparatus:	PRSA		
Surface configuration	**Gap opening, Yi [mm]**	**Ignition distance, Zi [mm]**	**Mean max pressure [barg]**
Undamaged	0.98 (MESG)	14	2.40
PH-7.2.3	0.98	14	3.20
Undamaged	1.10	14	2.25
PH-7.2.3	1.10 (MESG)	14	3.03

From Table 4-4 it can be seen that the mean maximum pressure for the undamaged slits are significantly lower than the mean maximum pressure for the slits with multiple crosswise grooves. Even at an gap opening that is 0.12 mm wider the pressure build up is 0.63 bar(g) greater for the slit with configuration PH-7.2.3, compared with an undamaged slit. This indicates that there is a decisive effect of the crosswise grooves that leads to more resistance in the gap. This will be further discussed in section 4.4.2.

From Figure 4-8 it is shown that the pressure development for the slit configuration PH-7.2.3 differs from the pressure development for an undamaged slit at the same gap opening. The first 25 milliseconds the pressure development is approximately equal for the two slits, from 25 milliseconds to the peak the pressure increases more rapid for the slit with multiple crosswise grooves. From Table 4-4 it is shown that the mean maximum pressure is 0.80 bar higher for slit with configuration PH-7.2.3 than for undamaged slits. From the pressure development it can also be observed that it takes approximately 20 milliseconds more to reach a gauge pressure of zero in the primary chamber for the surface with crosswise grooves, than it does for the slit with undamaged gap surface. This will be further debated in section 4.4.2.

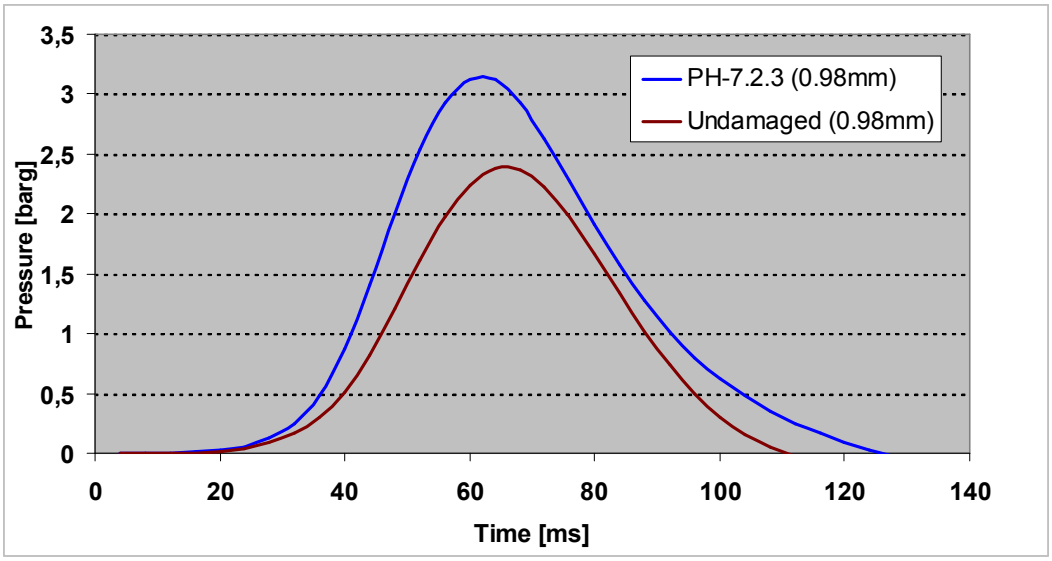

Figure 4-8: *Pressure development in the primary chamber for explosions performed with undamaged gap surface and gap surface with configuration PH-7.2.3. The gap opening is set to a width of 0.98 mm at both slit configurations. The ignition position is 14 mm.*

From Figure 4-9 it can be seen that the maximum pressure build up for the slit with configuration PH- 7.2.3 is noticeable higher than the maximum pressure build up for the undamaged slit with gap openings at their respective MESG values. The maximum pressure is approximately 0.6 bar higher for the slit with configuration PH-7.2.3, despite the fact that the gap opening at MESG for this configuration is 0.12 mm greater than for an undamaged slit. Consequently the venting area is significantly larger for the slit with crosswise grooves. It can also be seen from Figure 4-9 that it takes approximately 10 milliseconds more to reach a gauge pressure of zero for the slit with configuration PH-7.2.3 than it does for the undamaged slit.

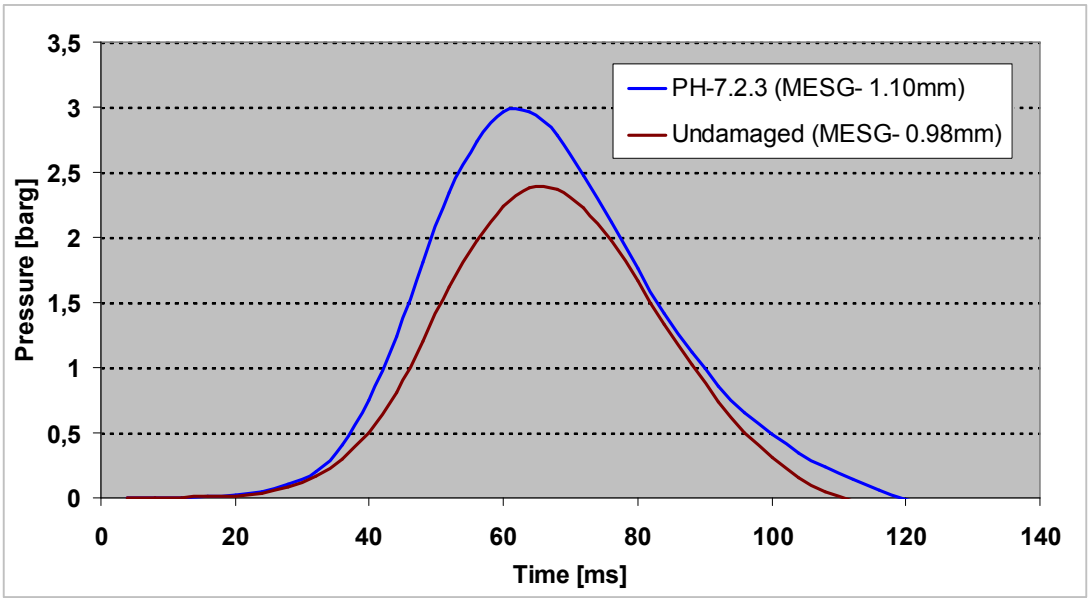

Figure 4-9: *Pressure development in the primary chamber for explosions performed with an undamaged gap surface and a gap surface with configuration PH-7.2.3. The gap opening is at their respective MESG values (0.98 mm for undamaged and 1.10 mm for PH-7.2.3), the ignition position is Zi: 14 mm.*

4.4.2 Discussion

From several experiments performed in this work and by (Grov 2010) it is proved that a slit surface with multiple crosswise grooves reduce the probability for re-ignition of a surrounding explosive gas mixture. It is stated that the maximum explosion pressure in the primary chamber increases with crosswise grooves on the gap surface. An increase in the maximum pressure indicates that the flowing gases meet more resistance through the gap. This resistance must be caused by the rough surface which leads to more friction in the gap.

(Grov 2010) proposed in his master thesis that the increased pressure in the primary chamber due venting through a slit with crosswise grooves lead to a greater velocity of the hot combustion gases through the gap, this is in disagreement with the experimental observations and calculations (see Appendix B) made in this thesis. The statement for the disagreement is given below.

In fluid dynamics the friction factor, f is used. This is a dimensionless number for the friction (see section 2.3.9). When the pressure drop over a pipe is calculated the friction factor adjusts for the pressure loss caused by resistance at the gap wall. Let us consider what effect the crosswise grooves have on the friction factor, and consequently the velocity of the hot combustion gases through the gap and the pressure in the primary chamber. From section 2.3.9 it can be seen that the friction factor is a function of the relative roughness, k/D. If one look into the configuration of the slit with crosswise grooves, it can be seen that the grooves are abnormally large in relation to the total diameter of the gap (see Figure 4-10). This gives an extraordinary high value of the relative roughness. This indicates that the resistance in the gap due to wall friction is extraordinary great. The consequence of the great resistance is that the combustion gases struggle more to get through the gap, and consequently the flux through the gap decreases. A decrease in the flux of combustion gases through the gap means that the primary chamber empties more slowly, which leads to a greater maximum explosion pressure in the primary chamber. The pressure build up in the chamber is therefore significantly larger when the venting is performed with a slit with multiple crosswise grooves compared to an undamaged slit. The results presented in Figure 4-8 verifies this, it can be seen that it takes approximately 20 milliseconds more to reach gauge pressure of zero for the slit with multiple crosswise grooves than it does for a undamaged slit. This indicates that the velocity and consequently the flux through the gap is less for slits with crosswise grooves. Consequently it takes more time to empty the primary chamber for hot combustion gases due to venting with a slit surface with multiple crosswise grooves.

There are several possible consequences of a reduction in the flux of warm combustion gases out of the primary chamber. If the flux of warm combustion gases is reduced, the ignition source is to some extend reduced, because there will be less warm gases exposed to the explosive atmosphere in the secondary chamber at any given time. The heat will not accumulate in such great extend in the turbulent and “cold” environment straight above the gap opening.

Another consequence of the reduced flux is that the warm combustion gases got more time to be cooled down before they enter the secondary chamber. This is in agreement with the temperature measurements presented in section 0. The resistance in the gap prevents a large quantity of hot gases to enter the secondary chamber immediately after the combustion. This means that the hot combustion gases have to stay in the primary chamber some milliseconds more when using a slit with multiple crosswise grooves compared to an undamaged slit.

These milliseconds can be enough to cool the hot gases sufficient down and may contribute to prevent a re-ignition of the surrounding explosive atmosphere.

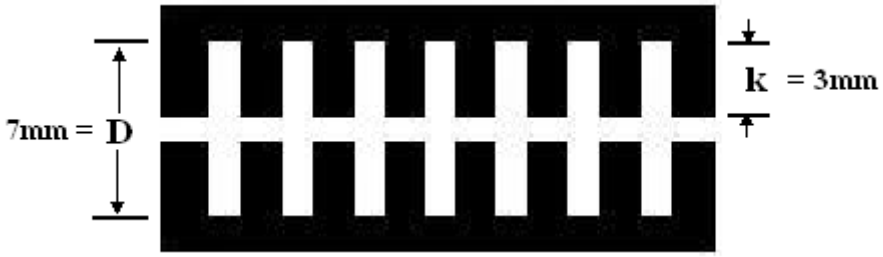

Figure 4-10: *Slit with multiple crosswise grooves. The height of the groove, k is called the roughness parameter and D is total diameter from the bottom of the grooves.*

4.5 High speed camera recordings- comparison of slit with multiple crosswise grooves and undamaged slit

The reason for shooting several experiments with high speed camera was to investigate if there were any difference in the re-ignition process for undamaged gap surface and multiple crosswise grooves. The gap opening was set to a width close to the MESG value (0.02-0.03 mm greater) for the two different gap surfaces. The camera used was a Casio EX-F1, that can record 1200 frames per second (see Appendix C-1).

4.5.1 Results

From ten recorded experiments with an undamaged gap surface it was stated that the re-ignition occurred as a detached sphere at a given altitude above the gap opening. From Figure 4-11 it can be seen that the re-ignition occurs approximately one centimeter above the gap opening. The gap opening is set to 1.02 mm, which is a gap opening 0.04 mm greater than the MESG value for an undamaged slit.

Figure 4-11: *Re-ignition with undamaged at gap opening 1.02 mm. 1200 frames/sec.*

An interesting observation was made when shooting the re-ignition process for the multiple crosswise grooves. The re-ignition occurred at a lower altitude than for the undamaged slit. The observed re-ignition looks like a jet penetrating out from the flame gap (Figure 4-12), and

not as a detached sphere above the gap opening, which was observed in the experiments performed with the undamaged slits.

Figure 4-12: *Re-ignition with slit configuration PH-7.2.3 at gap opening 1.12 mm. 1200 frames/sec.*

4.5.2 Discussion

In the experiments performed in the present work two events of re-ignitions is observed in the secondary chamber, through high speed recordings. During the explosion tests with an undamaged slit a detached sphere where the re-ignition occurred is observed, this is in accordance to Phillips theory that is discussed in section 2.5.1. He described that the ignition occurred at the head of a spherical vortex a given distance away from the orifice (see Figure 2-19). From the recordings of the explosion where a slit with seven perforated crosswise grooves were used it was observed that the ignition occurred at a lower altitude. The shape of the ignition area looked like a jet that penetrated out from the gap opening and not like an ignition at the head of the vortex as described by Phillips in section 2.5.1.

From the review of (Tennekes and Lumley 1994) theory (see section 2.3.8) they introduced the terms of different regions in the hot jet that penetrates out from the primary chamber. Tennekes and Lumley stated that the hot jet would not ignite the mixture completely up to the gap opening in the secondary chamber but a given distance from it, as Phillips described. They explained that the time of contact between hot and cold gas is to short and may be insufficient for igniting the explosive gas mixture close to the gap exit because of the extremely high velocity and the rapid expansion of the hot flowing gas. This is in accordance to the high speed recordings from the experiments performed with undamaged slit, but it is not in accordance to the observations made from the recordings of the re-ignition process for the slit with multiple crosswise grooves, although the initial pressure is noticeably higher in the primary chamber. Therefore it can be stated that the theory of Tennekes and Lumley is not valid for any hot jet that penetrates through a narrow hole, the configuration of the gap surface has to be evaluated.

Tennekes and Lumley theory of regions which is described in section 2.3.8 is restated below. The theory now considers the slit with multiple crosswise grooves and how the gas flows through it (an illustration is given in Figure 4-13). When there is an ignition inside the primary chamber, first cold unburned gas and then hot combustion gas will start to flow through the slit. At a given distance inside the slit the flame will be quenched and only hot

combustion products will penetrate through the slit. As soon as the flame is quenched and the jet of hot combustion gas enters the next groove the flow start to behave as it would do if it had emerged from the gap exit at undamaged state. This means that the jet moves from the core region to the transition region inside the slit and not at the exit of the slit. Consequently there is no longer constant velocity, temperature and concentration in the core of the penetrating jet inside the slit. The turbulence intensity increases and consequently the interference between hot and cold gas and the fluid- wall contact area increases through the slit. These mechanisms lead to a more efficient cooling process and it leads to a lower jet temperature which is supported by the results in section 0 and the theory of (Ceylan and Kelbaliyev 2003) in section 2.4.1. From the equation (2.14) by Phillips in section 2.5.1 a low value of T favors no combustion in the secondary chamber. But if the gap opening is sufficiently wide (1.10 mm) the flame can penetrate a small distance further into the gap and the temperature will not decrease in the same extend through the gap. This, combined with the disintegrated fluid path through the flame gap, can give rise to a hot jet that achieve the conditions that are favorable for re-ignition at a lower altitude above the gap opening than what an undamaged gap surface would achieve (see Figure 4-12). This may explain the observed re-ignition close to the gap opening under explosion tests with multiple crosswise grooves. It should be mentioned that this is only a suggestion for the explanation of the great difference in the re-ignition scenarios for the two slit configurations.

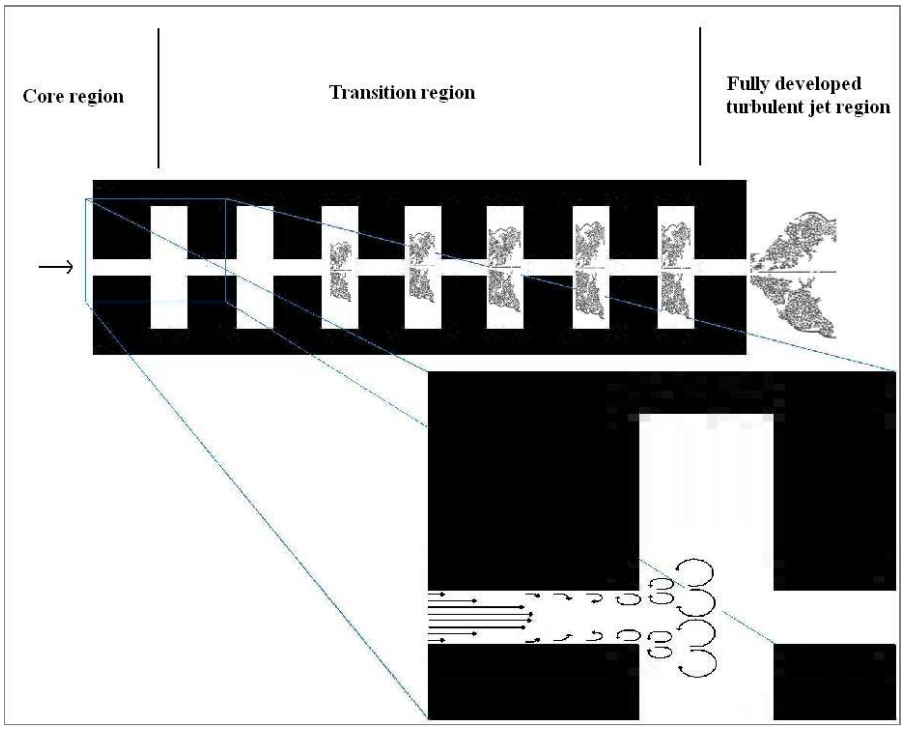

Figure 4-13: *Suggestion for distribution of regions in a slit with multiple crosswise grooves. The Core region is characterized with constant velocity, temperature and concentration in the core of the jet. The transition region is where the jet develops to a fully turbulent jet. The fully developed jet is the region where the cooling of the hot combustion gases is at the maximum.*

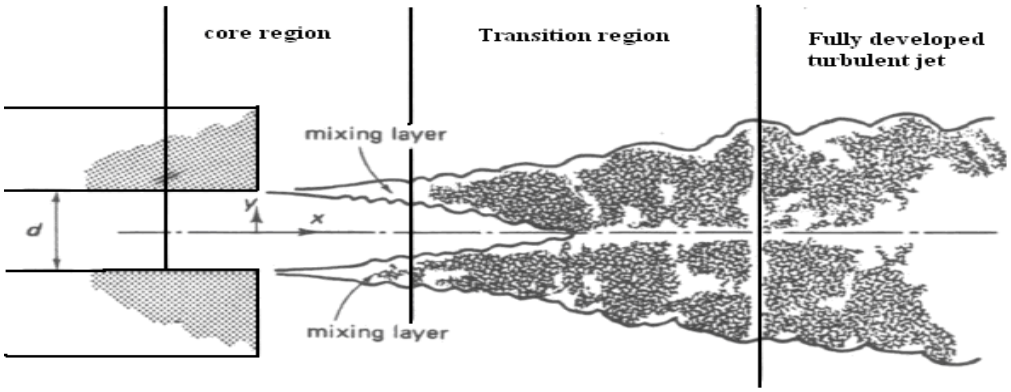

Figure 4-14: *Distribution of the core, transition and fully developed turbulence jet regions at an undamaged slit. From (Tennekes and Lumley 1994).*

Another possible explanation of the two different re-ignition scenarios is that the flame penetrates straight through the slit with configuration PH-7.2.3. Then the observation is not a re-ignition in the secondary chamber but a lasting flame that penetrates from the primary chamber to the secondary chamber. The MESG value for the slit with configuration PH-7.2.3 is 0.12 mm greater than the MESG value for the slit with undamaged gap surface. This implies that the passage for a penetrating flame is significantly larger for the slit with multiple crosswise grooves than for the slit with undamaged gap surface at their respective MESG values. So a possible solution for the two different ignition scenarios in the secondary chamber is that if the MESG value of 1.10 mm is exceeded for the slit configuration PH-7.2.3, it is not necessarily the hot combustion gases that causes an ignition in the secondary chamber, but it may be a flame that penetrates straight through the slit from the primary chamber, due to the "wide" gap opening. But this is a controversial theory due to the great pressure behind the flame and the rough flame gap surface which combined causes a great deal of turbulence. Literature reviewed in section 2.5.2 by (Ballal and Lefebvre 1975) agrees up on the fact that an increase in the turbulence increases the probability for quenching a flame.

4.6 Result and discussion from experiments performed with slits with different depths on the multiple crosswise grooves

Several experiments were performed on each slit configuration to locate the different MESG values. Ten subsequent explosions with no re-ignition in the secondary chamber verify the MESG and from these ten experiments the mean pressure is recorded. The specification of the different slits can be found in section 3.5.5. The results from the experiments are shown in Table 4-5.

4.6.1 Results

Table 4-5: *MESG values found and pressure measured from experiments performed with slits with different depths on the seven crosswise grooves.*

Date:	23.05-09.07.2010		
Apparatus:	PRSA		
Surface configuration	**Zi [mm]**	**MESG [mm]**	**Mean Pressure at MESG [barg]**
PH-7.2.3	14	1.10	2.97
PH-7.2.2	14	1.05	2.78
PH-7.2.1	14	1.09	2.05 (N/A)
PH-7.2.0,5	14	1.08	2.54
Undamaged	14	0.98	1.93

From Table 4-5 it is shown that all of the tested slits with crosswise grooves have a higher MESG than the undamaged slit set. The slit with the highest MESG is the slit with the deepest crosswise grooves. This is the slit with configuration PH-7.2.3, but it can be seen from the table that there is no clear correlation between the depth of the grooves and the MESG found. An example of this is that the MESG for the slit set with grooves of 0.5 mm depth, is 0.03 mm greater than the slit set with grooves of 2 mm depth.

The mean maximum pressure in the primary chamber for the explosions performed with grooves of different depth is shown in Table 4-5. If the pressure measurement for the slit with configuration PH-7.2.1 is disregarded, it can be seen that there is a coupling between the depth of the grooves and the mean maximum pressure at MESG in the primary chamber. The result from the experiments carried out indicates that pressure decreases with decreasing depth of the perforated crosswise grooves. The pressure measurements for the slit with configuration PH-7.2.1 can be disregarded because the pressure gauge failed in five out of ten experiments and showed abnormal pressure values for the rest of the experiments.

To verify that there was a correlation between the depth of crosswise grooves and the pressure, the different slit sets were fastened at a constant gap opening of 1.05 mm and the pressure was measured. The result from these experiments is presented in Table 4-6 and Figure 4-15.

Table 4-6: *Pressured measured from experiments carried out with a gap opening at 1.05 mm and slits with various depths on the perforated crosswise grooves.*

Date:	02.07-09.07.2010		
Apparatus:	PRSA		
Surface configuration (depth of grooves [mm])	**Yi[mm]**	**Zi [mm]**	**Mean Pressure [barg]**
PH-7.2.3	1.05	14	3.11
PH-7.2.2	1.05	14	2.78
PH-7.2.1	1.05	14	2.57
PH-7.2.0,5	1.05	14	2.55
Undamaged	1.05	14	1.93

From the experiments shown in Table 4-6 it is stated that the pressure increases with increasing depth of the perforated crosswise grooves. From the values in the table it can be seen that the pressure increases with 32.1 % when adding seven crosswise grooves with a depth of 0.5 mm and a width of 2 mm to an undamaged slit surface. The pressure increases to the greatest extend when the depths of the grooves are changed from 2 mm to 3 mm. Then the pressure in the primary chamber increases with approximately 12 %. The MESG value also shows the same tendency and increases to the greatest extend when changing from grooves with depth of 2 mm to a depth of 3 mm.

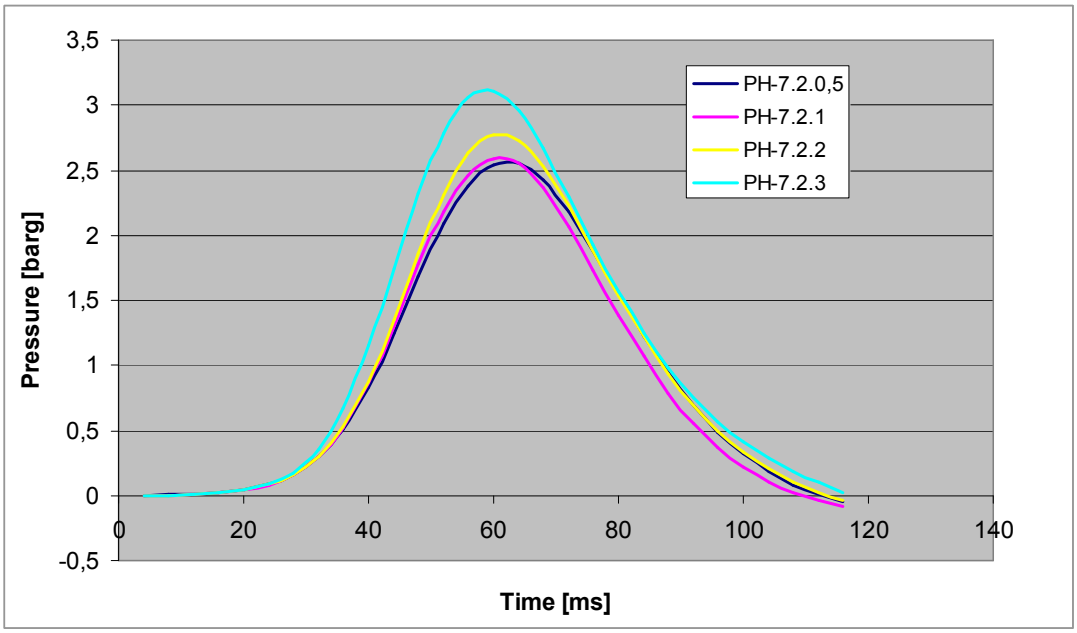

Figure 4-15: *Pressure development with a gap opening of 1.05 mm for slits with different depths on the perforated crosswise grooves. The light blue curve is for crosswise grooves with a depth of 3 mm, the yellow is for 2 mm, the pink is for 1 mm and the dark blue for 0.5 mm.*

From Figure 4-15 it is shown that the first seven milliseconds the pressure build up is approximately the same for every slit, subsequent the pressure increases the most for the slit with deepest grooves and the least for the slit with the shallowest grooves.

4.6.2 Discussion

From the experiments performed in this section it is stated that the pressure increases with increasing depth of the grooves. This is in accordance with the literature reviewed in section 2.4.1, where an increase in the relative roughness leads to a greater friction factor. An increase in the friction factor implies increased resistance through the gap, which leads to a decrease in the velocity of the hot combustion gases. Calculations that support this is presented in Appendix B. As discussed earlier a decrease in the flux of hot combustion products from the primary chamber, leads to a greater pressure drop inside the channel and a greater maximum pressure in the primary chamber.

The general improvement of the gap efficiency when adding multiple crosswise grooves to the gap surface can also be a result of the increased heat transfer to the wall, due to the increased fluid-wall contact area when the flow becomes more turbulent, as described in section 2.4.1. The equations in section 2.4.1 presented by (Ceylan and Kelbaliyev 2003) shows that surface roughness is of great importance considering the heat transfer to the wall in a turbulent flow. Ceylan and Kelbaliyev stated that if the relative roughness of the wall is greater than the thickness of the viscous sub-layer inside the tube, then the turbulence in the boundary layer becomes dominant. The thickness of the boundary layer may be estimated from equation (2.7). From calculation shown in Appendix B it can be seen that the relative roughness is greater than the thickness of the boundary layer for all of the four slits with different depth on the crosswise grooves. Ceylan and Kelbaliyev also proclaimed that the flow close to the wall would be fully rough turbulent and independent of the Reynolds number if the relative roughness was, $\xi \geq 2000 / Re$. As a result of this they presented a simple equation (2.8) for estimation of the friction factor, which is only dependent on the relative roughness. The four slits examined in this section fulfil these requirements (see Appendix B). The flow inside the slits may therefore be counted as a rough turbulent flow. All reviewed literature agrees that turbulent flow increases the heat transfer from fluid to solid. (Mottahed and Molki 1996) proposed that the heat transfer coefficient may increase up to 350 % if a smooth pipe wall is roughened. It is therefore conceivable that heat loss to the wall is a significant phenomenon that contributes to improve of the gap efficiency for all of the four slit sets with multiple crosswise grooves.

The temperature measurements carried out in this work (presented in section 4.3.1) gave an interesting and surprising result that may support the importance of heat transfer to the wall through the gap. The temperature measured 1 mm above the gap opening decreased with approximately 50 % when the undamaged slit set was replaced by a slit set with seven crosswise grooves, PH-7.2.3. The thermocouples were placed as close to the gap opening as possible to record the temperature of the hot gas before it started to mix with cold gas in the external chamber. A difference of 300 degrees Celsius at position 1 mm above the gap opening for the two slit sets indicates that there is an important cooling phenomenon inside the slit, which contributes to the temperature reduction as discussed in section 0.

The pressure gauge failed in 5 out of 10 experiments carried out for the slit with configuration PH-7.2.1. In addition the pressure gauge showed abnormal values for the rest of the experiments. The mean maximum pressure may therefore be ignored for these experiments.

The experiments performed in this section shows that an increase in the depth of the grooves leads to an increase in the maximum pressure in the primary chamber. How the pressure conducts at greater depths is unknown. There is possibly a limiting depth of the grooves

where the pressure appears to stabilize; at this point an increase in depth does not affect the resistance in the gap either. For further work it could be interesting to see how much deeper the grooves can be before the pressure and additional the MESG value stabilizes or decreases.

4.7 Result and discussion from experiments performed with slits with different width on the perforating crosswise grooves

A slit with seven crosswise grooves of 1 mm width and depth of 3 mm were constructed. This was to investigate if there was any clear difference in the gap efficiency between a slit with seven crosswise grooves of 2 mm width and a slit with grooves of 1 mm width. The specification of the slit can be found in section 3.5.6. The result from the experiments carried out is presented in Table 4-7.

4.7.1 Results

Table 4-7: *Comparison of slits with different width of the perforating crosswise grooves, in addition the slit with undamaged gap surface is presented.*

Date:	02.07-09.07.2010		
Apparatus:	PRSA		
Surface configuration	**Zi [mm]**	**MESG [mm]**	**Mean Pressure at MESG [barg]**
PH-7.2.3	14	1.10	3.03
PH-7.1.3	14	1.00	2.48
Undamaged	14	0.98	2.40

From Table 4-7 it can be seen that the MESG for the slit width configuration is found to be 1.00 mm. This is a MESG that is 0.02 mm greater than the MESG for an undamaged slit surface, but 0.10 mm lower than the value for a slit with seven crosswise grooves of width 2 mm and depth 3 mm. The MESG value drops 9 % due to a decrease in the width of 1 mm. This indicates that the width of the crosswise grooves is of great importance due to the gaps ability to prevent a transmission of an explosion.

The mean pressure for the slit with configuration PH-7.1.3 is 16.5 % lower than the mean pressure measured of the slit with grooves that are 1 mm wider. This indicates that the resistance in the gap decreases with decreasing width of the perforating crosswise grooves.

In Figure 4-16 the pressure development for the different slit sets are compared. The gap opening is constant at 0.98 mm. The maximum pressure for the slit set with grooves of width 1 mm is approximately 24 % lower than the maximum pressure for the slit set with grooves of 2 mm at gap opening 0.98 mm. This is a significant difference that will be discussed in section 4.7.2. From Figure 4-16 it can be seen that the time for the pressure to reach its maximum is the least for the slit with the widest grooves, despite the slit with the widest grooves uses longest time to reach a gauge pressure of zero. It uses approximately 10 ms longer than the slit with crosswise grooves of 1 mm width. This implies that the time it takes to empty the primary chamber for hot combustion gases is greatest when the venting is performed with the slit set of the widest perforating crosswise grooves.

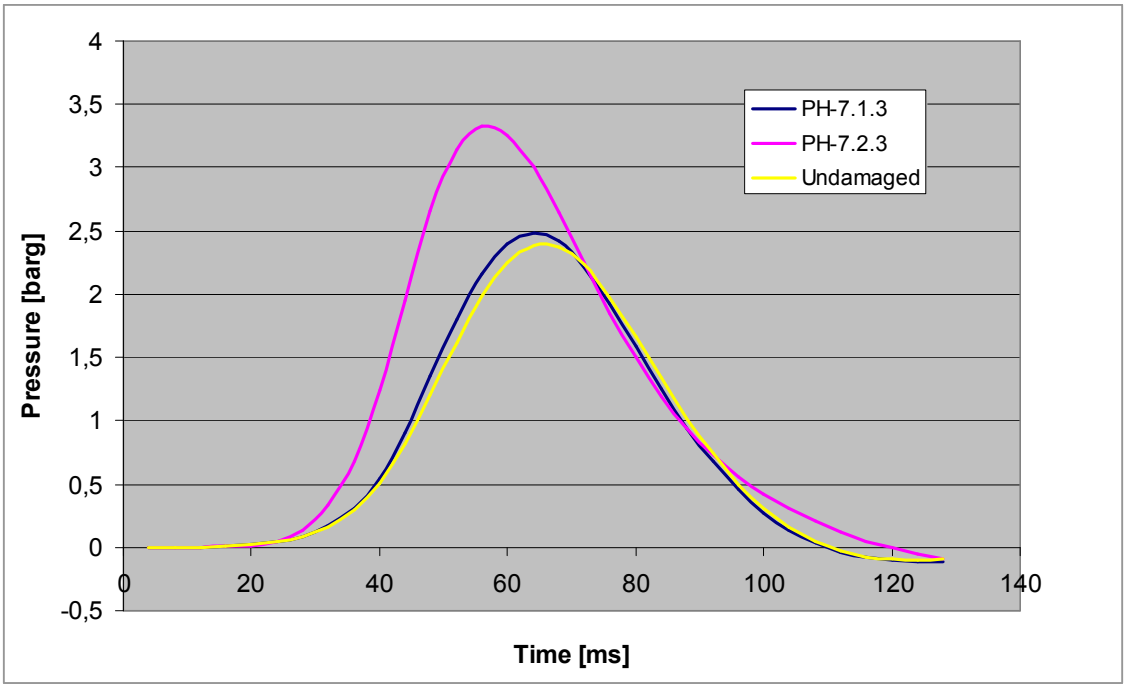

Figure 4-16: *Pressure development due to slits with different width on the perforating grooves compared with pressure development for an undamaged slit. The gap opening is constant at 0.98 mm. The blue curve represents the slit with crosswise grooves of 1 mm width and the pink curve represents the slit with crosswise grooves of 2 mm width.*

4.7.2 Discussion

From Table 4-7 it can be seen that the ability to prevent a re-ignition in the external chamber is almost the same for the undamaged slit and the slit with crosswise grooves of width 1 mm. The MESG value only increases with 2 % when adding seven perforating grooves of width 1 mm on an undamaged slit. Compared, the increase of the MESG value is 12 % when adding seven crosswise grooves of width 2 mm to the surface. This means that the width of the grooves is of great importance considering gap efficiency. The pressure measurements presented in Figure 4-16 shows that there is only a slightly increase in the maximum pressure when adding seven crosswise grooves of width 1 mm to an undamaged slit. This means that the resistance in these two gaps is surprisingly similar despite the great difference in the gap configurations. On the other hand the maximum pressure increases 34 % for the slit with crosswise grooves of width 2 mm. This implies a great increase in resistance through the flame gap, which further leads to a decrease in the flux of the hot combustion gases through the gap, as discussed in section 4.4.2. It can therefore be stated that the width of the perforating multiple crosswise grooves, is of great importance due to the gaps ability to prevent a re-ignition of an external explosive atmosphere.

The great difference in the maximum pressure for the two slits indicates that the definition of relative roughness (see section 2.3.9) is not fully accurate for the calculation of fluid flow through gaps with perforating grooves. This is because the relative roughness parameter only takes into account the ratio between the lowest and the highest height of the grooves and not the width. This means that the two slit configurations of PH-7.2.3 and PH-7.1.3 has the same relative roughness, despite the difference in the width of the grooves.

It should be mentioned that the investigation of the effect of different widths on the perforated crosswise grooves optimally should have been based on several sets with different width on the perforated grooves, not only two. It was not designed several sets with different width because it is not enough space on the slit surface for seven grooves with greater width than 2 mm. For further investigation the total number of multiple perforated grooves on the slit surface should be reduced, so it can be made several sets of different width on the crosswise grooves.

4.8 Result and discussion from experiment on flame gap surface of Plexiglas with seven perforating crosswise grooves

A slit made of Plexiglas with crosswise grooves was tested. The slit had the same configuration as PH-7.2.3. This implies seven crosswise grooves of width 2 mm and depth 3 mm. The reason for testing this slit was to investigate the effect of heat transfer from the penetrating hot combustion gases to the material of the rough slit set.

4.8.1 Result

During the first explosion the crosswise grooves were damaged. The "walls" between the grooves started melting and the entire flame gap start bending (see Figure 4-17). Thus the slit with crosswise grooves made of Plexiglas was useless for any further investigation.

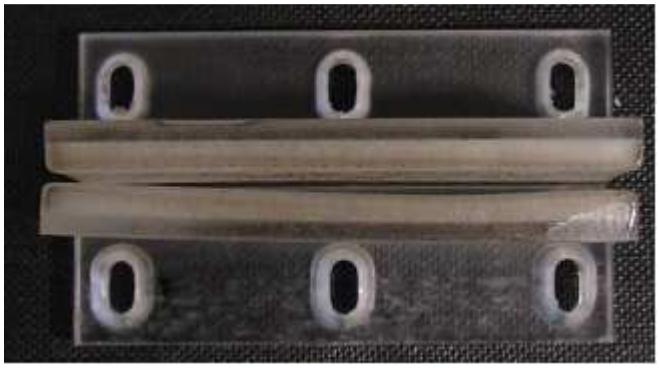

Figure 4-17: *Damaged Plexiglas slit, the flame gap walls has bowed.*

4.8.2 Discussion

The slit made out of Plexiglas had seven grooves of width 2 mm. The consequence of a large number of grooves is that the distance (the walls) between the grooves is relatively small, approximately 1 mm. A one millimetre wide Plexiglas wall is extremely fragile. An explosion pressures of 3 bar(g) and combustion temperatures greater than 1000 degree Celsius proved to be more than enough to demolish the walls. For further investigation it should be made slits with a lower number of grooves, so the walls between the grooves get wider and more robust. Alternatively, change to another material of low thermal conductivity that can withstand the high temperatures. It will then be possible to investigate what diverse effects a material of "low" thermal conductivity and a material of "high" thermal conductivity have on the gap efficiency at a rough turbulent state.

4.9 Result and discussion from Experiments performed with dust inside the flame gap of the PRSA and the PCFA

In this section the result from several experiments carried out with aluminium and pollen dust inside the flame gap is presented. The dust was weighted and placed in the gap with a spatula. All of the experiments were performed with an undamaged slit and a gap opening lower than the slits MESG value (0.98 mm for PRSA and 0.95 mm for PCFA). This was to ensure that the hot penetrating combustion gas could not cause a re-ignition in the external chamber. The only potential source of ignition was combustible dust. The results from the experiments are presented in section 4.9.1 and section 4.9.3.

4.9.1 Results from experiments in the PRSA

Table 4-8: *Experiments performed with aluminium dust placed in an undamaged flame gap.*

Gap opening, Yi [mm]	Quantity of aluminium per experiment [g]	Number of experiments	Number of re-ignitions
0.95	0.01	10	7
0.45	0.01	10	5
0.40	0.01	10	5

Table 4-9: *Experiments performed with pollen dust placed in an undamaged flame gap.*

Gap opening, Yi (mm)	Quantity of aluminium per experiment [g]	Number of experiment	Number of re-ignitions
0,95	0.01	10	0
0,45	0.01	10	0

From Table 4-8 it can be seen that re-ignitions occurred in the external chamber at all of the gap openings that was tested, 0.95 mm, 0.45 mm and 0.40 mm. The gap opening of 0.40 mm is a legal gap opening for use in the industry according to the standard (IEC 2007a) (see Figure 2-4 in section 2.2). This is a very interesting finding that will be discussed further in section 4.9.2

It was not found any clear correlation between the gap opening and the number of re-ignitions in the external chamber. From high speed recordings it is observed that all of the re-ignitions occur at the top of the secondary chamber, approximately 25-30 cm from the gap opening (see Figure 4-18). The time it takes from the explosion is trigged in the primary chamber to the explosive gas mixture ignites in the secondary chamber is about 10 to 14 milliseconds. In half of the experiments it was no re-ignition. During these experiments a burning jet of aluminium dust was observed, penetrating through the explosive gas mixture in the secondary chamber without causing an ignition.

From Table 4-9 it can be seen that no re-ignitions occurred when pollen was placed in the flame gap. It was observed that a small cloud of pollen dust was dispersed in the external chamber during the explosion in the primary chamber, but no burning particles could be seen.

In Figure 4-18 the development of a burning jet of aluminium that penetrates into the explosive gas mixture of propane/air in the secondary chamber is shown. The high speed

camera recorded 600 pictures per second. From the first to the second picture the aluminium dust has travelled a distance of approximately 20 cm. This corresponds to a dust velocity of 120 m/s.

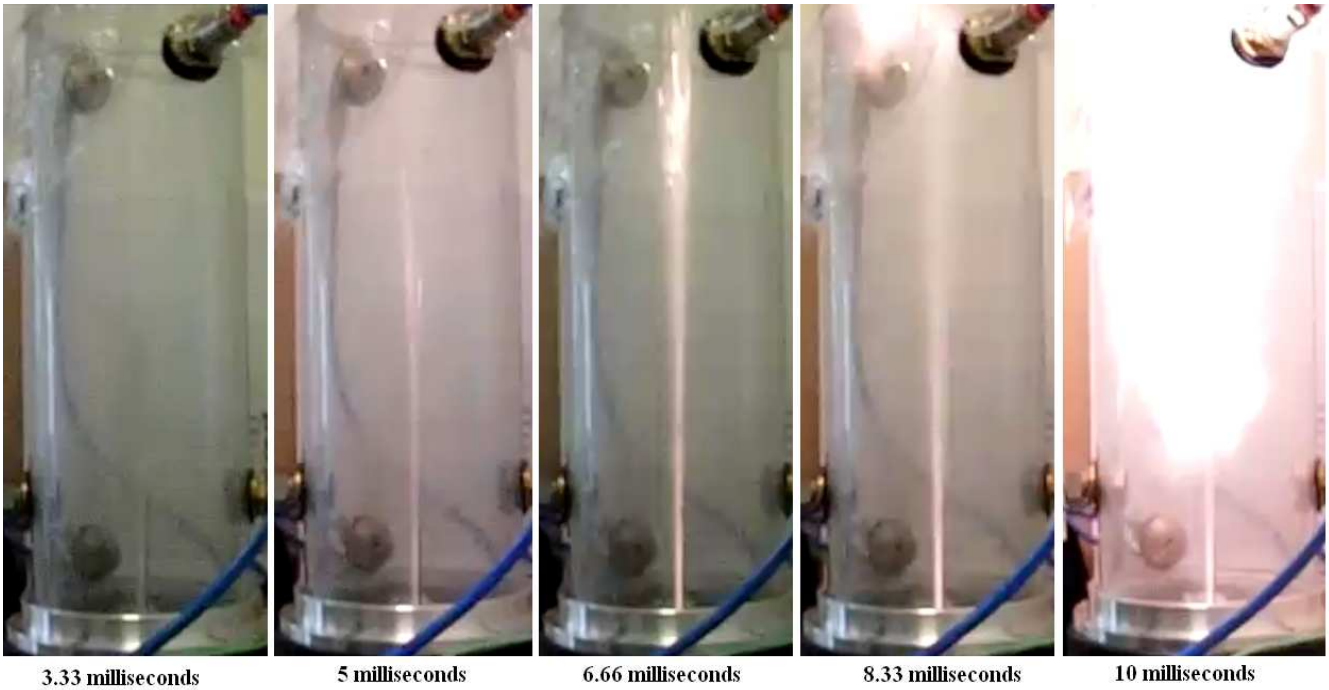

Figure 4-18: *Development of burning aluminium dust that penetrates through an undamaged slit at gap opening 0.40 mm and into a chamber filled with a gas mixture of 4.2 vol % propane in air.*

4.9.2 Discussion from experiments performed in the PRSA

From photographs of the dust in section 3.5.8 it can be seen that atomized aluminium has a smaller particle size than the pollen particles. The atomized aluminium consists of flakes and not spherical particles as pollen. The flakes of aluminium has a thickness of approximately 0.1 µm, this implies that the aluminium requires noticeably lower energy to ignite (MIE) than the spherical particles of pollen of a diameter of approximately 10-25 µm. As stated in section 2.7.3 the minimum ignition energy is strongly coupled to the particle size. The experiments performed in this work also indicate this. The aluminium ignited in 17 of 30 experiments, while the pollen dust did not ignite in one out of 20 experiments.

The gap opening of 0.40 mm is an allowed gap opening according to the standard of (IEC 2007a) for flameproof enclosures located in hazard zones 1 and 2. In half of the experiments with aluminium at this gap opening a re-ignition in the secondary chamber occurred. This result is quite surprising. From experiments performed by (Goroshin, Bidabadi et al. 1996) the quenching distance for a laminar burning dust cloud of atomized aluminium of diameter 5.5 µm is found to be 5 mm. They carried out their experiments without the presence of an explosive gas cloud. From the experiments performed in this work it can be stated the combination of increasing initial pressure, increasing turbulence level and a propane-containing atmosphere leads to a drastic reduction of the quenching distance for atomized aluminium dust.

When the pollen dust and atomized aluminium were placed in the flame gap with a spatula it was observed that some of the dust felled through the flame gap and into the main volume of the primary chamber. This implies that some of the dust will be dispersed and possibly ignited in the primary chamber during the initial gas explosion. The explosion causes great pressure and fluctuations of fluids inside the chamber, which increases the initial turbulence level of the explosive dust cloud. From literature reviewed in section 2.7.4 it can be seen that the minimum ignition energy for different substances of dust increases with increasing turbulence level of the dust cloud, but it is also stated by (Garcia-Agreda, Di Benedetto et al. 2010) that a hybrid mixture of gas and dust can lead to a lower flammability limit for both dust and gas mixtures (see section 2.7.6). From the experiments performed in this thesis it is shown that the aluminium powder can easily ignite in the primary chamber and penetrate through the required width of 0.40 mm (IEC) during an internal gas explosion. Which physical mechanisms that contributes the most to this observation is somewhat uncertain and more investigation is needed.

The incident of dust falling through the flame gap and into the primary chamber does not imply that the experiments are unsuccessful. This shows that the examined dust substances can find its way through a narrow gap without a great pushing force behind. And further be ignited in the Ex"d" enclosure before it penetrates back to the external atmosphere, where it possibly can re-ignite the explosive gas cloud and cause a great fatality. To investigate whether the burning dust that penetrated back to the external chamber was ignited inside the flame gap or in the primary volume of the enclosure, it was decided to perform experiments in an apparatus (PCFA, see section 3.6) where the flame gap is placed horizontal to the external chamber. Consequently the dust will not fall into the primary volume due to the gravitation when it is placed on the flame gap. The result from these experiments is presented in section 4.9.3.

From Figure 4-18 it can be seen that the penetrating jet causes a re-ignition of the explosive gas cloud at the top of the secondary chamber. From high speed recordings it can be seen that the same course of event is valid for all of the re-ignitions caused by the aluminium dust. An explanation of this scenario can be that the gas mixture has a given chemical induction time (see theory in section 2.3.6). This means that there is an ignition delay from the gas is exposed for high temperature until it ignites. This delay is caused by the formation of intermediate radicals as described in section 2.3.4. The velocity of the burning aluminium jet is possibly so high that the intermediate radicals do not have enough time to react. The ignition of the explosive gas cloud occurs when the velocity of the jet is dramatically reduced at the cling film covering the top of the secondary chamber. For further investigation it could be interesting to see if the gas cloud would ignite if the burning jet of aluminium particles hadn’t been obstructed by the cling film. Then the burning particles possibly had quenched before their velocity was low enough to ignite the explosive gas. If so, it is especially critical with any obstruction in front of the flame gap of a flameproof enclosure.

From Figure 4-18 it can also be seen that the flame at 10 milliseconds is yellow. This indicates that it is a low concentration of oxygen in the chamber. This corresponds to the fact that the burning jet of aluminium has consumed some of the oxygen in the secondary chamber before the gas mixture ignites.

4.9.3 Results and discussion from experiments performed with dust inside the flame gap of the PCFA

Forty experiments were performed in the Plane Circular Flange Apparatus to investigate the effect of dust on the flame gap. The dust was weighted and placed on the horizontal circular flame gap. Subsequently the primary and secondary chambers were filled with a uniform mixture of 4.2 vol. % propane in air. The result is presented in Table 4-10 and Table 4-11.

4.9.4 Results from experiments in the PCFA

Table 4-10: *Experiments performed in the PRSA with atomized aluminium.*

Gap opening, Yi (mm)	Quantity of aluminium per experiment [g]	Number of experiments	Number of re-ignitions
0.93	0.03	10	3
0.90	0.03	10	0

Table 4-11: *Experiments performed in the PRSA with pollen.*

Gap opening, Yi (mm)	Quantity of aluminium per experiment [g]	Number of experiments	Number of re-ignitions
0.93	0.03	10	0
0.90	0.03	10	0

From Table 4-10 it can be seen that re-ignition occurred in three experiments at gap opening 0.93 mm, this is a gap opening 0.02 mm narrower than the MESG value for an undamaged flame surface in the PCFA. When the gap opening was reduced to 0.90 no re-ignitions occurred.

From Table 4-11 it can be seen that pollen dust did not cause any re-ignition in the secondary chamber. It was not observed one single spark in the secondary chamber during the experiments with pollen.

From Figure 4-19 the development of the re-ignition process can be seen. From the recordings it is observed that atomized aluminium start to pour into the secondary chamber immediately after the ignition source is trigged in the primary chamber. After approximately 11 milliseconds the burning aluminium dust enters the secondary chamber and causes a re-ignition of the explosive propane atmosphere. Subsequent combustion of both dust and the gas were seen in the secondary chamber. It is observed from the recordings that all of the three re-ignition processes occur at the same place inside the secondary chamber. The location for the re-ignition is straight from the ignition source that is placed 14 mm horizontal into primary chamber.

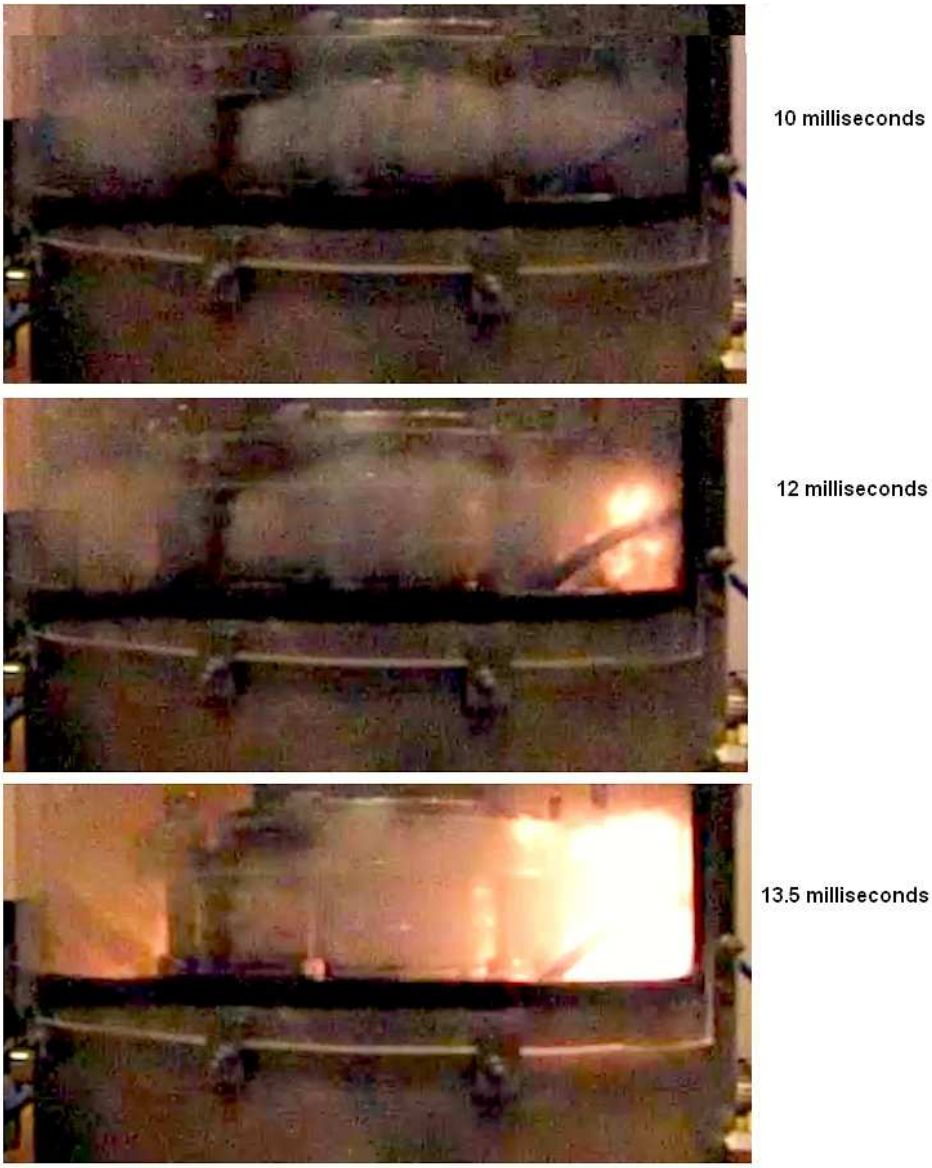

Figure 4-19: *Atomized aluminium penetrating into the secondary chamber due to an initial explosion in the primary chamber. The Gap opening is 0.93 mm.*

4.9.5 Discussion

The experiments carried out with atomized aluminium gave three re-ignitions at a gap opening of 0.93 mm, which is a gap opening 0.02 mm lower than the MESG value for an undamaged slit. This indicates that dust located inside the flame gap can ignite. A flame gap quenches the flame at a given position inside the gap. This implies that the flame is present a short distance into the gap. From this information it is assumed that the aluminium dust that is located closest to ignition source in the primary chamber ignites, because the flame front reaches this point first (see Figure 4-20). This is supported by high speed recordings as shown in Figure 4-19, where the re-ignition scenario is located close to the ignition source inside the primary chamber.

From the results shown in Table 4-10 it can be seen that no re-ignitions occurred at 0.90 mm, this indicates that the flame is quenched at such an early stage in the flame gap that it does not

have time or energy enough to ignite the atomized aluminium located on the flame gap surface.

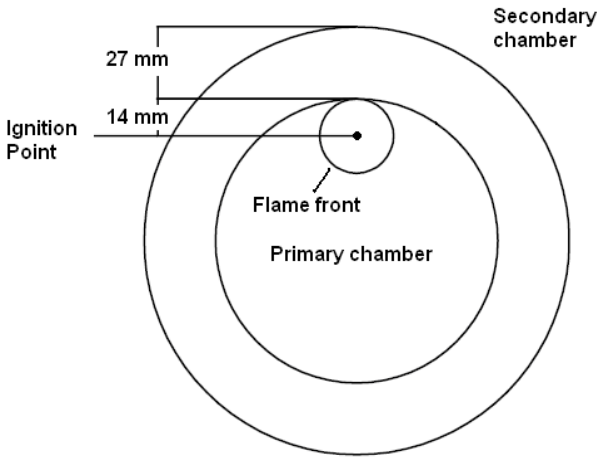

Figure 4-20: *Illustration of the flame front which reach the flame gap at a given location first.*

It should be mentioned that the maximum explosion pressure measured in the Plane Circular Flange Apparatus is approximately thirty times lower than the pressure in the PRSA, due to the great difference in the venting area. The low explosion pressure in the PCFA implies a decrease in the pushing force behind the aluminium dust, which leads to a lower velocity of the penetrating atomized aluminium. This can possibly affect the ignition process of the combustible aluminium. Ideally the different experiments presented in section 4.9.1 and section 4.9.3 should have been conducted in two apparatus that gave the same pushing force (pressure) behind the dust. This would provide more equal conditions for ignition.

From the experiments performed in this section it can be stated that the probability for a re-ignition in the secondary chamber increases slightly when the dust is located on a flame gap horizontal to the ground. But according to the experiments presented in section 4.9.1 the dust can easily fall into the primary chamber. Where the atomized aluminium ignited and penetrated back to the external chamber at burning state, and caused re-ignition in half of the experiments at an legal gap opening of 0.40 mm, according to the standard (IEC 2007a).

5 Conclusions

The examined slit sets, with rust and multiple crosswise grooves on the gap surface are both in the category of damaged flame gap surfaces. Current international standards (IEC) require that the mean roughness of the flame gap surface of Ex"d" enclosures is less than 6.3 µm. The standard also requires that the flame gap shall be restored to its original quality if it is damaged, but there is no guidance that defines which damages that is considered as significant. This implies that flameproof enclosures with minor visible damages on the flame gap surface will be dismantled and repaired, or replaced by new flameproof enclosures, without knowing if the damage on the flame gap surface reduces the gap efficiency and thus reduce the safety.

1. Throughout the present experimental work 4.2 vol. % propane in air has been used as the test gas. MESG has been used as a judgement if the gap efficiency increases or decreases, due to different damages on the gap surface. The MESG for a slit with roughness in accordance to the requirements of IEC (< 6.3µm) has been used as a reference slit. The MESG for the undamaged reference slit is found to be 0.98 mm in the Plane Rectangular Slit Apparatus (Grov 2010). The flame gap openings of flameproof enclosures are made with a given safety barrier, which varies with the volume of the enclosure and the length of the flame gap. A enclosure with the same configurations as the apparatuses used in the present work has an allowed gap opening of 0.40 mm, in accordance to the standard (IEC 2007a).

2. The maximum experimental safe gap (MESG) for a gap configuration depends strongly on the distance from the ignition position to the gap entrance, as shown by (Larsen 1998). He found that it exists an optimal ignition distance for re-ignition of a surrounding explosive gas mixture. All of the experiments carried out in this thesis were performed at this “worst case ignition position”. For an undamaged slit surface (Grov 2010) found that the “worst case ignition position” was 14 mm from the gap opening in the PRSA. In the present work, it is shown that the “worst case ignition position” for a slit with severe damages (multiple crosswise grooves) is equal to the ignition distance of 14 mm from the gap entrance, found by (Grov 2010).

3. Three main series of experiments were conducted in this thesis, experiments with rusted slit sets, experiments with multiple crosswise grooves on the gap surface and experiments with the presence of dust inside the flame gap. The conclusions after the investigation can be summarized as:

4. Rusted flame gap surfaces

- Five slits of different gap opening were placed at sea side for three months to rust. All of the five slit sets were explosion tested at undamaged state, prior to the rusting. Two of the slit sets gave 100 % re-ignition in undamaged state, two slit sets gave no re-ignitions and the last slit set gave three re-ignitions out of ten experiments. After rusting it was not observed one single re-ignition for the five different slit sets, despite the fact that all of the five rusted slit sets had a gap surface with an average roughness much higher than the required value of < 6.3 µm from (IEC 2007a). The overall conclusion from these experiments it is therefore that the requirement of surface roughness is arbitrary chosen.

5. Multiple crosswise grooves

- Temperature measurements carried out in this thesis shows that the temperature of the hot combustion gases, that flow out from a slit with multiple crosswise grooves (PH-7.2.3) is approximately 300^{o}C lower than the temperature of the hot gases that flow out from an undamaged slit, despite identical explosion conditions.

- Pressure measurements performed in the present work confirm that the flux of hot combustion gases through the flame gap decrease when multiple crosswise grooves are added to the flame gap. It is seen from different pressure graphs that the time it takes to empty the internal chamber for hot combustion gases increases when multiple crosswise grooves is added to an undamaged flame gap surface. Consequently, the hot gases get more time for cooling inside the flameproof enclosure before they enter the external atmosphere. Thus the external explosive atmosphere is exposed to less hot combustion gases per unit of time, than it would have been if the flame gap was undamaged.

- Two different re-ignition scenarios are detected through high speed recordings for the undamaged slit and the slit with multiple crosswise grooves. The re-ignition occurs at a lower altitude and looks like a jet during the experiments with multiple crosswise grooves. The re-ignition scenario for an undamaged slit looks like a detached sphere a given distance above the gap opening, which is in accordance to literature reviewed in chapter 2.5.

- The MESG is found for different slit sets with multiple crosswise grooves of different width and depth in the present work. The overall conclusion from these experiments is that the gap efficiency does not get reduced if perforating multiple crosswise grooves are added to an undamaged gap surface. There is no clear correlation between the MESG value found and the depth of the grooves, but it is shown that the pressure in the primary chamber increases with increasing depth of the grooves. It is also shown that a decrease in the width of the grooves from 2 mm to 1 mm leads to a decrease in the MESG from 1.10 mm to 1.00 mm. This implies that the width of the grooves is of great importance due to the gap efficiency.

6. Experiments with dust inside the flame gap

- Two different apparatuses were used in the investigation of dust inside the flame gap. The PRSA and the Plane Circular Flange Apparatus. The PCFA has a flame gap located horizontal to the ground, which implies that the dust cannot fall into the primary chamber due to gravity. Two dust types where used in the present work; atomized aluminium and pollen.

- The experiments performed in the PRSA shows that both of the dust types can easily fall through the flame gap and into the main volume of the primary chamber. The atomized aluminium penetrated back to the external chamber at a burning state and caused a re-ignition in more than half of the experiments. Even at the allowed gap opening of 0.40 mm, according to the standard (IEC 2007a) the atomized aluminium caused re-ignition in half of the experiments. Pollen did not cause any re-ignitions in the external chamber.

- Pollen did not cause any re-ignition in the PCFA either. The experiments performed with atomized aluminium in the PCFA caused a slightly reduction of the gap efficiency. No re-ignitions were observed for gap openings narrower than 0.93 mm. It can therefore be stated that combustible dust represents a much greater danger if it find its way through the flame gap and into the primary chamber, prior to a gas explosion.

- The overall conclusion from these experiments is that the presence of combustible dust in areas where flameproof enclosures are located must not be underestimated as a potential hazard. It is shown through several experiments that dust possibly can cause re-ignition of an external explosive atmosphere, at gap openings where it is impossible to get an ignition of the surrounding explosive atmosphere with only gas present. Even at the allowed gap opening of 0.40 mm (according to the standard (IEC 2007a)) external ignition occurred in half of the experiments.

6 Recommendations for Further Work

Rusted flame gap surfaces

The experimental work in the present thesis has showed that rust on the flame gap surface can increase the Maximum Experimental Safe Gap (MESG), but more systematic work on rusted flame gap surfaces are needed to verify the effect of rust formation on the flame gap surface. Suggestion for further work is listed below:

- Place several slit sets at the sea side for rusting for different periods of time, and then investigate how the gap efficiency varies with the degree of rust formation on the flame gap surface.

- Establish a system in the Plane Circular Flange Apparatus (PCFA) so the flanges can be screwed together before rusting, and subsequently placed directly in the apparatus. This is to investigate if the same results will be obtained in the PCFA as one got for rusted flame gap surface in the Plane Rectangular Slit Apparatus (PRSA).

Mechanical damages on the flame gap surface

In the present thesis the main focus has been on multiple perforating crosswise grooves on the gap surface. Several other mechanical damages on the gap surface could be interesting to investigate. Some suggestions are given below:

- Grooves can be milled into the gap surface with a given angle in relation to the flow. This can be both single grooves and multiple grooves.

- More experiments are needed to investigate the effect of different widths on the slits with multiple crosswise grooves. In this thesis, it is only performed experiments of two different widths. To investigate if the MESG increases further with grooves of greater width new slits have to be made and examined.

- The effect of single stab damages on the gap surface. Such damages can occur during maintenance and reparation of the flameproof enclosures when a tool made of a hard material bump into the flame gap surface and forms a notch.

The presence of dust inside a flameproof enclosure

The investigation of dust inside the flame gap is a new approach of the experimental work with flameproof enclosures. The work performed in the present thesis with dust inside flameproof enclosures is therefore in the initial phase. More investigation has to be carried out to get more knowledge of this phenomenon. Suggestion for further work is given below:

- Conduct experiments with dusts types of different reactivity than the two tested in the present work, and find limiting values for particle sizes, MIE, heat of combustion etc. This is to get an a better understanding of which dust types that can cause re-ignition in the external atmosphere

- Perform experiments with metal particles that potentially can originate from a solid surface, which has lost some solid material due to maintenance and reparation performed with a screwdriver, or other “hard” tools in an industrial plant. And further see if it is possibly for these particles to ignite in the flameproof enclosure and penetrate through the flame gap.

Experimental setup

- Investigate how a more reactive gas affects the gap efficiency due to slits with different surface damages. It is likely to assume that a more reactive gas as ethylene is more sensitive to changes of the surface configuration. Experiments performed with different gases can give guidance to more theoretical understanding of the effect of surface damages on the flame gap.

- Investigate the re-ignition process in the secondary chamber with a Schlieren set up. A Schlieren system can be helpful in the investigation of the physical phenomenon of different re-ignition processes due to different configurations on the gap surface.

- Temperature measurements through the flame gap with multiple crosswise grooves could give information that can provide a better understanding of the cooling process through the gap.

- Turbulence measurements above the flame gap for different flame gap configurations could give information of the correlation between turbulence level and the probability for re-ignition of the external explosive gas mixture.

Numerical simulations of the transmission process of an explosion

- The transmission process of an explosion through a narrow gap is a complex phenomenon. A deeper theoretical study due to a CFD analysis can possibly give new and improved knowledge of this debated theme. A theoretical ignition and combustion model should be developed, so different cases could be investigated.

Ceylan, K. and G. Kelbaliyev (2003). "The roughness effects on friction and heat transfer in the fully developed turbulent flow in pipes." Applied Thermal Engineering **23**(5): 557-570.

Grov, A. (2010). An experimental study of the influence of major damage of flame gap surface in flameproof apparatus on the ability of the gaps to prevent gas explosion transmission. Department of Pyhsics programme of process safety. Bergen, University of Bergen. **Master in science**

McCabe, W. L., P. Harriott, et al. (2005). Unit operations of chemical engineering. Boston, McGraw-Hill.

Ballal, D. R. and A. H. Lefebvre (1975). "The influence of flow parameters on minimum ignition energy." **15**: 1473-1481.

Bardal, E. (1994). Korrosjon og korrosjonsvern, Tapir, 82-519-1173-7.

Bartknecht, W. (1987). "Staubexplosionen-Ablauf and Schutzmassnahmen." Springer Verlag, Berlin.

Beyer, M. (1996). Über den Zunddurchsclag explodierender Gasgemische an Gehäusen der Zündschutzart 'Druckfeste Kapselung'. VDI Reiche.

Beyling, C. (1906). Versuche zweks Erprobung der Schlagwettersichercherheit besonders geschutzer electrischer Motoren und Apparate. Glückaf**:** 42.

Chang, R. (2006). "Generell chemistry." **fourth edition**(0-07-111567-6).

Eckhoff, R. K. (2003). Dust explosions in the process industries. Amsterdam, GPP.

Eckhoff, R. K. (2005). Explosion Hazards in the Process Industries, Gulf Publishing Company.

Einarsen, R. I. (2001). Experimental determination of holes and slits in flameproof enclosures, for preventing transmission to external explosive gas clouds. Department of Pyhsics programme of process safety. Bergen, University of Bergen. **Cand.Scient**.

Engler, C. (1885). "Beitrage zur Kenntniss der Staubexplosionen " Chemische Industrie 171-173.

Ermakov, V. A., Razdobreev, et al. (1982). "Temperature of aluminium particles at the time of ignition and combustion." Fizika Goveniya i Vzryva **18**.

F.A.Williams (1985). "Combustion theory." Addison Wesley **2nd Ed.**

Frank-Kamenetskii, D. A. (1955). "Diffusion and heat exhange in chemical kinetics. ." Princeton university Press.

Friedman, R. and A. Macek (1962). "Ignition and combustion of aluminium particles in hot ambient gases." Combustion and Flame **6**: 9-19.

Garcia-Agreda, A., A. Di Benedetto, et al. (2010). "Dust/gas mixtures explosion regimes." Powder Technology **In Press, Corrected Proof**.

Glarner, T. (1984). "Mindestzündenenergie - Einfluss der temperatur." VDI Berichte, Düsseldorf **494**: 109-118.

Goroshin, S., M. Bidabadi, et al. (1996). "Quenching distance of laminar flame in aluminum dust clouds." Combustion and Flame **105**(1-2): 147-160.

Grobleben, K. H. (1967). "The emission of burned gases as a cause of external ignition in the case of flameproof enclosures " 12th international Conference of Mine Safety Research Establishment Dortmund **Paper 36**.

IEC (2002). IEC (2002): 60079-1-1:2002 Electrical apparatus for explosive gas atmospheres Part 1-1: Flameproof enclosures 'd' Method of test for ascertainment of maximum experimental safe gap, Central Office of International Electrotechnical Commission, Geneva, Switzerland.

IEC (2007a). "Explosive atmosphere." Equipment protection by flame proof enclosures **Part 1**.

IEC (2007b). 60079-19:2007 Explosive atmospheres - Part 19: Equipment repair, overhaul and reclamation. .

IEC (2007c). IEC(2007c):60079-17:2007 Explosive atmospheres. Part 17: Electrical installations inspection and maintenance.

J. Warnatz, U. M., R.W Dibble (2006). "Combustion." Springer Berlin Heidelber New York **4th Edition**.

Kalvatn, I. (2009). Experimental investigation of the optical measurement method for detecting dust and gas flames in a flame acceleration tube. Department of physics and technology. Bergen, University of Bergen. **Master Sc.**

Kanury, A. M. (1975). "Introduction to combustion phenomena: (for fire, incineration, pollution and energy applications),." New York, Gordon and Breach. .

Larsen, Ø. (1998). A Study of Critical Dimensions of Holes for Transmission of Gas Explosions and development & Testing of a Schlieren System for Studying Jets of Hot Combustion Products. Department of Pyhsics programme of process safety. Bergen, University of Bergen. **Cand.Scient.**

Mottahed, B. and M. Molki (1996). "Artificial roughness effects on turbulent transfer coefficients in the entrance region of a circular tube." International Journal of Heat and Mass Transfer **39**(12): 2515-2523.

Opsvik, H. E. Z. (2010). Experimental investigation of the influence of mechanical and corrosion damage of gap surfaces on the efficiency of flame gaps in flameproof apparatus. Department of physics and technology. Bergen, University of Bergen. **Master Sc.**

Pellmont, G. (1979). "Explosions- und Zündverhalten von hybriden Gemschen aus brennbaren Stäuben und Brenngasen." Doctoral Thesis No 6498 **6498**.

Perry, R. H. and D. W. Green (2008). Perry's chemical engineers' handbook. New York, McGraw-Hill.

Petroleum Safety Authority Norway, P. (2009). Trends in Risk Level in the Petroleum Activity on the Norwegian Continental Shelf. Ø. Tuntland**:** 36.

Petroleum, T. i. o. (2002). "Area classification code for installations handling flammable fluids." 2nd ed, August 2002 London.

Phillips, H. (1971). The Mechanism of flameproof protection**:** 86.

Phillips, H. (1988). The Safe Gap: Effect of explosion Pressure. IEE Conference Publication London**:** 5.

RKI-instruments (2010). http://www.rkiinstruments.com/pages/application_briefs/Accurately_measure_flammable_gases.htm.

Servomex (1991). Servomex 1410B. Infrared Analyser. Instruction Manual.

Smith, P. B. (1953). "The role of flanges in conferring protection on flameproof electrical enclosures." **77**.

Strehlow, R. A., J. A. Nicholls, et al. (1979). "An investigation of the maximum experimental safe gap anomaly." Journal of Hazardous Materials **3**(1): 1-15.

Tennekes and Lumley (1994). "A first course in turbulence " London, England, The MIT Press.

Turns, S. R. (1996). An introduction to combustion: concepts and applications. New York, McGraw-Hill.

Appendix

Appendix A – Experimental apparatus and procedures

A-1 Equipment data

Table- I: *Equipment list*

Equipment	**Type**
Gas Analyzer	Servomex 1400B4 SPX
Computer	Dell Latitude D630
DAQ	NI USB 6009
Pressure transducer	Kistler 701A
Charge Amplifier	5015A0000
Spark Generator	Tailor made (Appendix C-3)
Thermocouples	Tailor made (Appendix C-2.1)
Test gas	Propane (99.95 %)
Experimental Apparatus	Plane Rectangular Slit Apparatus (PRSA)
Experimental Apparatus	Plane Circular Flange Apparatus (PCFA)
Camera	Casio Exilim EX-F1
Welding apparatus for thermocouples	Tailor made (Appendix C-2.2)

A-2 Experimental procedure – The Plane Rectangular Slit Apparatus.

A-2.1 Adjusting Procedure - gap opening in the PRSA

From (Grov 2010)

1. Remove the external chamber, by turning the whole chamber counter clockwise.
2. Remove the top of the primary chamber where the flame gap is located.
3. Locate the distance "shims" in both sides through the gap (shown in Figure- I), make sure that the distance "shims" are through the whole gap width, to ensure uniform gap opening.
4. Fasten the two screws in the top of the gap (shown in Figure- I and Figure- II), with a torque of 20 cNM.
5. Fasten the four screws at the start of the gap with a torque of 20 cNm (shown in Figure- III and Figure- IV).
6. Fasten the six screws on the bottom of the gap with a torque of 1 Nm.

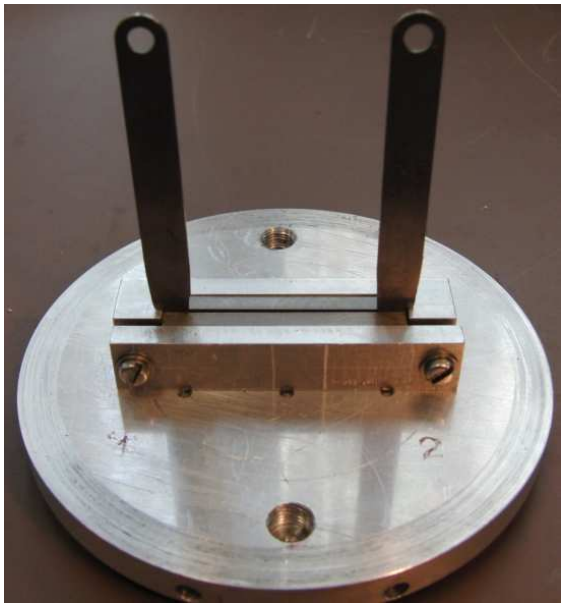

Figure- I: *Photograph of the upper part of the flame gap in the PRSA, with distance "shims" placed, the gap is fastened with a small torque applied on the screws seen in the photograph*

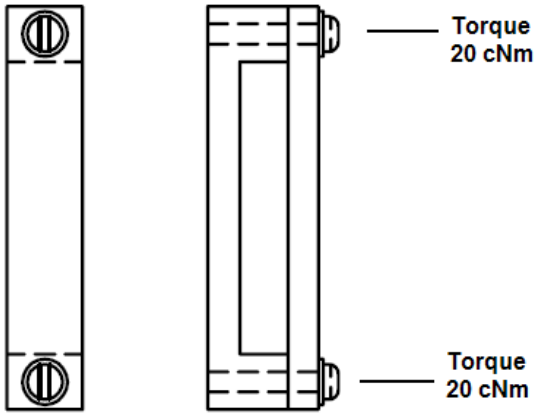

Figure- II: *Drawing of the clamp in the upper part of the flame gap, with the two screws that must be fastened with a torque of 20 cNM*

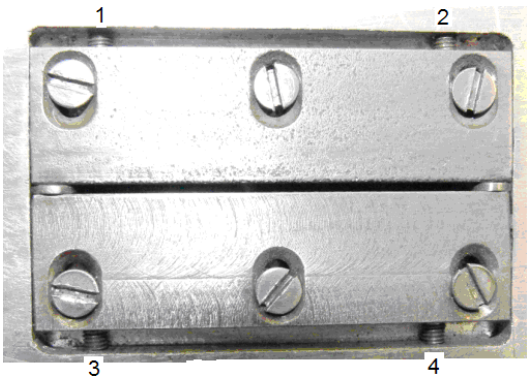

Figure- III: *Photograph of the lower part of the flame gap in the PRSA, this is the part which is inside the primary chamber. The numbers 1-4 on the photograph is the screws which are tightened with the same torque as the screws in the upper part of the flame gap, ensuring a uniform gap opening over the whole width of the gap. On the sides of the flame gap the distance "shims" can be seen*

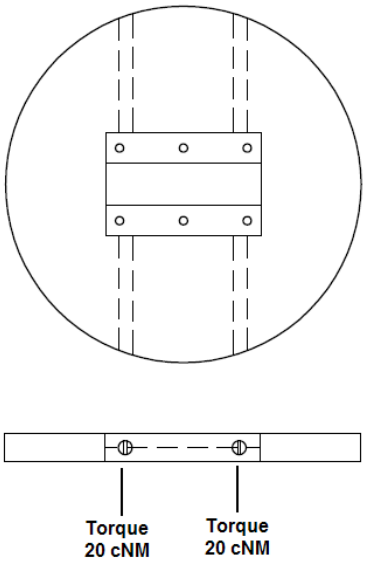

Figure- IV: *Drawing of the lower part of the flame gap inside the primary chamber of the PRSA. The drawing shows where the screws clamp the gap together on the position where the distance "shims" are located*

A-2.2 Experimental Procedure – the Plane Rectangular Slit Apparatus (PRSA)

From (Grov 2010)

After the gas analyzer is calibrated it has to be powered in the period the experiments is been performed. A power off situation requires a new calibration. When starting the gas analyzer in the morning, or after a longer brake, it's not mandatory, but prudent, to perform a zero point calibration, ref. point A.2.4 - Setting the zero.

The reference values in the procedure, with respect to flow, are based on experiences with a gas concentration of 4.2 % propane in air.

With reference to the schematic in Figure- V the following steps has to be accomplished:

1.) Install the plastic membrane on the top of the apparatus.

2.) Turn on the spark generator.

3.) Open utility valves (1, 2, 4 and 5). Close evacuating valve (7) and ensure that the 3 way valve (8) is in supply position. Service valve (6) shall be closed at all times during the experiments.

4.) Open the valve for air supply (9). Air pressure set to 0,5 barg.

5.) Start the gas analyzer pump.

6.) Open the valve for the gas supply (10). Gas pressure set to 0,5 barg.

7.) Adjust the air and gas flow preliminary to 75% and 15% respectively on the analyzers flow meters.

8.) Maximum gas flow is 1000 ml/minute.

9.) Monitor the gas concentration level on inlet and outlet from the apparatus, and adjust up/down on the air supply to achieve 4,2 % propane in air. Allow the analyzer to stabilize at least 60 seconds before reading out measurements.

10.) When the gas concentration level on the outlet reaches set point, start monitoring the gas concentration on the inlet of the experimental apparatus. Open the evacuating valve (7) and set the 3 way valve (8) to monitor the outlet. Close the utility valves (1, 2, 4 and 5).

11.) Secure the area.

12.) Wear ear protection.

13.) Activate the Labview program.

14.) Store the measurements by means of specifying a filename in Labview.

15.) Flush with air prior to new experiments.

16.) When the experiments are completed remember to close the gas- (10) and air supply (9).

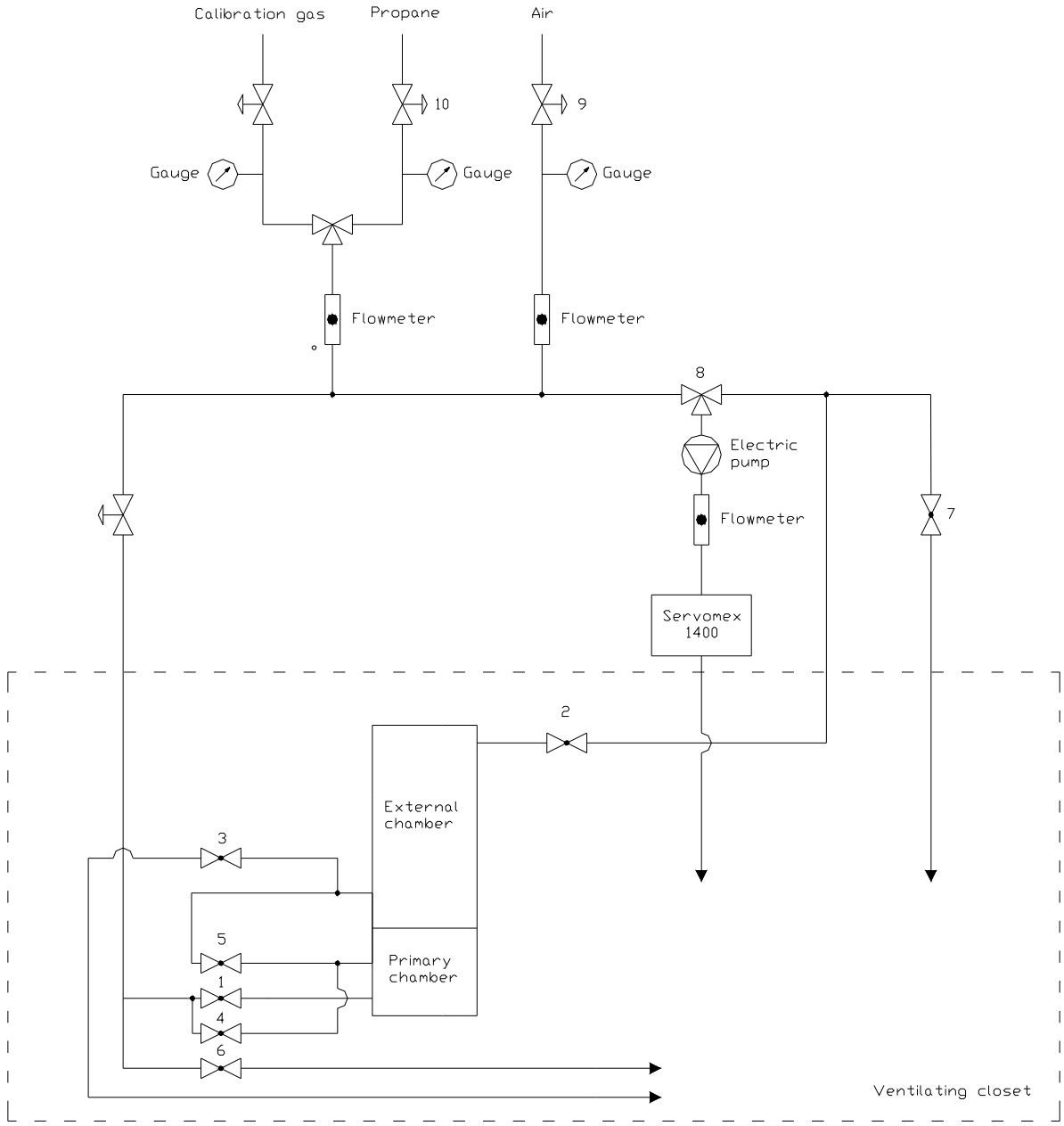

Figure- V: *PRSA with appurtenant tubing*

A-2.3 Experimental procedure - The Plane Circular Flange Apparatus (PCFA)

From (Opsvik 2010)

After the gas analyzer is calibrated it has to be powered in the period the experiments is been performed. A power off situation requires a new calibration. When starting the gas analyzer in the morning, or after a longer brake, it's not mandatory, but prudent, to perform a zero point calibration, ref. point A.2.4 - Setting the zero.

The reference values in the procedure, with respect to flow, are based on experiences with a gas concentration of 4,2 % propane in air.

With reference to the schematic in Figure- VI the following steps has to be accomplished:

1.) Install the plastic membrane on the top of the apparatus
2.) Turn on the spark generator
3.) Open utility valves (1, 2, 3 and 4). Close evacuating valve (7) and ensure that the 3 way valve (8) is in supply position
4.) Open the valve for air supply (5). Air pressure set to 0,5 barg
5.) Start the gas analyzer pump
6.) Open the valve for the gas supply (6). Gas pressure set to 0,5 barg
7.) Adjust the air and gas flow preliminary to 75% and 15% respectively on the analyzers flow meters
8.) Maximum gas flow is 1000 ml/minute
9.) Monitor the gas concentration level on inlet and outlet from the apparatus, and adjust up/down on the air supply to achieve 4,2 % propane in air. Allow the analyzer to stabilize at least 60 seconds before reading out measurements
10.) When the gas concentration level on the outlet reaches set point, start monitoring the gas concentration on the inlet of the experimental apparatus. Open the evacuating valve (7) and set the 3 way valve (8) to monitor the outlet. Close the utility valves (1, 2, 3 and 4)
11.) Secure the area
12.) Wear ear protection
13.) Activate the Labview program
14.) Store the measurements by means of specifying a filename in Labview
15.) Flush with air prior to new experiments
16.) When the experiments are completed remember to close the gas- (6) and air supply (5)

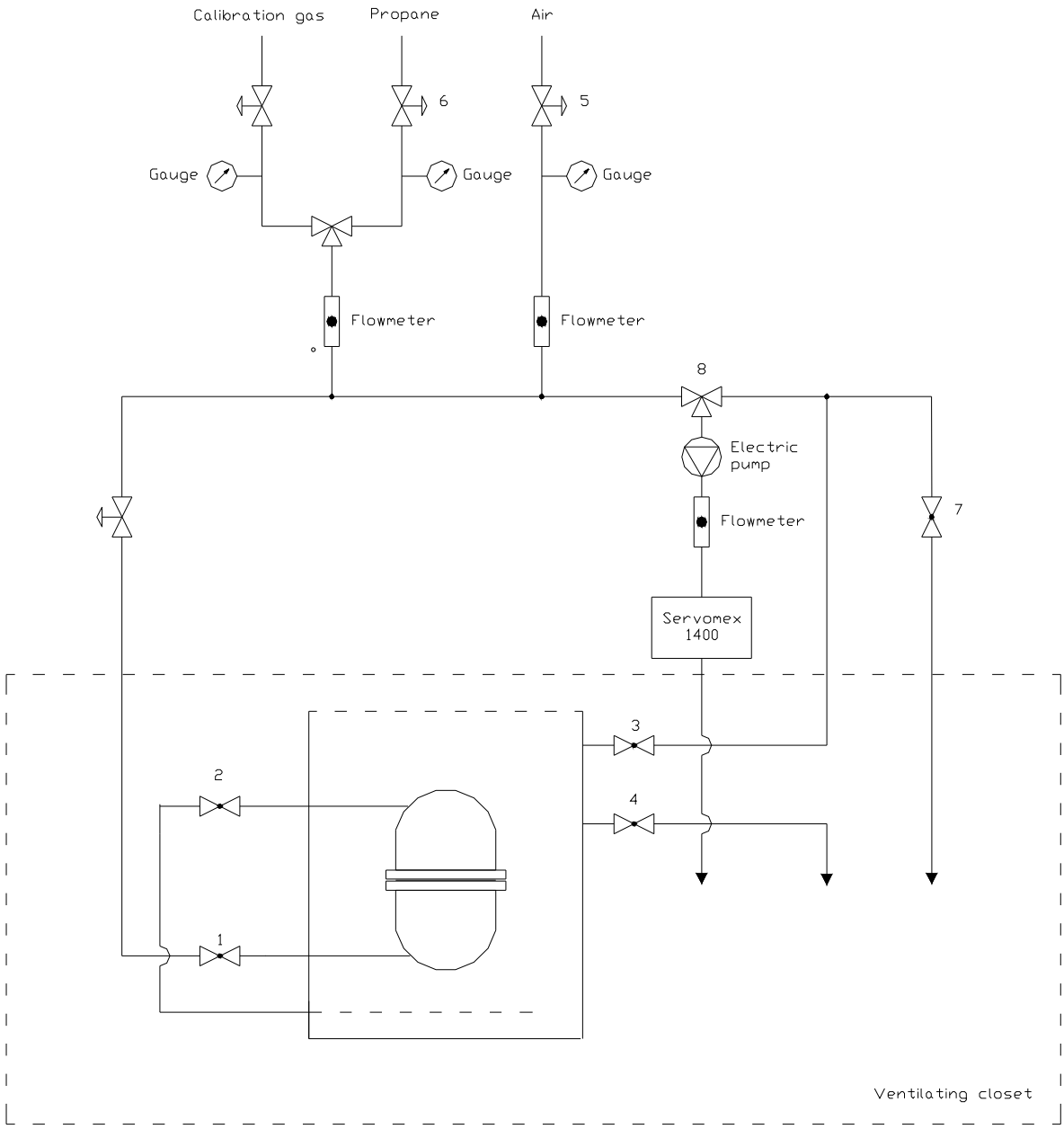

Figure- VI: *The PCFA with appurtenant tubing*

A-2.4 Calibration procedure - Gas Analyzer

From (Opsvik 2010)

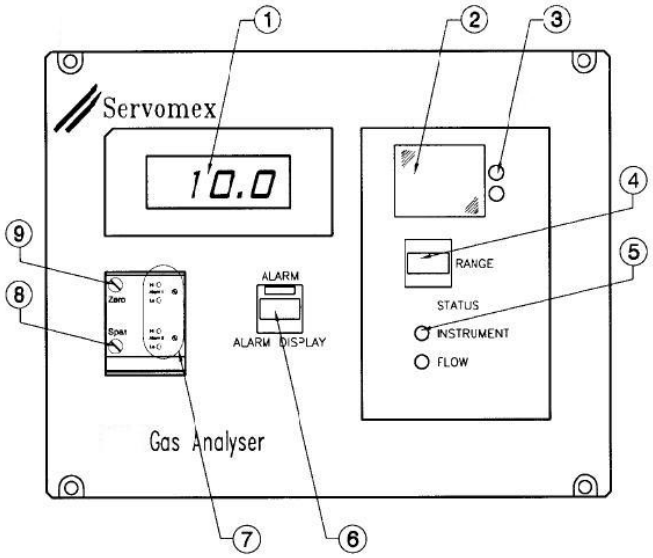

① Digit Display
② Range label
③ Range Indicator
④ Range selection switch
⑤ Instrument status indicator
⑥ Sample flow failure indicator
⑦ Span setting control (2)
⑧ Span setting control (1)
⑨ Zero calibration

Figure- VII: *Servomex 1410 B - Infrared Gas Analyzer*

For optimum accuracy allow a minimum of four hours from power on for the monitor to stabilise before performing a calibration.

When connecting the calibration gases allow at least 60 seconds for the internal pipe work and cell to flush out completely before making adjustments to the calibration. The analyzer should be calibrated at the temperature at which it will operate.

Servomex recommendations with respect to calibration intervals:
Weekly: Check Zero
Monthly: Check Zero and span. Adjust as necessary

Setting the Zero

i) Open the air supply valve. Adjust air pressure to 0,5 barg and flow to 1,0 liter/minute

ii) Ensure that gas supply valve is closed

iii) Start pump. Allow operation for approximately two minutes

iv) Adjust display to 0,00 - if necessary. Use the Zero calibration potentiometer in the front of the analyzer, indicated as number ⑨ in Figure- VII. Turning the potentiometer clockwise gives a increase in the display and vice versa

Setting the span

i) Close the air supply

ii) Open the calibration gas supply. The calibration gas consists of 5% propane and 95% Nitrogen

iii) Adjust gas pressure to 0,5 barg and flow to 1 liter/minute

iv) Adjust display to 5.00 % - if necessary. Use the Span calibration potentiometer in the front of the analyzer, indicated as number ⑧ in Figure- VII. Turning the potentiometer clockwise gives an increase in the display and vice versa

The span potentiometer to the right is only in use if a second span gas is introduced. The method would be precisely the same as described in point **iv)** above.

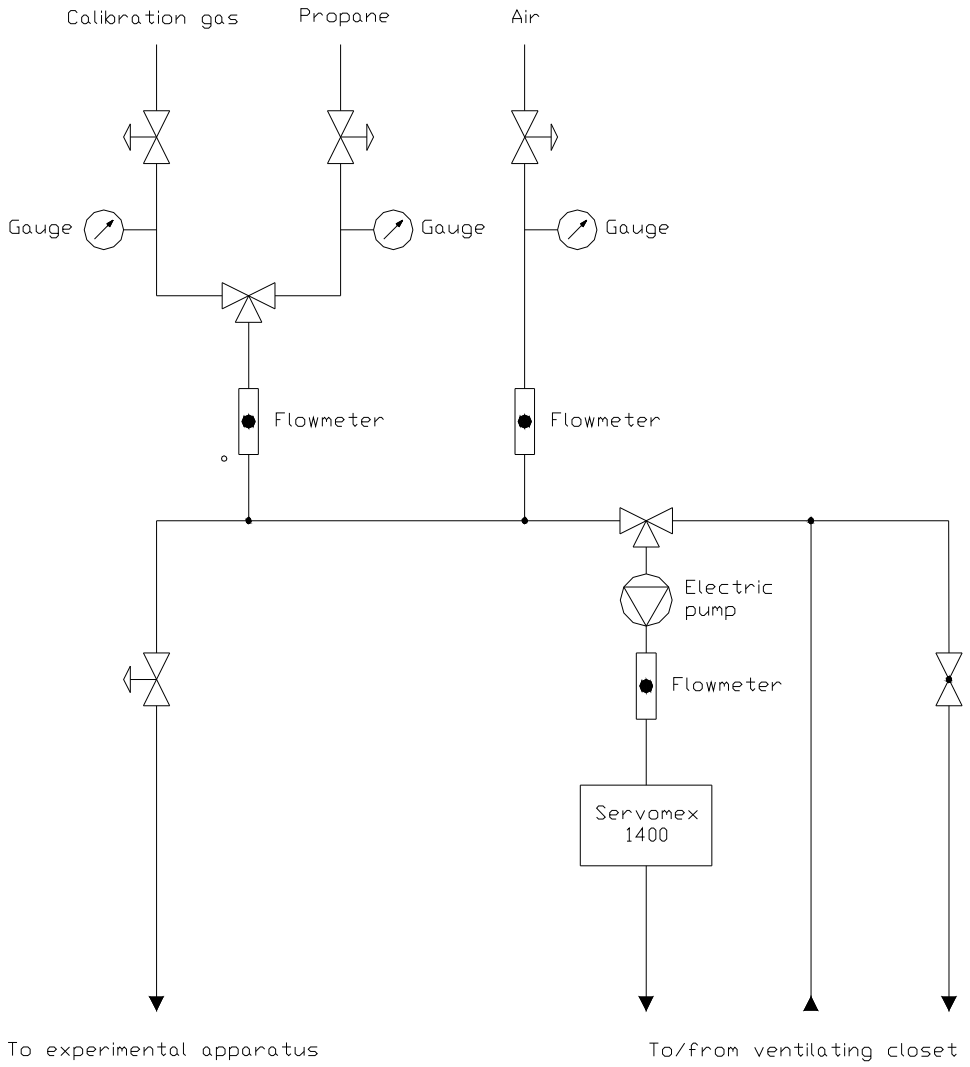

Figure- VIII: *Servomex 1410 B - Infrared Gas Analyzer with appurtenant pipe work and fixtures*

A-2.5 Data Acquisition System

From (Opsvik 2010)

A simplified user guide for the Labview program for running the experiment

A program was made, based on Labview, in order to run the experiment. In the front panel of the program, shown in Figure- IX and Figure- X, the experiments it's getting controlled. In the block diagram, shown in the same figure, input/output-channel settings can be chosen by the use of the data acquisition (DAQ) assistants. To activate the experiment, press the arrow button in the upper left corner of the front panel. After every experiment it is important that the file name for the logging file is saved. This is done via the file path dialog box.

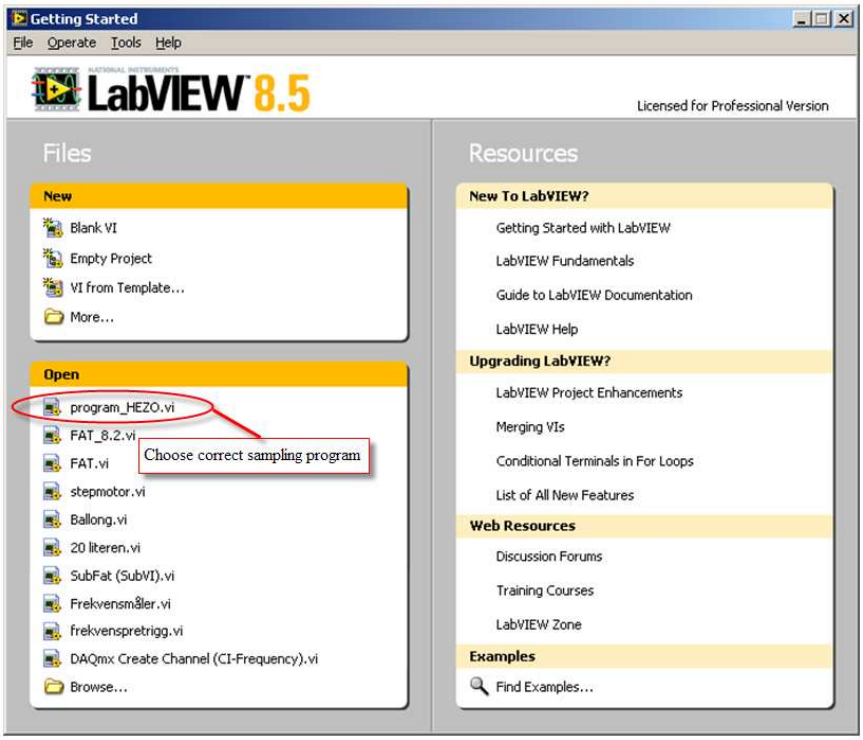

Figure- IX: *Initial Labview dialog box*

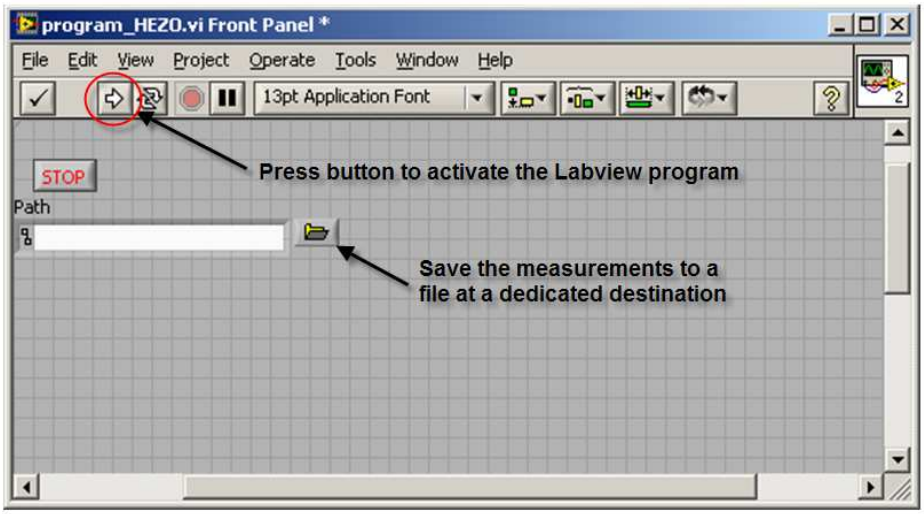

Figure- X: *Main Labview dialog box*

Appendix B - Flow calculations

To support the discussion in section 4.6 with respect to the experimental results in the Plane Rectangular Flange Apparatus simplified calculations has been carried out.

Assumptions

Several assumptions are made to simplify the calculation for the fluid flow through the gap. The calculations were made to show that the velocity of the hot combustion gases decreases when multiple crosswise grooves is added to an undamaged gap surface.

A reduced velocity through the gap leads to an increase in the pressure inside the primary chamber which is in accordance to pressure measurements presented in section 4.4. It is conceivable that other new physically mechanism also is applicable due to the great roughness and the shape of the perforating crosswise grooves on the gap surface, but these effects is neglected.

The hot combustion products that flow throughout the gap consist mainly of CO_2, water vapor and N_2. To simplify the calculations it is assumed that the only gas present in the flow is N_2, which is the substance that the hot combustion gas consist most of.

The temperature of the combustion gas is quite uncertain through the gap. In the calculations a temperature of 1000 ^{0}C is chosen.

The velocity, temperature and pressure will change through the gap. Consequently the density of the hot combustion products will change throughout the gap. To simplify the calculations equation for incompressible gas is used.

Formulas

The constant and formulas used in calculations are found in (McCabe, Harriott et al. 2005) (Ceylan and Kelbaliyev 2003) and in (Perry and Green 2008).

The formulas for Reynolds number, equivalent diameter and friction factor that are used in the calculations can be found in section 2.3.9 and section 2.4.1.

The average velocity, through the gap is deduced from the Bernoulli equation and the equation for the friction factor as a function of the pressure loss due to skin friction:

$$P_1 - P_2 = \frac{1}{2}.\rho\overline{V}^2 + \Delta P_s \qquad \textbf{(A-1)}$$

$$f = \frac{\Delta P_s}{2\rho\overline{V}^2} \cdot \frac{D_h}{L} \qquad \textbf{(A-2)}$$

A combination of these two equations gives the equation for the gas velocity:

$$\bar{V} = \sqrt{\frac{P_1}{(\frac{1}{2}+\frac{2fL}{D_h})\rho}} \qquad \textbf{(A-3)}$$

Where:

$\bar{V}$ = average velocity of gas

P1 = gauge pressure in the primary chamber

P2 = gauge pressure in the secondary chamber

ΔPs= pressure loss due to skin friction

L= length of channel

f= Fanning friction factor

ρ = density of gas

The density of the gas is given by the equation of state:

$$\rho = \frac{P}{RT} \qquad \textbf{(A-4)}$$

Where:

R = The individual gas constant

Constants and parameters:

Table- II: *Fixed parameters*

Gap length	25 mm
Gap opening (Yi)	1.05 mm
Equivalent diameter (D	0.00187
Gas constant (N_2)	296.8 J/kg K
Temperature (combustion products)	1270 K
Viscosity (N_2)	4.6* 10^{-4} Poise (Pa s)

Table- III: *Variable parameters*

Slit configuration	**Depth of grooves, k (mm)**	**Measured gauge pressure in primary chamber [Pa]**	**Density N_2 (kg/m^3)**
Undamaged	0	193000	0,77
PH-7.2.0,5	0,5	255000	0,93
PH-7.2.1	1	257000	0,94
PH-7.2.2	2	278000	1,00
PH-7.2.3	3	311000	1,08

Calculations

It is assumed that the flow is fully rough turbulent, the friction factor can then be found from the equation (2.8) given by (Ceylan and Kelbaliyev 2003).

Slit configuration	**Relative roughness ξ, (k/D□)**	**Friction factor**	**Velocity, hot gas [m/s]**
Undamaged	0	0,03	438,7
PH-7.2.0,5	0,26	0,133	260,2
PH-7.2.1	0,53	0,173	230,7
PH-7.2.2	1,07	0,226	206,3
PH-7.2.3	1,60	0,263	195,7

It can be seen from calculations above that the velocity of the hot combustion products decreases with increasing roughness of the gap surface. The velocity is further used to calculate the Reynolds number and subsequently the thickness of the boundary layer, equation (2.7).

Slit configuration	**Reynolds number**	**2000/Re**	**Thickness, boundary layer**
Undamaged	13733	0,15	0,043
PH-7.2.0,5	9838	0,20	0,050
PH-7.2.1	8817	0,23	0,053
PH-7.2.2	8386	0,24	0,055
PH-7.2.3	8590	0,23	0,054

(Ceylan and Kelbaliyev 2003) stated that the flow is fully rough turbulent and the friction factor is independent of the Reynolds number if the relative roughness, $\xi \geq 2000 / Re$. The relative roughness for all of the slits with multiple crosswise grooves has a relative roughness greater than the 2000/Re and the flow can therefore be stated as fully rough turbulent for these slits. Consequently the equation for the heat transfer process from fluid to wall presented in section 2.4.1 is valid.

Appendix C - Experimental equipment

C-1 High speed camera

Figure- XI: *Casio Exilim EX-F1*

The camera used in the present experimental work is a Casio Exilim EX-F1. It's a six-megapixel SLR-style camera with a 12x optical zoom lens. It has an ultra-high-speed CMOS sensor and LSI image processor and other speed enhancements giving it the ability to shoot full-resolution 2816 x 2112 pixel stills at 60 frames a second with a maximum shutter speed of 1/40,000th of a second, or to shoot video at 1,200 frames per second, allowing slow-motion shooting at up to 40x reduced speed.

C-2 Thermocouples and welding apparatus

C-2.1 Thermocouples

Based on (Kalvatn 2009)

A thermocouple consists of a junction of two different metals. The junction creates a small voltage that increases with temperatue. There is a variety of different thermocouples and they are classified by wich materials the junction is made of. The most common type of thermocouples is type k, which is used in this project, where the two materials in use are Nickel-Chromium and Nickel-Aluminium. Its temperature range is from -200 ^{o}C to 1100 ^{o}C, its sesitivity is approximately 41 μV/ ^{o}C and they got an accuracy of about ±2.5 ^{o}C. The thickness of the metal wires is 0.3 mm. As shown in Figure- XII the use of thermocouples can be very easy using only a voltmeter.

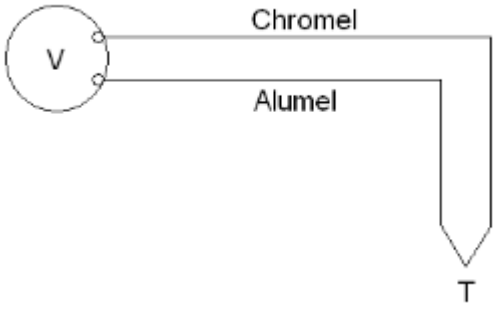

Figure- XII: *Schematic of temperature measurement using a voltmeter and a thermocouple. From* (Kalvatn 2009).

C-2.2 Welding apparatus for thermocouples

From (Kalvatn 2009)

Figure- XIII shows the apparatus that has been made for welding together the two metal wires that the thermoelement consists of. The basic principle behind the apparatus is to first charge a condensator with power from the regular power net via a rectifier, and then to discharge it across the two wires. This is done by, at one end of the cable, connecting one wire to the positive part of the condensator and the other to the negative part. At the other end of the cable the two wires are gently pushed against each other until contact is made, and the condensator then discharge through the wires. The wires are then welded together.

To further improve the result, argon is added to the welding point during the process in an attempt to exel oxygen from the welding zone. This will, to some extent, prevent combustion to take place, and the melting/welding of the two materials will be the more dominant process.

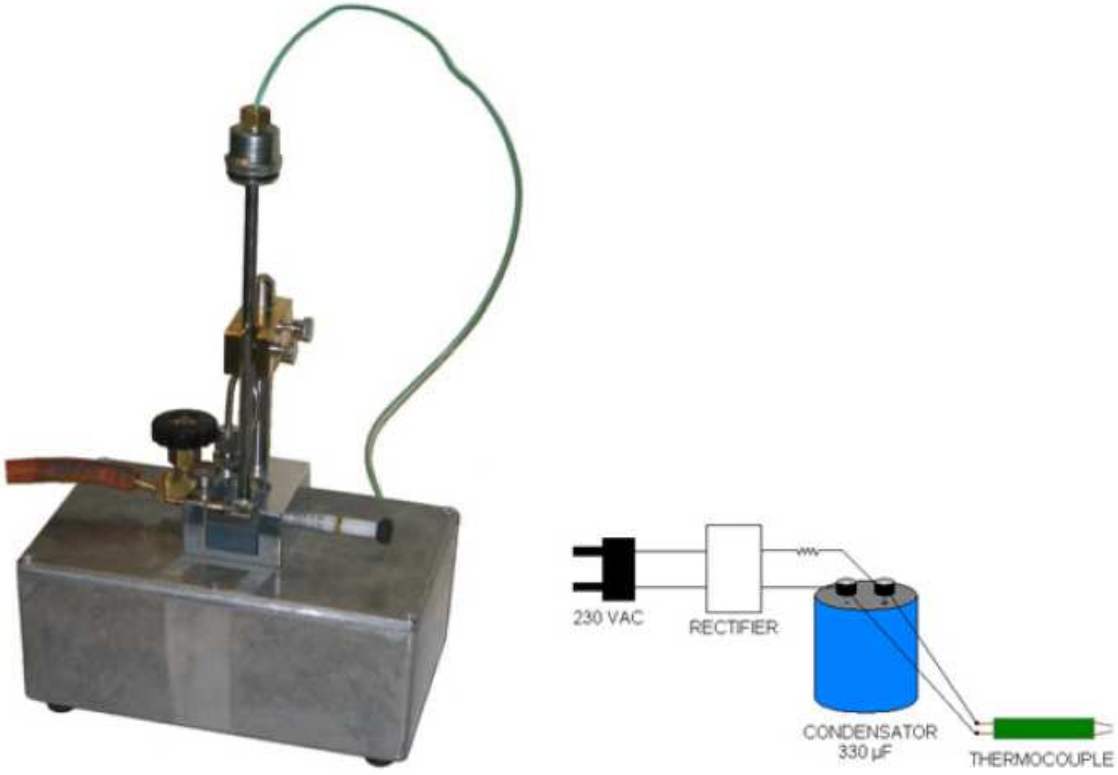

Figure- XIII *Apparatus used for welding thermocouples.*

C-3 Spark generator

From (Kalvatn 2009)

An electric spark generator has been made for preliminary experiments for both this project and others e.g. the modified balloon experiment. However, it did not generate enough energy to ignite pure dust clouds and was therefore only used for gas mixtures and hybrid mixtures with gas and dust. The energy generated has been estimated at around 50 mJ. Figure A-3 shows the schematic for the generator. The part list is shown in Table B-1 The electronics of the generator is built into a cabinet with the size of 25 x 20 x 11 cm (L x W x H) and a handle on the top. The electrical circuit board within the spark generator has been made at the UiB.
The basic principle of the generator is to discharge a capacitor that has been loaded by electricity from the regular power net. Either a negative or a positive flank of voltage can manually, or externally trigger the spark generator. The desired setting is chosen on the front panel of the spark generator. The possibility to externally trigger the spark discharge makes it easy to trigger the spark from a computer, thus it is implemented in the Labview program for running the FAT experiment. Figure- XIV below shows the inner parts of the generator.

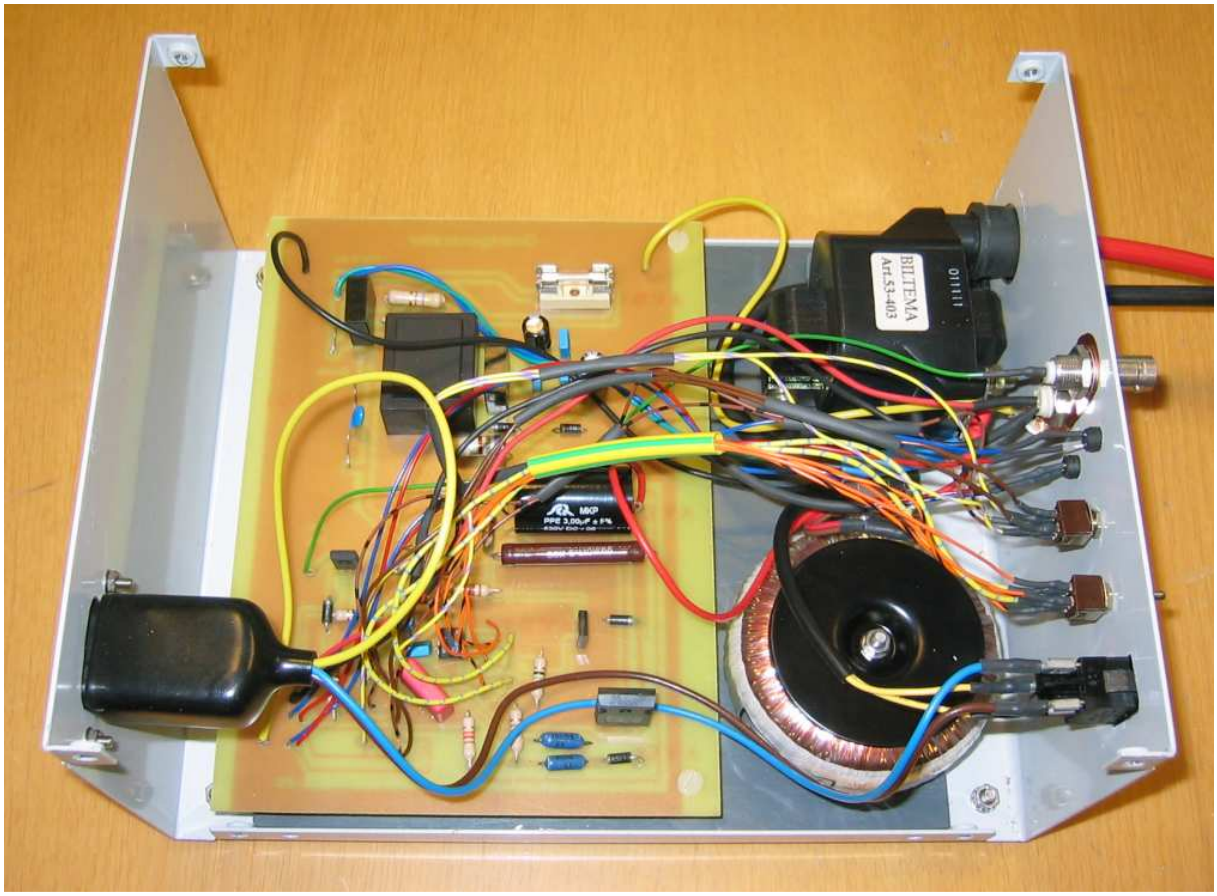

Figure- XIV: *Inner parts of the electric spark generator*

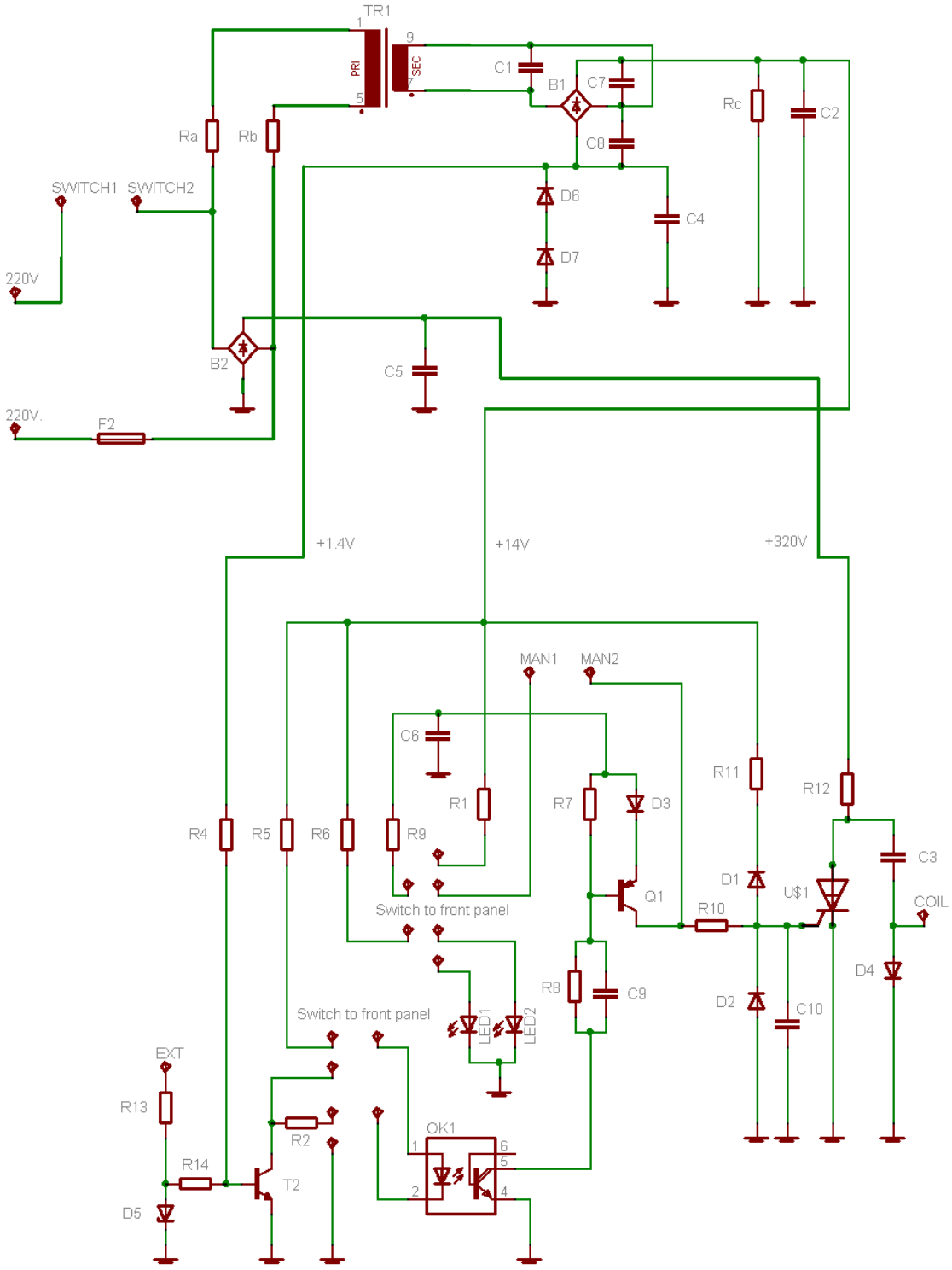

Figure- XV: *Electrical circuit for spark generator*

Table- IV: *Part list for spark generator*

Part	Value	Device	
C3	1u/500V	C-EU275-113X316	capacitor
C6	2.2u	C-EU050-025X075	capacitor
C9	0.1u	C-EU025-024X044	capacitor
C10	0.1u	C-EU050-025X075	capacitor
D1	1N4004	1N4004	diode
D2	1N4004	1N4004	diode
D3	1N4004	1N4004	diode
D4	1N4004	1N4004	diode
D5	1N821	1N821	diode
LED1		LED5MM	led
LED2		LED5MM	led
OK1	4N33	4N33	optocoupler
Q1	BD140	BD140	transistor-pnp
R1	100	R-EU_0207/10	resistor
R2	15	R-EU_0207/10	resistor
R4	10k	R-EU_0207/10	resistor
R5	680	R-EU_0207/15	resistor
R6	1.2k	R-EU_0207/10	resistor
R7	1.2k	R-EU_0207/10	resistor
R8	1.2k	R-EU_0207/10	resistor
R9	220	R-EU_0207/10	resistor
R10	15	R-EU_0207/10	resistor
R11	100	R-EU_0207/10	resistor
R12	58K/2W	R-EU_0617/22	resistor
R13	470	R-EU_0207/10	resistor
R14	120	R-EU_0207/10	resistor
T2	BD139	BD139	transistor
U$1	30TPS08	30TPS08	triac
B1		SKB	rectifier
B2		SKB	rectifier
C1	0.1u	C-EU050-025X075	capacitor
C2	100u	C-EU050-025X075	capacitor
C4	100u	C-EU050-025X075	capacitor
C5	0.01u/400V	C-EU275-093X316	capacitor
C7	0.1u	C-EU050-025X075	capacitor
C8	0.1u	C-EU050-025X075	capacitor
D6	1N4004	1N4004	diode
D7	1N4004	1N4004	diode
F2		SH22,5A	fuse
Ra	470/1W	R-EU_0411/15	resistor
Rb	470/1W	R-EU_0411/15	resistor
Rc	680/1W	R-EU_0411/15	resistor
TR1		EI30-1	trafo
coil		Art.53-403	Biltema

C-4 Scale

Sartorius TE212 Portable Battery Powered Electronic Scale, used for weighting dust.

Figure- XVI *Sartorius TE212 Portable Battery Powered Electronic Scale.*

Table- V: *specifications scale.*

Brand	Model	Capacity	Readability	Reproducibility
Sartorius	TE212 Portable scale	200g	0.01 g	< = ± 0.01 g

Appendix D - Different measurement data from experiments performed in the present work

An excerpt from the measurement data obtained through the experimental work is presented in this section.

Experiments performed with attached slit sets prior to rusting, and after exposure of rust.

		Undamaged slits, 27 april 2010		Rusted slits, 20 july 2010	
Gap opening, Yi [mm]	**Ignition position, Zi [mm]**	**Pmax [barg]**	**Re-ignition**	**Pmax [barg]**	**Re-ignition**
1,01	14	2,34	Yes	2,68	No
1,01	14	2,28	Yes	2,59	No
1,01	14	2,30	Yes	2,58	No
1,01	14	2,30	Yes	2,55	No
1,01	14	2,28	Yes	2,55	No
1,01	14	2,29	Yes	2,54	No
1,01	14	2,30	Yes	2,52	No
1,01	14	2,29	Yes	2,52	No
1,01	14	2,32	Yes	2,52	No
1,01	14	2,28	Yes	2,52	No
Mean		2,30		2,56	
1,00	14	2,44	Yes	1,55	No
1,00	14	2,38	Yes	1,44	No
1,00	14	2,37	Yes	1,46	No
1,00	14	2,35	Yes	1,45	No
1,00	14	2,36	Yes	1,44	No
1,00	14	2,32	Yes	1,43	No
1,00	14	2,38	Yes	1,43	No
1,00	14	2,35	Yes	1,40	No
1,00	14	2,36	Yes	1,40	No
1,00	14	2,35	Yes	1,40	No
Mean		2,37		1,44	
0,99	14	2,41	No	3,43	No
0,99	14	2,41	Yes	3,32	No
0,99	14	2,40	No	3,31	No
0,99	14	2,37	Yes	3,27	No
0,99	14	2,36	No	3,29	No
0,99	14	2,38	No	3,29	No
0,99	14	2,43	No	3,28	No
0,99	14	2,36	No	3,27	No
0,99	14	2,38	Yes	3,26	No
0,99	14	2,42	No	3,27	No
Mean		2,39		3,30	
0,98	14	2,40	No	3,61	No
0,98	14	2,39	No	3,53	No
0,98	14	2,41	No	3,53	No
0,98	14	2,41	No	3,49	No
0,98	14	2,38	No	3,48	No
0,98	14	2,40	No	3,45	No
0,98	14	2,38	No	3,48	No
0,98	14	2,40	No	3,50	No
0,98	14	2,39	No	3,50	No
0,98	14	2,43	No	3,49	No

Mean		2,40		3,51	
0,97	14	2,77	No	3,88	No
0,97	14	2,75	No	3,69	No
0,97	14	2,77	No	3,64	No
0,97	14	2,77	No	3,57	No
0,97	14	2,76	No	3,54	No
0,97	14	2,76	No	3,46	No
0,97	14	2,76	No	3,54	No
0,97	14	2,76	No	3,55	No
0,97	14	2,78	No	3,50	No
0,97	14	2,73	No	3,49	No
Mean		2,76		3,59	

Temperature measurements at different altitudes above the gap opening for an undamaged slit and a slit with multiple crosswise grooves (PH-7.2.3):

Date:	**19.05-27.05.2010**	
Surface configuration	**Undamaged**	
Apparatus	**PRSA**	
Gap opening [mm]	**1mm**	
Temperature °C		
1mm	**2cm**	**4cm**
647	**323**	**208**
633	**305**	**237**
632	**313**	**227**
N/A	**333**	**206**
631,8	**313**	**225**
Mean temperature		
635,95	**317,4**	**220,6**

Date:	**19.05-27.05.2010**	
Surface configuration	**PH-7.2.3**	
Apparatus	**PRSA**	
Gap opening [mm]	**1mm**	
Temperature °C		
1mm	**2cm**	**4cm**
330	**150**	**87**
335	**112**	**85**
N/A	**132**	**85**
335	**108**	**87**
313	**154**	**88**
Mean temperature		
328,25	**131,2**	**86,4**

Pressure measurements at different ignition positions for a slit with multiple crosswise grooves at gap opening 1.20 mm:

Date:	28.06.2010		
Surface configuration:	PH-7-2-3		
Apparatus:	PRSA		
Gap opening, Yi [mm]	**Zi [mm]**	**Pmax [barg]**	**Re- ignition**
1,20	5	2,63	No
1,20	5	2,59	No
1,20	5	2,64	No
1,20	5	2,62	No
1,20	5	2,58	No
1,20	5	2,62	No
1,20	5	2,60	No
1,20	5	2,59	No
1,20	5	2,61	No
Mean Pressure		2,61	

Date:	29.06.2010		
Surface configuration:	PH-7-2-3		
Apparatus:	PRSA		
Gap opening, Yi [mm]	**Zi [mm]**	**Pmax [barg]**	**Re- ignition**
1,20	10	2,71	Yes
1,20	10	2,68	No
1,20	10	2,70	Yes
1,20	10	2,70	Yes
1,20	10	2,73	No
1,20	10	2,71	Yes
1,20	10	2,69	Yes
1,20	10	2,68	Yes
1,20	10	2,69	No
Mean Pressure		2,70	

Date:	29.06.2010		
Surface configuration:	PH-7-2-3		
Apparatus:	PRSA		
Gap opening, Yi [mm]	**Zi [mm]**	**Pmax [barg]**	**Re- ignition**
1,20	14	2,73	Yes
1,20	14	2,75	Yes
1,20	14	2,74	Yes
1,20	14	2,72	Yes
1,20	14	2,72	Yes
1,20	14	2,74	Yes
1,20	14	2,75	Yes
1,20	14	2,72	Yes
1,20	14	2,73	Yes
Mean Pressure		2,73	

Date:	30.06.2010		
Surface configuration:	PH-7-2-3		
Apparatus:	PRSA		
Gap opening, Yi [mm]	**Zi [mm]**	**Pmax [barg]**	**Re- ignition**
1,20	20	2,86	No
1,20	20	2,89	No
1,20	20	2,84	No
1,20	20	2,88	No
1,20	20	2,86	No
1,20	20	2,86	No
1,20	20	2,87	No
1,20	20	2,89	No
1,20	20	2,85	No
Mean Pressure		2,87	

Date:	30.06.2010		
Surface configuration:	PH-7-2-3		
Apparatus:	PRSA		
Gap opening, Yi [mm]	**Zi [mm]**	**Pmax [barg]**	**Re- ignition**
1,20	25	2,90	No
1,20	25	2,91	No
1,20	25	2,91	No
1,20	25	2,89	No
1,20	25	2,92	No
1,20	25	2,92	No
1,20	25	2,88	No
1,20	25	2,90	No
1,20	25	2,91	No
Mean Pressure		2,90	

Pressure measurements at MESG for slit with undamaged surface and slits with multiple crosswise grooves:

Date:	27.04.2010		
Surface configuration:	Undamaged		
Apparatus:	PRSA		
Gap opening, Yi [mm]	**Zi [mm]**	**Pmax [barg]**	**Re- ignition**
0.98	14	2,40	No
0.98	14	2,39	No
0.98	14	2,41	No
0.98	14	2,41	No
0.98	14	2,38	No
0.98	14	2,40	No
0.98	14	2,38	No
0.98	14	2,40	No
0.98	14	2,39	No
Mean Pressure		2,40	

Date:	24.05.2010		
Surface configuration:	PH-7.2.3		
Apparatus:	PRSA		
Gap opening, Yi [mm]	**Zi [mm]**	**Pmax [barg]**	**Re- ignition**
0.98	14	3,16	No
0.98	14	3,13	No
0.98	14	3,14	No
0.98	14	3,12	No
0.98	14	3,11	No
0.98	14	3,15	No
0.98	14	3,33	No
0.98	14	3,32	No
0.98	14	3,30	No
Mean Pressure		3,20	

Date:	27.05.2010		
Surface configuration:	Undamaged		
Apparatus:	PRSA		
Gap opening, Yi [mm]	**Zi [mm]**	**Pmax [barg]**	**Re-ignition**
1,10	14	2,25	Yes
1,10	14	2,25	Yes
1,10	14	2,23	Yes
1,10	14	2,23	Yes
1,10	14	2,30	Yes
1,10	14	2,10	Yes
1,10	14	2,38	No
1,10	14	2,07	Yes
1,10	14	2,64	Yes
1,10	14	2,07	Yes
Mean Pressure		2,25	

Date:	28.05.2010		
Surface configuration:	PH-7.2.3		
Apparatus:	PRSA		
Gap opening, Yi [mm]	**Zi [mm]**	**Pmax [barg]**	**Re- ignition**
1,10	14	3,01	No
1,10	14	3,00	No
1,10	14	3,07	No
1,10	14	2,97	No
1,10	14	2,95	No
1,10	14	2,96	No
1,10	14	2,98	No
1,10	14	3,15	No
1,10	14	3,11	No
1,10	14	3,08	No
Mean Pressure		3,03	

Appendix E- Certificates

E-1 Calibration gas

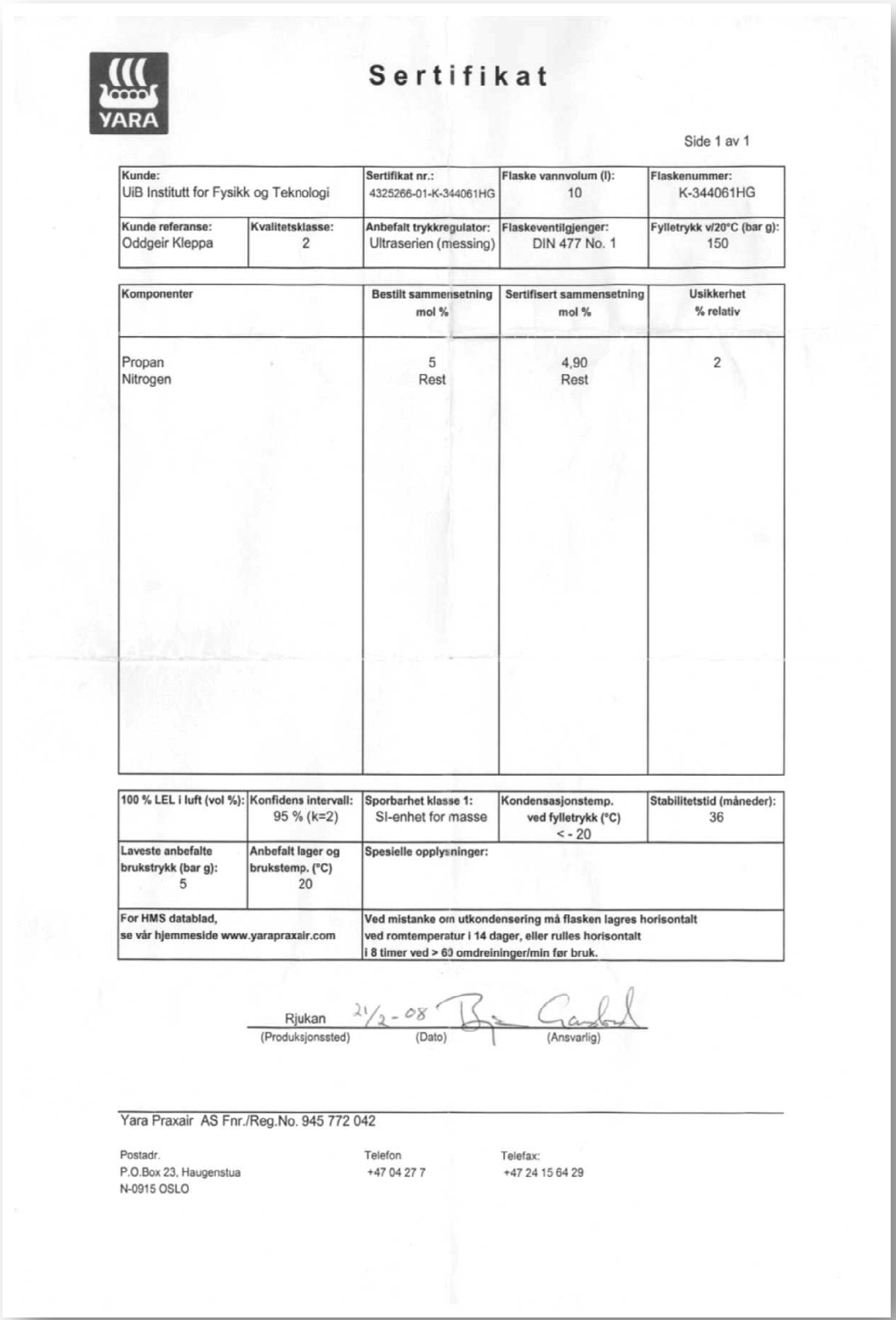

YARA

Sertifikat

Side 1 av 1

Kunde:		Sertifikat nr.:	Flaske vannvolum (l):	Flaskenummer:
UiB Institutt for Fysikk og Teknologi		4325266-01-K-344061HG	10	K-344061HG
Kunde referanse:	**Kvalitetsklasse:**	**Anbefalt trykkregulator:**	**Flaskeventilgjenger:**	**Fylletrykk v/20°C (bar g):**
Oddgeir Kleppa	2	Ultraserien (messing)	DIN 477 No. 1	150

Komponenter	Bestilt sammensetning mol %	Sertifisert sammensetning mol %	Usikkerhet % relativ
Propan	5	4,90	2
Nitrogen	Rest	Rest	

100 % LEL i luft (vol %):	Konfidens intervall:	Sporbarhet klasse 1:	Kondensasjonstemp. ved fylletrykk (°C)	Stabilitetstid (måneder):
	95 % (k=2)	SI-enhet for masse	< - 20	36
Laveste anbefalte brukstrykk (bar g): 5	**Anbefalt lager og brukstemp. (°C)** 20	**Spesielle opplysninger:**		
For HMS datablad, se vår hjemmeside www.yarapraxair.com		**Ved mistanke om utkondensering må flasken lagres horisontalt ved romtemperatur i 14 dager, eller rulles horisontalt i 8 timer ved > 60 omdreininger/min før bruk.**		

Rjukan 21/2-08 [signature]

(Produksjonssted) (Dato) (Ansvarlig)

Yara Praxair AS Fnr./Reg.No. 945 772 042

Postadr.
P.O.Box 23, Haugenstua
N-0915 OSLO

Telefon
+47 04 27 7

Telefax:
+47 24 15 64 29

E-2 Test gas

2

Salgsspesifikasjon

Dok.id.nr.: SS141
Gyldig fra: 2004-06-30
Revisjon: 05
I alt 2 sider

Propan 3.5

1. Spesifikasjon:

Propan(C_3H_8)	>	99,95 %
Vann (H_2O)	<	10 ppm
Oksygen (O_2)	<	10 ppm
Nitrogen (N_2)	<	50 ppm
Karbondioksid (CO_2)	<	20 ppm
Andre hydrokarboner (C_nH_m)	<	400 ppm

2. Flasketyper

Størrelse	**Innhold**	**Varenummer**
10 liter	4,2 kg	500317
50 liter	21,0 kg	500318

Se også HMS-datablad på vår hjemmeside www.yara.no
(Gass og Kjemikalier -> Produkter og tjenester -> HMS-datablad -> "produktnavn")

Yara Industrial AS forbeholder seg retten til å endre spesifikasjonene uten varsel

Postadresse
Yara Industrial AS
Postboks 23 Haugenstua
N-0915 Oslo

Telefon
24 15 76 00

Telefax
24 15 75 50

Internett
www.yara.no

E-3 Charge amplifier

KISTLER
measure. analyze. innovate.

Kalibrierschein Ladung
Calibration Certificate Charge

Type **5015A0000** Serial No. **1683268**

Kalibriert durch Calibrated by		Datum Date
R. Büchele		19.05.2008
Referenzgeräte Reference Equipment	**Typ** Type	**Serien-Nr.** Serial-No.
Ladungskalibrator Charge Calibrator	5395A1	530626
Umgebungstemperatur Ambient Temperature °C		**Relative Feuchte** Relative Humidity %
24		40

Geräteeinstellungen
Instrument settings

HP Filter HP Filter	LP Filter LP Filter kHz	Ausgangsbereich FS Output Range FS V
DC (Long)	1,0	10

Messergebnisse Results of Measurement

Nullpunktabweichung ohne Filter Offset Voltage Filter off mV	Nullpunktabweichung mit Filter Offset Voltage Filter on mV	Measure Sprung Measure Jump mV	Drift Drift pC/s; mV/s
0,8	0,7	-0,1	0,00

Filter 30 kHz; obere Grenzfrequenz (-3 dB) Filter 30 kHz; upper cutoff frequency (-3 dB) kHz	Obere Grenzfrequenz bei voller Bandbreite (-3 dB) Upper cutoff frequency at full bandwidth (-3 dB) kHz
30,2	196

Bereichseinstellung Range setting pC	Eingangs-Ladung Input charge pC	Abweichung Spannungsausgang Voltage output error %	Abweichung Anzeige Readout error %
4,990	-4,990	-0,1	-0,1
9,990	-9,990	-0,1	-0,1
49,90	-49,90	0,0	0,0
99,90	-99,90	0,0	0,0
499,0	-499,0	0,0	0,0
999,0	-999,0	0,0	0,0
4'990	-4'990	0,0	0,0
9'990	-9'990	0,0	0,0
49'900	-49'900	0,0	0,0
99'900	-99'900	0,0	0,0
219'900	-219'900	0,0	0,0
1'099'000	-1'099'000	0,0	0,0
2'000'000	-2'000'000	0,0	0,0

Bestätigung Confirmation

Wir bestätigen, dass das oben identifizierte Gerät nach den vorgeschriebenen Verfahren geprüft wurde. Alle Messmittel sind auf nationale Normale rückverfolgbar. Kistler betreibt die SCS (Swiss Calibration Service) Kalibrierstelle Nr. 049, akkreditiert nach ISO 17025. Das Kistler Qualitätsmanagement System ist nach ISO 9001 zertifiziert.

We confirm that the device identified above was tested by the prescribed procedures. All measuring devices are traceable to national standards. the SCS (Swiss Calibration Service) Calibration Laboratory No. 049 is operated by Kistler and accredited per ISO 17025. The Kistler Quality Management System is certified per ISO 9001.

Kistler Instrumente AG
Eulachstrasse 22
PO Box
CH-8408 Winterthur
Tel. +41 52 224 11 11
Fax +41 52 224 14 14
info@kistler.com
ZKB Winterthur 8C 732
Swift: ZKBKCHZZ80A
Account: 1132-0374.628
IBAN: CH67 0070 0113 2003 7462 8
VAT: 229 713
ISO 9001 certified
www.kistler.com

E-4 Pressure transducers

KISTLER
measure. analyze. innovate.

Kalibrierschein DRUCK
Calibration Certificate PRESSURE

Type **701A** Serial No. **1740583**

Kalibriert durch Calibrated by	Datum Date
U. Köhler	20.10.2008

Referenzgeräte Reference Equipment	Typ Type	Serien-Nr. Serial No.
Gebrauchsnormal Working Standard	Kistler 7005-350	634580
Ladungsverstärker Charge Amplifier	Kistler 5011A Kistler 5011A	572386 572385
Ladungskalibrator Charge Calibrator	Kistler 5395A	530633

Umgebungstemperatur Ambient Temperature °C	Relative Feuchte Relative Humidity %
23	41

Messergebnisse Results of Measurement

Kalibrierter Bereich Calibrated Range bar	Empfindlichkeit Sensitivity pC / bar	Linearität Linearity ≤ ± %FSO
0 ... 250	-80,60	0,11
0 ... 25	-79,49	0,04
0 ... 2,5	-79,22	0,04

Messverfahren **Kontinuierliche Kalibrierung, Vergleichsverfahren**
Measurement Procedure Continuous Calibration, Comparison Method

Bestätigung Confirmation

Die Geräte halten die Herstelltoleranzen gemäss Spezifikationen der Datenblätter ein. Wir bestätigen, dass das oben identifizierte Gerät nach den vorgeschriebenen Verfahren geprüft wurde. Alle Messmittel sind auf nationale Normale rückverfolgbar. Kistler betreibt die SCS (Swiss Calibration Service) Kalibrierstelle Nr. 049, akkreditiert nach ISO 17025. Das Kistler Qualitätsmanagement System ist nach ISO 9001 zertifiziert.

The equipment meets the manufacturing tolerances according to the specification data sheets. We confirm that the device identified above was tested by the prescribed procedures. All measuring devices are traceable to national standards. The SCS (Swiss Calibration Service) Calibration Laboratory No. 049 is operated by Kistler and accredited per ISO 17025. The Kistler Quality Management System is certificied per ISO 9001.

Kistler Instrumente AG
Eulachstrasse 22
PO Box
CH-8408 Winterthur
Tel. +41 52 224 11 11
Fax +41 52 224 14 14
info@kistler.com
ZKB Winterthur BC 732
Swift: ZKBKCHZZ80A
Account: 1132-0374.628
IBAN: CH67 0070 0113 2003 7462 8
VAT: 229 713
ISO 9001 certified
www.kistler.com

Appendix – F Magnified Photos of Dust

F-1 Atomized aluminum

Magnified photography's of the atomized aluminum used in the experimental work.
The photos are taken at the Laboratory for Electron Microscopy at the University of Bergen with Zeiss Supra 55VP (electron microscope).

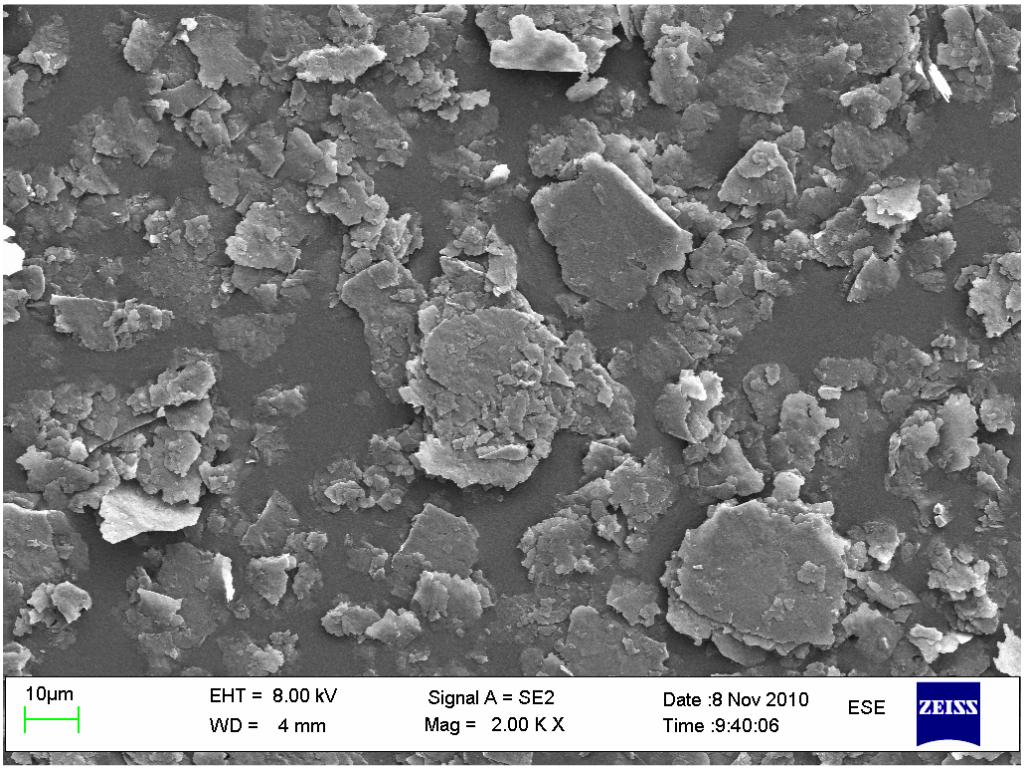

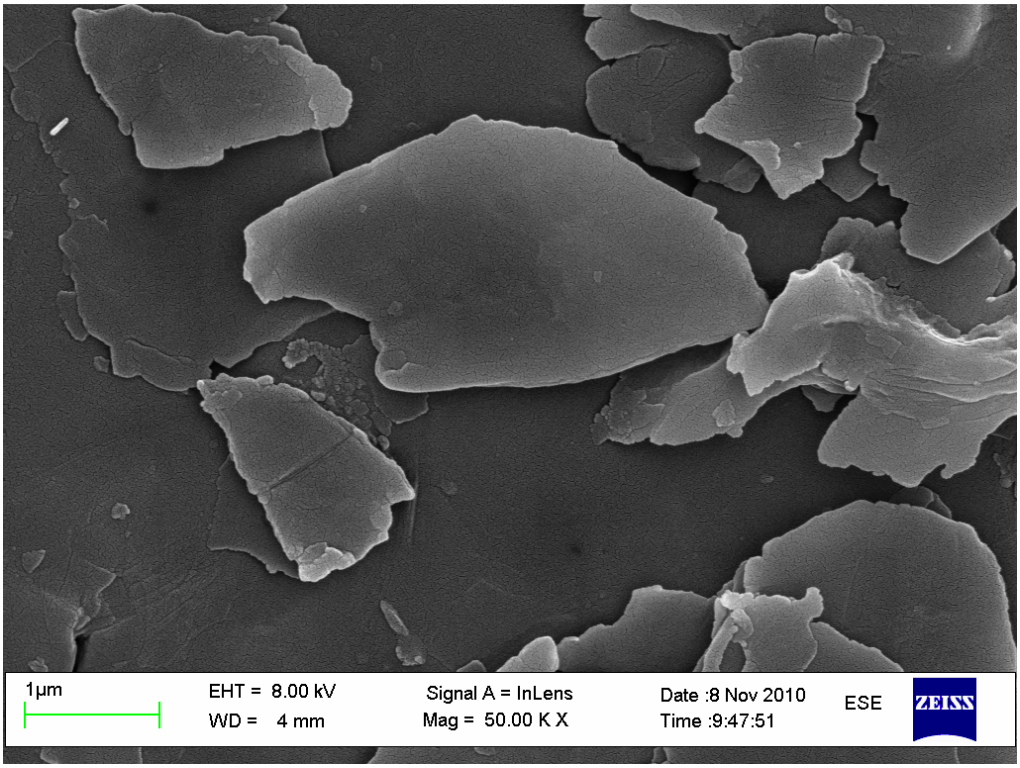

F-2 Pollen dust

Magnified photography`s of pollen dust used in the experimental work.
The photos are taken at the Laboratory for Electron Microscopy at the University of Bergen with Zeiss Supra 55VP (electron microscope).

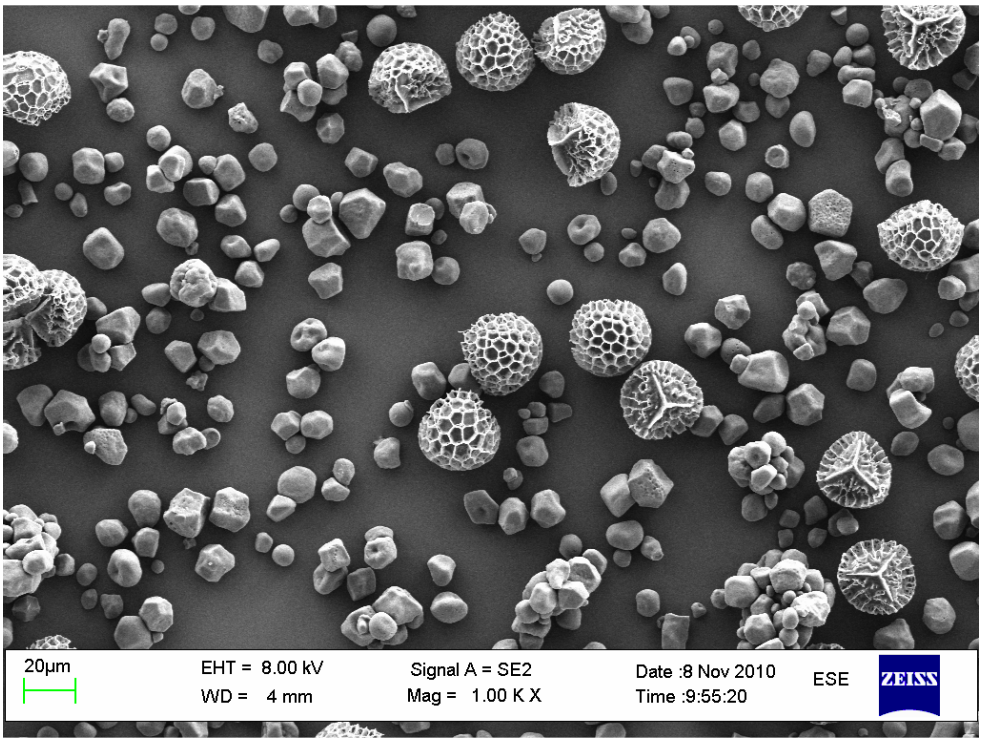

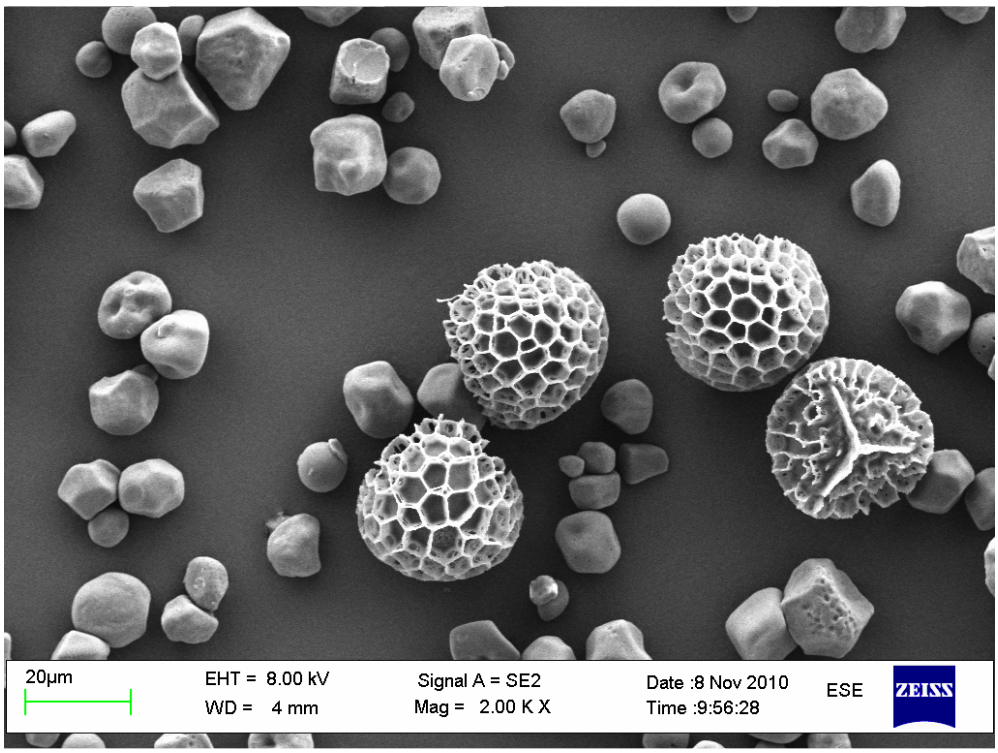

Ceylan, K. and G. Kelbaliyev (2003). "The roughness effects on friction and heat transfer in the fully developed turbulent flow in pipes." Applied Thermal Engineering **23**(5): 557-570.

Grov, A. (2010). An experimental study of the influence of major damage of flame gap surface in flameproof apparatus on the ability of the gaps to prevent gas explosion transmission. Department of Pyhsics programme of process safety. Bergen, University of Bergen. **Master in science**

Kalvatn, I. (2009). Experimental investigation of the optical measurement method for detecting dust and gas flames in a flame acceleration tube. Department of physics and technology. Bergen, University of Bergen. **Master Sc.**

McCabe, W. L., P. Harriott, et al. (2005). Unit operations of chemical engineering. Boston, McGraw-Hill.

Opsvik, H. E. Z. (2010). Experimental investigation of the influence of mechanical and corrosion damage of gap surfaces on the efficiency of flame gaps in flameproof apparatus. Department of physics and technology. Bergen, University of Bergen. **Master Sc.**

Perry, R. H. and D. W. Green (2008). Perry's chemical engineers' handbook. New York, McGraw-Hill.